Satellite cell molecular clock regulation on muscle mitochondria, contractile function, and muscle repair

Kahn, Ryan

Kahn, Ryan (2025). Satellite cell molecular clock regulation on muscle mitochondria, contractile function, and muscle repair [PhD Thesis]. Australian Catholic University. DOI: https://doi.org/10.26199/acu.913xq

Satellite cell molecular clock regulation on muscle mitochondria, contractile function, and muscle repair

Submitted by:

Ryan E. Kahn

B.Sc (exercise science), MSc (human physiology)

A thesis in fulfillment of the requirements for the degree of

Doctor of Philosophy

Ph.D. with Publication

Exercise and Nutrition Research Program

Mary MacKillop Institute for Health Research

Australian Catholic University

Melbourne, Victoria, Australia

September 2024

Statement of Authorship and Sources

This thesis contains no material that has been extracted in whole or in part from a thesis that I have submitted towards the award of any other degree or diploma in any other tertiary institution.

No other person's work has been used without due acknowledgment in the main text of the thesis.

All research procedures reported in the thesis received the approval of the relevant Ethics/Safety Committees (where required).

The extent of collaboration with another person or persons has been acknowledged accordingly where necessary.

Signed:

Ryan Kahn

Date: 27 August 2024

Acknowledgements

Firstly, I'd like to thank my Ph.D. supervisors Professor John Hawley, Dr. Sudarshan Dayanidhi, and Dr. Leonidas Karagounis. I've grown a great deal under their supervision and I am extremely grateful for having had the chance to pursue my interests and love for science under their guidance. All of your input and guidance has helped me to become the scientist I'd like to be and hopefully, will continue to grow into. I'm very grateful to have had this opportunity. John, I cannot thank you enough for taking a chance on me and giving me the opportunity to grow as a scientist. Your guidance over the years has helped me grow in so many ways and I'm extremely grateful I've had the good fortune to learn from someone with so much experience like yourself. What you've accomplished in the research fields of exercise/muscle physiology and the translatability of that work to sports-performance is something I admire and what initially drew me to want to pursue a Ph.D. under you. I'm hopeful I will find ways to translate the research-findings in my niche of muscle physiology similarly to the world of sports and pave my path forward with the blueprint for success that you've trailblazed.

Leon, you're help has been insurmountable in my progress as a Ph.D. student. You work at an incredible rate, and I've learned a great deal from your guidance. Your broader perspective for how research applies to real-world scenarios has helped me improve my translational thinking regarding my current and future research and I'm very appreciative of our chats we've had over the course of the Ph.D. Thank you for all your time and effort you've put in to help me along this journey.

Lastly, Sudarshan, to put it bluntly, my young scientific career just would not have gone this well so far if it were not for you. I had just finished my master's, was feeling isolated and out on an island not knowing my next step forward, and we were visiting family in Chicago when I

decided to cold email you to grab coffee and chat muscle nerdiness things. You took the time to grab coffee with a muscle-scientist-wannabe, saw something in me, and then offered me a job to work with you on some pretty cool muscle projects (that ended up working out rather well ☺). Fast-forward a year, COVID hits, the world shuts down, John and I are out of options to get me into Australia to start my Ph.D., and again you were a lifeline and together, you and John formed a collaboration between ACU and Shirley Ryan Ability Labs that let me start the Ph.D. from Chicago. Without you, all the great pre-Ph.D. work we did, and the Ph.D. work itself would never have been possible. I'm forever grateful for you believing in me, having faith in me, and always encouraging and guiding me in every possible way in science and in life. It has been a blessing and a privilege to have someone like you in my corner looking out for me. Cheers to you, my friend; and thank you for everything.

I'd also like to thank our collaborator, Dr. Richard Lieber. The wealth of knowledge I've gained in muscle mechanics and overall, as a scientist under your guidance has been instrumental to my development and I'm extremely grateful to have had the opportunity to work with you. The weekly data meetings we had during "peak season" of our muscle mechanics experiments where we would get into the weeds and go back-and-forth about all kinds of contractile related mechanisms was some of the most fun I've had during the whole Ph.D. and are some of my favorite core memories of the journey.

Thank you to my lab mates at Shirly Ryan Ability Labs/Northwestern University as well as at ACU. The day-to-day chats of muscle-nerdiness related things is what I looked forward to everyday and what made this journey so fun for me. Particularly, I'm very grateful to Dr. Raji Pichika for always looking out for my best interest. Whenever I had to troubleshoot or was in need of some veteran-experimental guidance, she was always willing to help and share with me her

incredible knowledge-base and experience. Additionally, thank you to my external panel members Drs. Andy Domenighetti and Justin Hardee. Your guidance and encouragement have greatly added to not only the experimental work but also to my growth as a scientist. I'm very grateful to you both.

To my friends and family, thank you all for your continued support and interest. To my older sister Brianna, thank you for always being a reassuring ear to chat to whenever I was feeling overwhelmed. Having your support throughout the Ph.D journey has helped me navigate many unforeseen obstacles and I'm truly grateful for all your support. To the Dunlaps, Dane, Lance, and Nadine, you guys have always been there for me and I couldn't be more grateful to call some of the most caring, kind, and simply remarkable individuals my family. I've loved coming back home to Florida on breaks and fully unplugging, playing lots of tennis, and always laughing (and eating way too many chocolate squares) until I'm cramping. Your genuine interest and asking about all the muscle-nerdy things I find myself doing these days is something I really appreciate and cherish. Having you guys in my corner has and continues to give me the foundation and belief in myself that I can do anything, and no dream is too big to chase. To Kevin and Kathy Tunney, both of your endless love and support has meant the world to me. You guys have helped me navigate the ups/downs of the winding journey of this Ph.D. and in life and I'm extremely grateful to have you both in my life. Some of the most "feel-good" memories I've accrued since we've moved to Chicago back in 2020 have been the time Mere and I have spent with you both. Whether it's the holidays or just a trip out to the suburbs with you guys, I always have a blast and can always count on coming home with a new hat (stolen from Kevin's collection of course ☺). It's the feelings that I get from being around you both and Mere that have made Chicago "home" for me and I couldn't be more grateful to have such incredible people in my life. I didn't know what I was missing ☺

Lastly, thank you to my wife, Meredith Tunney-Kahn. You must have heard me talk about these little creatures called satellite cells over a million times by now and every time you are as genuine as the last in listening to me ramble about all things muscle-nerdiness. Through all the peaks and valleys of this Ph.D. journey, you've been through it all with me. We've moved coast-to-coast across the US twice, and now have literally moved across the globe and back. We've gone from a couple, to engaged, to married and have made the most incredible memories with each other, family, and friends (new and seasoned ones) over the years. Throughout this Ph.D. journey, you've been there to encourage me, console me, laugh with me, and all the while establishing yourself and paving your way forward in your own career and life journey. And, most importantly, you've always helped me to maintain a healthy perspective on what matters most in our life together even in the face of the more grueling years our careers have demanded of us. You can be the best in the world at whatever it is you do but, it doesn't mean a thing if you aren't the person you want to be in the eyes of the person you love in this world. Above all else, that is and always will be my north star. I'm incredibly blessed to call you my wife, and forever grateful for all your love and support throughout this journey.

Table of contents

List of Publications from Thesis

Kahn RE, Dinnunhan F, Meza G, Lieber RL, Lacham-Kaplan O, Hawley JA, & Dayanidhi S. (2024). Time-of-day mitochondrial respiration in glycolytic and oxidative skeletal muscle in the presence and following ablation of satellite cells. *Revised and resubmitting to MSSE.*

Kahn, R. E., Lieber, R. L., Dinnunhan, F., Lacham-Kaplan, O., Dayanidhi, S., & Hawley, J. A. (2024). Satellite cells differentially regulate *ex vivo* force production according to time-of-day. *American Journal of Physiology-Cell Physiology* https://doi.org/10.1152/ajpcell.00157.2024

Kahn, R. E., Dayanidhi, S., Lacham-Kaplan, O., & Hawley, J. A. (2023). Molecular clocks, satellite cells, and skeletal muscle regeneration. *American Journal of Physiology-Cell Physiology*. https://doi.org/10.1152/ajpcell.00073.2023

Kahn RE, Zhu P, Roy I, Peek C, Hawley JA, & Dayanidhi S. (2024). Ablation of satellite cell-specific clock gene, *Bmal1*, alters force production, muscle damage, and repair following contractile injury. *Submitted to FASEB.*

List of Conference Presentations

Kahn RE, Dayanidhi S, Lieber RL, Hawley J, Lacham-Kaplan, O. Time-of-day variation in mitochondrial function following satellite cell depletion. *Orthopedic Research Society 2023 Annual Meeting*, 2023, Dallas, TX.

Kahn RE, Dayanidhi S, Lieber RL, Hawley J, Lacham-Kaplan, O. Time-of-day variation in muscle mitochondria and contractility function following satellite cell depletion. *The Skeletal Muscle Stem Cells and Regeneration Conference*, 2022, New Orleans, LA.

Kahn RE, Dayanidhi S, Hawley J, Lacham-Kaplan, O. Time-of-day variation in mitochondrial function following satellite cell depletion. 18*th International Biochemistry of Exercise Conference (IBEC)*, 2022, Toronto, Canada.

Kahn RE, Dayanidhi S, Hawley J, Lacham-Kaplan, O. Time of day variation in muscle mitochondrial function and contractility following satellite cell depletion". Northwestern Research Conference: 16th Annual Lewis Landberg Research Day, 2022, Chicago, IL.

List of Figures

List of Tables

List of abbreviations

ANOVA	analysis of variance
ATP	adenosine-triphosphate
Bmal1	brain and muscle like arnt-1
BSA	bovine serum albumin
BW	body weight
CCCP	carbonyl cyanide m-chlorophenyl hydrazone
CE	core-enhancer
CI	mitochondrial electron transport chain complex-I
CII	mitochondrial electron transport chain complex-II
CIII	mitochondrial electron transport chain complex-III
CIV	mitochondrial electron transport chain complex-IV
CLOCK	circadian locomotor output cycle kaput
Cox1	Cyclooxygenase 1
Cry1	cryptochrome circadian regulator 1
Cry2	cryptochrome circadian regulator 2
CS	citrate synthase
CSA	cross sectional area
CV	mitochondrial electron transport chain complex-CV
Ca^{++}	calcium
DI	distilled
DNA	deoxyribonucleic acid
E-C	excitation-contraction

E_{CI+II}	Maximal oxidative phosphorylation capacity of ETC
ECM	extracellular matrix
EDL	extensor digitorum longus
ES	electrically stimulated
ETC	electron transport chain
Fis1	fission 1 protein
G-0	phase zero during gap phase in cell cycle
G-Alert	alert-phase in between zero and one during gap phase in cell cycle
G1	phase one during gap phase in cell cycle
Gapdh	Glyceraldehyde 3-phosphate dehydrogenase
H&E	hematoxylin and eosin
Hif1a	hypoxia induced factor 1a
Hz	hertz
Igf1	insulin like growth factor 1
Igf2	insulin like growth factor 2
IHC	immunohistochemistry
IgG	immunoglobular domain
J	joules
KD	knockdown
KO	knockout
Kg	kilograms
L	liter
L_f	fiber length

L_f /s	fiber-lengths per second
L_o	muscle length
M	mass
MC	molecular clock
MPC	myogenic progenitor cell
Mrf4	myogenic factor 6
MRFs	myogenic regulatory factors
Myf5	myogenic factor 5
MyoD	myoblast determination protein 1
N	newtons
N/cm^2	newton/centimeters squared
NAD+	nicotinamide adenine dinucleotide + hydrogen
NADH	nicotinamide adenine dinucleotide
Nm	newton meters
O2	oxygen
Opa1	optic atrophy 1
OxPhos	oxidative phosphorylation
Pax7	paired box 7
PBS	phosphate buffered saline
Pgc1a	Peroxisome proliferator-activated receptor gamma coactivator 1-alpha
P_{CI}	Complex-I mediated oxidative phosphorylation
P_{CI+II}	Complex-I-II mediated oxidative phosphorylation
PCR	polymerase chain reaction

PCSA	physiological cross-sectional area
Pdk4	pyruvate dehydrogenase kinase 4
Per1	period 1
Per2	period 2
PFA	Paraformaldehyde
P_o	maximal isometric force
RER	respiratory exchange ratio
RNA	ribonucleic acid
ROX	residual oxygen consumption
Rev-erba	nuclear receptor subfamily 1 group D
S	synthesis phase in cell cycle
SA-HRP	streptavidin-horseradish peroxidase
SC	satellite cell
SCN	superchiasmatic nucleus
SEM	standard error of mean
SOL	soleus
SUIT	substrate-uncoupler-inhibitor titrations
TA	tibialis anterior
TCA	tricarboxylic acid cycle
Tmem176b	transmembrane protein 176b
TPT	time to peak tension
V	volts
$VO2_{max}$	maximal volume of oxygen consumption

$VO2_{peak}$	peak volume of oxygen consumption
ZT	zeitgeber hour
ddPCR	droplet digital polymerase chain reaction
dpi	days post injury
eMHC	embryonic myosin heavy chain
g	grams
h	hour
mL	milliliter
mM	millimolar
mRNA	messenger ribonucleic acid
mTORC1	mammalian target of rapamycin complex one
min	minutes
mmol	millimole
ms	milliseconds
mtDNA	mitochondrial deoxyribonucleic acid
ng	nanogram
nm	nanometer
rpm	revolutions per minute
s	seconds
uL	microliter
°C	Celsius
½ RT	half relaxation time
µg	microgram

ρ	fiber density

Abstract

Background: Circadian rhythms are an evolutionary conserved mechanism that underpin diurnal variance in biological and physiological processes. These rhythms are produced by a central molecular clock located in the suprachiasmatic nucleus (SCN) and are communicated to "peripheral" clocks located in peripheral tissues and organs. Of the peripheral clocks, several studies have demonstrated skeletal muscle houses some of the most robust rhythmicity in molecular clock oscillations throughout a 24 h day. A wide range of muscle biological/physiological processes are under molecular clock control including exercise-capacity, mitochondrial metabolism, contractile-function, and muscle repair/regeneration. However, there are *two* myogenic molecular clock sources within muscle: myonuclei and satellite cells (SC). Recent evidence has demonstrated that SCs house a functioning molecular clock with the transcription of several genes related to mitochondrial metabolism, muscle contractile function, and myogenesis exhibiting circadian expression patterns. Additionally, as other works have demonstrated that mitochondrial function, contractility, and muscle repair are all molecular clock regulated aspects of muscle physiology, this suggests the SC molecular clock may also play a role in such regulations. Systematic evaluation of mitochondrial function, contractile function, and muscle repair across different times of the day and in the presence/absence of SC-molecular clocks will provide novel information on the role that SC-molecular clocks may have in these processes.

Methods: Using the Pax7DTA ($Pax7^{CRE\text{-}ERT2/+}$; $Rosa26^{DTA/+}$) mouse model capable of inducible depletion of SC's, muscle mitochondrial function was assessed in the tibialis anterior (TA) (glycolytic muscle) and soleus (oxidative muscle) in the morning, afternoon, and evening (0700h,

1500h, 1900h). Mitochondrial citrate synthase activity, ETC-I activity, copy number, mitochondrial and molecular clock gene expression were undertaken at the same timepoints/SC-conditions in the TA and quadriceps. At time points demonstrating oscillatory clock gene expression*, ex vivo* submaximal muscle fatigue in the EDL was assessed to determine if fatiguing contractions reliant on mitochondrial-energy also demonstrate time-dependent variance. Next, utilizing the Pax7DTA mouse model, *ex vivo* maximal contractile function and eccentric injury of the EDL were assessed in the morning and afternoon (0700h and 1500h) in the presence and absence of SCs. Immunohistochemical methods were used to quantify dystrophin^{negative} fibers, cross sectional area, and SC abundance in these muscles. Gene expression was performed in contralateral, uninjured TA muscle. Finally, utilizing a mouse model capable of inducible depletion of molecular clock gene, *Bmal1,* in SCs (SC-*Bmal1*^{iKO}) muscle damage, SC progression, and muscle repair following *in vivo* eccentric contractile injury were compared to control animals (SC- *Bmal1*^{Cntrl}). Baseline *in vivo* torque and *ex vivo* specific force were quantified in both groups who underwent *in vivo* contractile injury consisting of 200 eccentric contractions. All mechanical experiments were performed at the same time of day (1000 h). Following injury, animals were sacrificed at 24 h, 72 h, and 7 days. Muscles were frozen, sectioned, and histologically and/or immunohistologically labeled for markers of muscle damage, neutrophil content, muscle repair, and satellite cell myogenic progression.

Results/Discussion: The results from these studies demonstrate that SC presence/absence does not affect time-of-day mitochondrial respiration. In line with peak, trough *Bmal1* and *CLOCK* gene expression, mitochondrial-dependent submaximal fatigue showed ~35% greater fatigue-resistance in the morning versus afternoon. Collectively, SCs are not a factor that influence time-

of-day mitochondrial function and therefore time-of-day differences in submaximal fatigue I (and others) observe may not be due to time-of-day regulations (SC, muscle, or otherwise) on mitochondrial respiration. With notable diurnal differences observed in *submaximal* contractile-fatigue, maximal contractile function with respect to time-of-day and SC presence/absence was evaluated in a separate study at the same timepoints. Morning-SC^{+} animals demonstrated reduced maximal tetanic and eccentric specific forces compared to SC^{-} counterparts. However, no such differences were observed between Afternoon-SC^{+}/SC^{-} groups. Consequently, Morning-SC^{+} animals experienced reduced extents of contractile injury (less force-loss and $dystrophin^{negataive}$ fibers) compared to SC^{-} counterparts, whereas no differences were noted between afternoon groups. These findings demonstrate that the regulatory role of SCs over contractility is time-of-day specific. Evaluations of *ex vivo* caffeine-contracture force, a surrogate for maximal Ca^{++} availability to contractile units, revealed similar patterns of lower force in Morning-SC^{+} versus SC^{-} counterparts indicating lower volumes of Ca^{++} may be underpinning the lower forces observed in these animals. These observations suggest SCs influence maximal force-production in the morning but, not in the afternoon and thus the extent of injury is concordant with the level of maximal force produced at specific times of day and the prevailing status of SCs. To further unravel SC-molecular clock regulation on contractile injury and how that may impact repair, a mouse model allowing for inducible depletion of SC-specific clock gene, *Bmal1*, was utilized for the last experiments. Following *in vivo* contractile injury, these animals demonstrated lesser extents of fiber-necrosis (24 h, 72 h), neutrophil content (24 h, 72 h), eMHC+ fibers (7 dpi), and centralized nuclei (7 dpi) compared to control animals. Of note, as SC-*Bmal1*^{iKO} animals produced lower torque and specific forces, these animals may have sustained less damage/repair in-line with the established notion that higher forces lead to higher

damage. As necrosis delays SC kinetics, the lesser necrosis noted in SC-*Bmal1*^{iKO} animals may have led to the earlier peaks in SC activation/proliferation (24 h versus 72 h in control animals). The extent of SC activation (Pax7+/MyoD+) was approximately two-fold higher in SC-*Bmal1*^{iKO} animals, suggesting that SC-*Bmal1* has an additional role on the temporal and volumetric regulation of MyoD during SC-mediated repair.

Conclusion: The results of the experiments performed provide evidence that SC-molecular clocks play a regulatory role in contractile function and muscle repair. While past works have shown *muscle* molecular clocks regulate these events, the results from the experiments undertaken for this thesis provide novel insights to demonstrate that *satellite cell specific* molecular clocks also regulate these processes. Collectively, the results from these studies provide preliminary insight suggesting that SC-molecular clocks, in part, regulate maximal force-production, contractile injury-induced muscle damage/repair, and SC-mediated myogenic progression. Future work will be able to use these initial studies as foundational knowledge to further explore the mechanisms of how SC-molecular clocks regulate muscle physiology according to time-of-day.

Chapter 1: Introduction and Overview

Circadian rhythms, produced by molecular clocks, exist in nearly all cells which render a variety of biological/physiological processes as rhythmic events (1). Circadian rhythms are generated from the "central" molecular clock residing in the suprachiasmatic nucleus (SCN) of the brain and these rhythmic signals are then relayed to "peripheral" clocks in most tissues and organs (2, 3). Independent of central rhythms, peripheral tissue molecular clocks can also generate their own distinct rhythmicity from stimuli such as contractile activity (4). Of the peripheral tissues, skeletal muscle molecular clocks produce some of the most robust circadian rhythms (1, 5). Notably, these rhythmic signals from muscle molecular clocks regulate a variety of critical muscle biological/physiological processes such as muscle mitochondrial metabolism, contractile function, and repair/regeneration (6-14). A literature review (Chapter 2) provides in in-depth discussion of such regulations by muscle molecular clocks.

Within the muscle microenvironment, a muscle stem cell population (i.e., satellite cells, SC) exists to facilitate muscle reparative/regenerative needs following muscle damage or injury (15, 16). Recently, it was discovered that SCs house their own molecular clocks that exhibit rhythmic clock gene expression over the course of 24 h (17). Additionally, SC specific genes related to mitochondrial metabolism, contractile function, and myogenesis exhibited circadian expression patterns (17), suggesting SC molecular clocks may play a role in these critical processes of muscle physiology. As noted, muscle molecular clocks exert regulatory roles over numerous aspects of muscle physiology. SCs may also harbor such regulatory functions over mitochondria, contractility, and myogenesis as well. Indeed, preliminary evidence supports the notion that SC molecular clocks have such regulatory capacity (see chapter 2). However, a comprehensive evaluation of the roles SC molecular clocks play in mitochondrial metabolism, contractile

function, and muscle repair is lacking. Therefore, the general aims of the experiments undertaken for this thesis were to systematically evaluate SC molecular clock regulations over:

1. Muscle mitochondrial metabolism
2. Muscle contractile function
3. Contractile-induced injury and repair

To address these aims, three related but inter-dependent experimental studies were conducted (described in detail in chapters 3, 5,8). Study-1 (chapter 3) specifically addressed aim-1 by assessing *ex vivo* mitochondrial function in the morning, afternoon, and evening in the presence and absence of SCs in both oxidative and glycolytic muscle. These experiments utilized a mouse-model capable of inducible depletion of SCs ($Pax7^{CRE\text{-}ERT2/+;}$ $Rosa26^{DTA/+}$, Pax7DTA). Aligned to time-of-day differences in clock gene expression, *ex vivo* submaximal contractile-fatigue reliant on mitochondria-energy was determined as well. The purpose of assessing mitochondrial function in the presence and absence of SCs across three times of day was to expose any time-of-day dependent regulations SCs may have on muscle mitochondria. Next, experiments for the second study (described in detail in chapter 5) addressed the second aim of this thesis by assessing *ex vivo* contractile function in the morning and afternoon in the presence and absence of SCs using the same mouse model as study-1. Timepoints chosen for this study were aligned to the significantly different timepoints arising from experiments conducted in study-1 (chapter 3). The purpose of assessing contractile function in the presence/absence of SCs in the morning and afternoon were to reveal any time-of-day dependent regulations SCs harbored over force-production. Additionally, to determine if any time-of-day dependent differences in force-production altered

the magnitude of subsequent contractile injury*, ex vivo* eccentric injury was carried out at both timepoints in the presence/absence of SCs. In study-3 (described in chapter 8), utilizing a mouse model capable of inducible depletion of molecular clock gene, *Bmal1* in SCs, *in vivo* eccentric contractile injury was undertaken to investigate SC-molecular clock regulations on SC myogenic progression and muscle repair.

Chapter 2: Literature review

2.1 Circadian molecular clocks

Circadian rhythms are highly conserved biological processes that are aligned to earth's daily rotation and subsequent light/dark cycles (1, 2). Circadian rhythms act as anticipatory mechanisms to changing environments on earth (light during the day, dark during night) functioning as "Zeitgebers" (timekeepers) for numerous biological processes across organs, tissues, and species (3, 18). On the cellular level, circadian rhythms are produced by a molecular clock located in nuclei of nearly all cells (19). Molecular clocks function as transcriptional/translational feedback loops that receive circadian signals (most notably photic-cues) and subsequently carry out appropriate responses which ultimately render biological/physiological processes as "circadian-regulated" events (18-20).

The molecular clock has mechanisms in place that can self-activate and repress itself comprised of a positive and negative "arm." The positive arm of the molecular clock, Bmal1 and CLOCK, bind to e-box sequences of promotor regions on target clock genes Per1/2, Cry1/2 (Fig 2.1). Once transcribed/translated, the expressed clock-genes Per1/2, Cry1/2 function as the negative arm of the molecular clock via re-entering the nucleus to repress/inhibit Bmal1/CLOCK's abilities for further transcription of clock genes (3, 19, 21) (Fig 2.1). This negative feedback loop operates on an oscillatory basis throughout a 24 h cycle and underpins the peaks and troughs in circadian rhythms (18, 19).

Although all cells contain molecular clocks, mammalian organisms house both a "central" clock located in the SCN of the brain and, "peripheral" clocks located in peripheral tissues (2). Circadian signals such as light are recognized by the SCN and are subsequently communicated to peripheral tissues' molecular clocks which interpret and undertake the appropriate time-of-day

physiological/biological responses (2, 22). In addition to photic cues, peripheral clocks are also responsive to diurnal cues such as exercise and/or feeding patterns (4). Of these peripheral clocks, circadian rhythmicity is most pronounced in brain, liver, and skeletal muscle (2, 20). In skeletal muscle, a wide variety of muscle physiological processes are regulated by these resident molecular clocks (7, 23, 24).

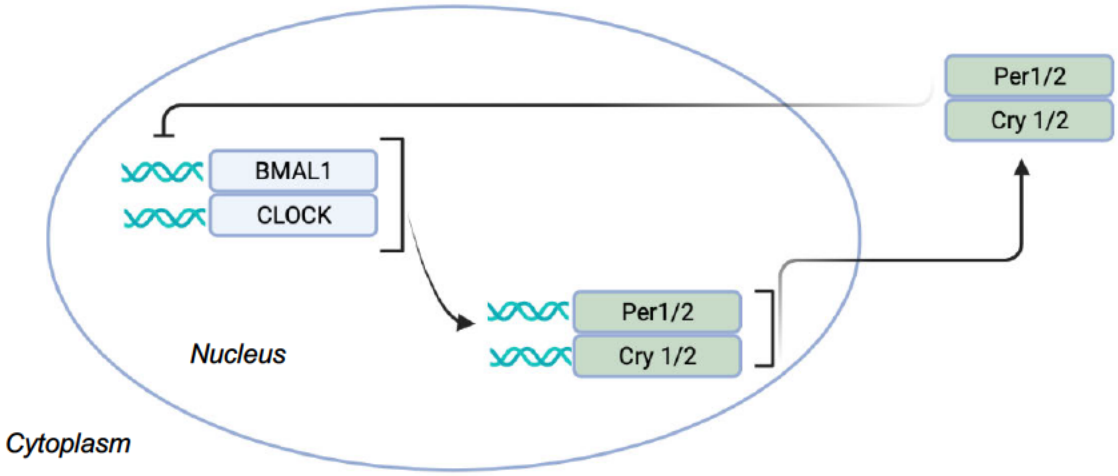

Figure 2.1: Molecular Clock

Bmal1 and CLOCK bind to the E-box region of clock genes Per1/2, Cry1/2 inducing their expression and exit of the nucleus. Per1/2 and Cry1/2 translocate back into the nucleus to then bind the E-box region of Bmal1 and CLOCK to repress their transcription of Per1/2, Cry1/2. This transcriptional/translational feedback loop is what comprises the oscillations of molecular clock output thus being "circadian rhythms."

2.2 Muscle molecular clocks and time-of-day regulation on muscle physiology: implications for satellite cell molecular clocks?

In skeletal muscle, molecular clocks regulate a vast landscape of muscle physiology consisting of (but not limited to) gene expression, exercise-capacity, contractile function, metabolism, and muscle repair (6-10, 23, 25-27). Of note, much of this evidence to demonstrate these roles has come from experiments involving circadian profiling of muscle physiological processes and whole-body/muscle-specific KO models of various molecular clock genes. Such investigations have provided data showing that the *muscle* molecular clock regulates a wide range of muscle processes. However, less is known about the *satellite cell* (SC) specific molecular clock (Fig 2.2). SCs, the muscle resident stem cell population, are mainly responsible for facilitating muscle repair (15, 16), and have recently been examined in a circadian context (17). Recent work has demonstrated that SCs house an oscillating molecular clock with rhythmic peaks in molecular clock gene expression (17). Numerous genes within SCs exhibited circadian expression profiles with several genes related to muscle metabolism, contractile function, and myogenesis observed to be oscillatory (17). Such findings suggest the SC molecular clock partially regulates previously observed aspects of muscle physiology that differ according to time-of-day (Fig 2.2). Additionally, muscle physiology operates on a spectrum with energy metabolism closely matching the demands of the prevailing contractile status (28, 29) such as exercise (30, 31). These contractile demands can lead to fatigue (32, 33) and/or muscle damage (34, 35), which requires muscle repair (36, 37). Molecular clock regulations on any one of these processes may inherently impact the other and therefore assessments of these processes should not be considered in isolation.

The following sections will first present physiological findings to show that exercise-capacity is a diurnal event, then provide the foundation to demonstrate how muscle metabolism and contractile force production that underpin exercise may be regulated by molecular clocks. Following this section, evidence of diurnal and molecular clock regulations on metabolism and

contractility will be discussed, as well as the proposed regulations by SC-molecular clocks (Fig 2.2). Finally, evidence will be presented showing that muscle repair following extreme/non-physiological injury is, in part, regulated by muscle and SC molecular clocks. This section will also introduce the notion that influence from the SC-molecular clock in *physiological* injury settings (resultant from eccentric contractions) may be impacted by existing evidence of molecular clock regulations on force-production.

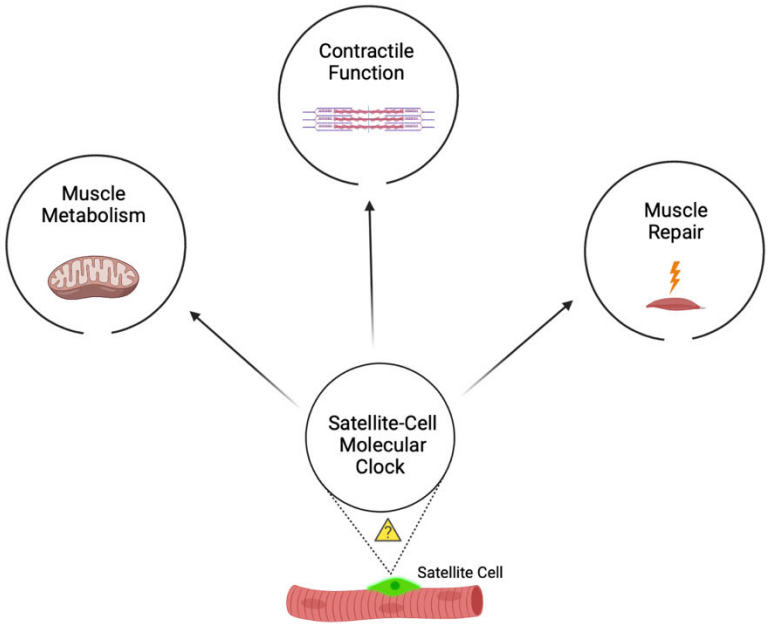

Figure 2.2: Satellite cell molecular clock regulation on muscle physiological processes

Simplified schematic of the potential nodes of regulation SC-molecular clocks may wield over muscle metabolism, contractile function, and muscle repair. Question mark indicates the unknown role SC molecular clocks may play in muscle metabolism, contractile function, and repair.

2.3 Molecular clock regulation of diurnal exercise-capacity

Exercise capacity differs with respect to time-of-day with evidence indicating molecular clocks are partly responsible for this diurnal variance (Table 2.1). Specific evidence was provided from a recent report demonstrating that exercise-capacity in mice peaked in the morning compared to other times of day (38). Furthermore, human exercise trials show a greater sustainment of $\%VO2_{max}$ and lower RER in the morning versus evening (25). Such diurnal patterns of exercise-capacity may be due to molecular clock regulations as various studies utilizing clock-gene KO mice have shown differences in exercise-capacity (39, 40). Specifically, Cry1/2 KO mice run faster and further compared to control animals (40). Exercise tests of "time-to exhaustion" performed at submaximal intensities largely dependent on aerobic energy metabolism demonstrate that exhaustion occurs earlier when animals exercised in the morning versus the afternoon (39). However, in the absence of Per2 and Bmal1, this timely variance in time-to-exhaustion was abolished possibly indicating that Per2 and Bmal1 have a critical role to play in regulating exercise-capacity (39). From a mechanistic perspective, "exhaustion" occurs when the metabolic supply of ATP fails to meet the demands of contractile-force production and consequently, muscle fatigue occurs (41). Muscle mitochondria are the predominant supply of ATP for contractile-demands during prolonged exercise (28). Therefore, the abovementioned observations of diurnal changes in exercise-capacity may be due to diurnal alterations in mitochondrial function. Additionally, although not assessed in the referenced works, the effect nutritional interventions have on the metabolism underpinning diurnal exercise-capacity has yet to be thoroughly investigated.

First Author	Species	Intervention	Intensity	Molecular clock and/or Time-of-day effects

Ezagouri 2019 (25)	C57BL/J6 (mouse)	Treadmill Running	Moderate	Enhanced endurance capacity at afternoon timepoint
	Per1/2 KO (mouse)			Differences abolished
	Human			Enhanced endurance capacity at morning timepoint
Adamovich 2021 (38)	C57BL/J6 (mouse)	Treadmill Running	Moderate	Enhanced endurance capacity at afternoon time point
	Bmal1 KO (mouse)			Differences abolished
	Per2 KO (mouse)			Differences abolished
Kiho 2006 (14)	Per2 KO (mouse)	Treadmill Running	Moderate/High	Reduced running capacity
Jordan 2017 (40)	Cry1/2, Cry1, Cry2 KOs (mouse)	Treadmill Running	High vs Low Intensity	Enhanced running capacity during high intensity running in Cry1/2 KO
Maier 2021 (39)	C57BL/J6 (mouse)	Treadmill Running	High Intensity	Enhanced endurance capacity at morning timepoint

Table 2.1: Molecular clock regulation of exercise-capacity

Table of studies that evaluated exercise-capacity based on time of day or alterations to the molecular clock

2.4 Molecular clock regulation of mitochondrial function

Since exercise-capacity is a diurnal event partly regulated by molecular clocks, this suggests mitochondrial function may also be regulated by time-of-day. Muscle mitochondria are integral to muscle metabolism as they supply the necessary ATP needed for the majority of contractile demands (28). Mitochondrial function differs by time-of-day with this phenomenon demonstrated across human and animal experiments (6, 10, 42). Such diurnal oscillations in function have been attributed to rhythmic oscillations in mitochondrial morphology (fusion/fission), since mitochondrial fusion and fission genes oscillate by time-of-day (6, 10, 43) (Fig 2.3). As mitochondria do not have nuclei of their own, their nuclear source for diurnal regulation must stem from muscle and/or SC molecular clocks. Work characterizing the muscle circadian transcriptome has shown that mitochondrial related genes are diurnally expressed suggesting diurnal variance in function may stem from the "muscle" molecular clock (26). Supporting this notion, whole body Bmal1 KO and muscle-specific Bmal1 KO animals display inhibited mitochondrial function (13, 44, 45), and in whole body Bmal1 KO animals, maximal mitochondrial oxidative phosphorylation capacities are reduced. However, as these mice were bred from birth lacking Bmal1 systemically, such deficits in function could, in part, be attributed to decreased mitochondrial abundance (13). Supportive of these findings, deficits in mitochondrial function were also observed in Bmal1 KO myotubes (44). These changes were attributed to alterations in the HIF1a pathway (44), with reports from the same group demonstrating the underlying mechanism may have been inhibitions on NAD+ metabolism, which concordantly altered mitochondrial function (45-47). Indeed, supplementing mice with NAD+ was able to rescue deficits in mitochondrial function (45). Importantly, the methodology in which these

investigations evaluated mitochondrial function involved measuring oxygen consumption in the presence of endogenous levels of substrate storages (carbohydrate, fat storages) (45, 47) that could possibly lead to a confound as different levels of endogenous substrates can alter mitochondrial function (48). To provide more clarity regarding diurnal and/or molecular clock-specific regulations on mitochondrial function, animals may need to be fasted to avoid any risks associated with different dietary eating habits that can lead to varying levels of endogenous substrates storages.

As discussed previously, a recent report that characterized the SC-specific transcriptome over the course of 24 h demonstrated that several metabolic/mitochondrial related genes were oscillatory (17), suggesting SC-molecular clocks may partially contribute to previously shown diurnal muscle mitochondrial function (6, 10). Two recent reports utilizing a mouse model capable of inducible depletion of SCs demonstrated that following SC ablation, exercise-capacity was reduced (49, 50). As mitochondria-derived ATP sustains the contractile-energetics of prolonged-exercise (28, 33), it is interesting to consider that while exercise-capacity was reduced in SC^- animals, mitochondrial abundance stayed the same (49). Although this study was conducted at a single time-of-day, this preliminary evidence suggests mitochondria may receive nuclear input from SCs and the lack thereof may affect mitochondrial function ultimately limiting exercise-capacity. Further evidence suggests a structural relationship between SCs and mitochondria with SC protrusion-like structures extending over myofibers and serving as a mode of communication shuttling metabolic/mitochondrial cargo between SCs and myofibers (51). Evidence of structural communication of mitochondrial cargo between SCs and myofibers (51), reduced exercise-capacity in SC-absence (49, 50), and diurnally expressed SC-specific mitochondrial genes (17)

collectively provide a mechanistic foundation to suggest SCs may have a diurnal regulation on mitochondrial function.

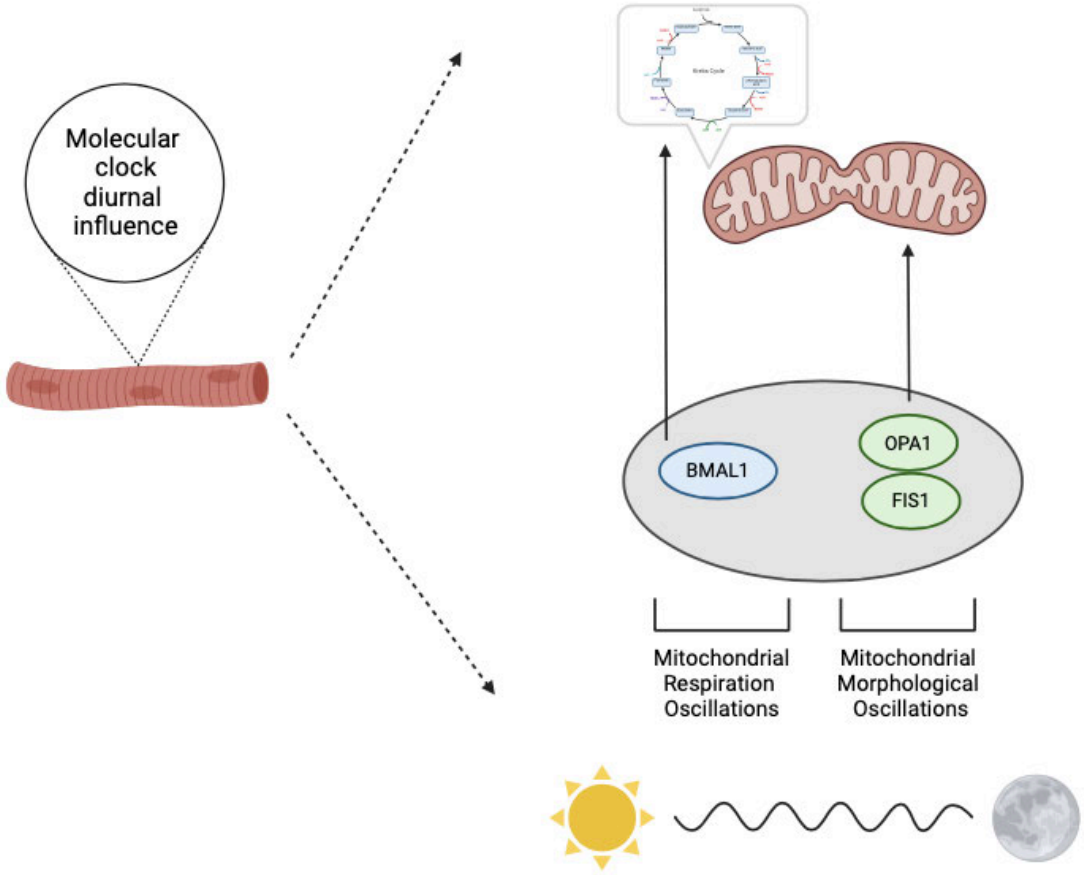

Figure 2.3: Molecular clock diurnal influence on muscle mitochondria

Mechanistic underpinnings of diurnal variance in mitochondrial function regulated by molecular clocks. Current evidence suggests diurnal variance in function may stem from concordant diurnal oscillations in mitochondrial morphology.

2.5 Molecular clock regulation of muscle contractility

As discussed (section 2.4), exercise capacity relies on a supply of readily available energy to sustain contractile force (28, 30, 33). Therefore, diurnal variation in exercise capacity may also

imply that contractile function is a diurnally regulated event. Accumulating evidence demonstrates that human muscle peak isometric torque follows a diurnal pattern with the highest forces occurring in the late afternoon (1600 h) (8). This is believed to be due to the molecular clock as the timing of peak torque in the late afternoon coincides with peak expression of molecular clock gene *Bmal1* in humans and animals (8, 9) (Table 2.2). In contexts of animal models investigating this relationship, whole body Bmal1 KO animals demonstrate decreased force-production in single fibers and whole muscle preparations (13). Furthermore, these deficits were observed in an inducible muscle-specific Bmal1 KO model following long-term ablation (28 and 52 weeks) (52, 53) (Table 2.2). A potential mechanism underpinning Bmal1's regulation of force production has been proposed to be alterations to the sarcomeric protein, titin (54, 55). These animals exhibit alterations in titin, which led to shortened sarcomere-lengths (54) and consequently may underpin decreased force-generation previously observed in this mouse model (13, 52). However, as human isometric torque data has been reported to oscillate with time-of-day in concordance with peak *Bmal1* expression (9), the mechanism by which molecular clocks regulate contractile function on a *diurnal* basis is likely distinct from those observed in long-term Bmal1-KO animal models.

Cry1/2 KO animals do not display any contractile force decrements (40), while Per2 KO animals harbor alterations in force-production (14) (Table 2.2). Interestingly, Per2 regulates calcium (Ca^{++}) related gene expression in muscle involved in the Ca^{++} kinetics of E-C coupling (56). This suggests Per2 regulates contractile function via calcium kinetics involved in E-C coupling. Such a notion would be in-line with previous work showing that molecular clocks regulate calcium-sensitive contractile machinery (i.e. myosin-light-chain-kinase) that influence force-production (26). However, diurnal expression of Ca^{++} related genes may not necessarily mean Ca^{++} is altered during the E-C coupling involved in muscle contractions. Therefore, future

studies should utilize *ex vivo* contractile assessments to measure Ca^{++} kinetics *during* contractions (57-59) to unravel if it is indeed the mechanistic culprit for molecular clock and/or diurnal influences on force production. Furthermore, molecular clocks in other tissue types have previously demonstrated regulatory control over calcium related functions offering further support for this potential mechanism in muscle (60-62).

Prior evidence has demonstrated that SC molecular clocks oscillate on a diurnal basis with several genes related to E-C coupling displaying diurnal variance (17). These data suggest that SCs may differentially regulate components of E-C coupling and thus, force-production by time-of-day, although experimental and mechanistic evidence in support of such a contention is lacking. To date, two studies have assessed whole muscle contractile function in mouse models after SC depletion (63, 64). In one such study, SC ablation in postnatal mice led to reduction in maximal contractile force (63). However, these changes were no longer observed when older mice were assessed, suggesting the deficits in contractile force may have stemmed from stunted muscle growth during post-natal development due to the requirement of SCs for muscle growth during this time period of life (63, 65, 66). In addition, a second study reported deficits in maximal contractile force following long-term SC ablation although these changes were attributed to long-term accumulation of excess ECM in the absence of SCs (64). Therefore, it is currently unknown if SCs affect force-production and if they do so in a time-of-day dependent manner. Future investigations should evaluate force-production following *short-term* SC-ablation and should do so in skeletal muscle from mature mice to avoid confounding effects (63, 64).

Additionally, it is likely that SCs time-of-day influence on force production is indirect via regulation on components of E-C coupling. As mentioned, the SC transcriptome has previously shown transcription of genes relevant to E-C coupling are expressed on a circadian basis (17)

suggesting downstream components of E-C coupling may be under circadian control thus, rendering force-production a diurnal event. However, as no studies have directly assessed this, whether SC molecular clocks influence force production via circadian regulation of E-C coupling is pure speculation. In this context however, it was recently discovered that muscle molecular clock gene *Per2* harbors a relationship with the Ca^{++} kinetics involved in E-C coupling (56). While SC molecular clocks were not evaluated in this study, evidence that molecular clocks have a functional link with the physiology of E-C coupling (56) vs simply transcription of the relevant components (26) may suggest SC molecular clocks may function similarly.

First Author	Species	Muscle	Molecular clock effect on contractile function
Kiho 2006 (14)	Per2 KO (mouse)	TA	Increased specific force
Andrews 2010 (13)	Bmal1 KO (mouse)	EDL	Decreased specific force
		EDL single fibers	Decreased maximally activated specific force
	CLOCK Mutant (mouse)	EDL	Decreased specific force
Schroder 2015 (52)	Muscle-Specific Bmal1 KO (mouse)	EDL	Decreased specific force

Jordan 2017 (40)	Cry1/2 KO (mouse)	EDL Soleus	No contractile differences
Dyar 2014 (53)	Muscle-Specific Bmal1 KO (mousse)	Plantar flexors	Decreased maximal torque

Table 2.2: Molecular clock regulations on contractile function

Studies that have evaluated contractile function in animal models of molecular clock disruption.

2.6 Molecular clock regulation of muscle repair

In the context of muscle repair, diurnal variance in force-production has implications that render muscle injury and consequent repair a function of time-of-day (Fig 2.4). Scaled degree of force-production induce concordant magnitudes of contractile injury (67, 68) and therefore, diurnal variance and/or molecular clock alterations to force-production may affect the extent of contractile injury and repair (Fig 2.4). Such a notion would infer that SCs, responsible for muscle repair/regeneration, may also harbor diurnal variance. Following injury, muscle enacts a highly conserved muscle regenerative response which involves the activation of SCs to orchestrate the cellular events required for successful muscle regeneration (15, 31, 69). Specifically, following activation, SCs will proceed down a myogenic lineage to proliferate, differentiate, and eventually fuse to the host myofiber to facilitate regenerative needs and replace damaged muscle architecture (15, 16, 36, 70-73). This myogenic progression of SCs is accomplished by sequential roles of the

myogenic regulatory factors namely, Myf5, MyoD, Mrf4, Myogenin, to act on the cell cycle to facilitate proliferative and differentiative events required for regeneration (74-76).

Studies in other fields of biology have shown that tissue repair following injury is a circadian event regulated by molecular clocks of tissue resident cells (77, 78). Furthermore, these circadian patterns of repair have been demonstrated across multiple tissue types suggesting molecular clock regulation on the process of repair itself may be a conserved circadian biological process (77-82). Although a vast array of work has characterized the cellular events involved in muscle repair/regeneration, relatively less work has focused on how/if molecular clocks influence muscle repair. In this regard, there is some insight into where and how molecular clocks may influence muscle repair/regeneration following injury (11, 12, 83-85). Previously, clock genes Cry and Per have both been shown to affect muscle regeneration following toxin induced injuries (83, 84). Specifically, whole-body Cry2 KO animals exhibited blunted muscle regeneration following injury as SC-derived myoblasts exhibited premature exit from the cell cycle and decreased expression of Myogenin (84). In the same study, lesser amounts of embryonic myosin heavy chain positive fibers were observed at a later timepoint following injury indicating these animals had indeed undergone lesser extents of muscle repair and could not fully meet the regenerative demands in the absence of Cry2 (84). Collectively, this suggests that Cry2 plays a critical role in regulating the myogenic response to accommodate repair following injury. Similarly, whole body Per1/2 KO animals exhibit alterations in myogenic progression (83). Following chemical injury, SCs of Per 1/2 KO animals display delayed SC proliferation which were suggested to be causal in deficits noted in myoblast differentiation/fusion *in vitro* (83). However, it is important to note that animals used in these studies were *whole-body* KOs of Cry and Per clock genes (83, 84), not SC-specific KO. Whether clock genes themselves have a direct effect on muscle regeneration or if

such effects are secondary to maladaptive phenotypes developed due to the systemic lack of these genes from birth is unknown.

Characterization of the muscle circadian transcriptome demonstrated that the myogenic regulatory factor, MyoD, exhibits circadian patterns of expression (26). Indeed, MyoD is expressed on a circadian basis (13, 26), with such rhythmicity hinging on upstream input from Bmal1 (as this rhythmicity is blunted in Bmal1-KO animals) (13, 26). The mechanism by which Bmal1 exerts its regulation on MyoD is through the core-enhancer (CE) region (86, 87) as specific ablation of this CE region abrogates MyoD's circadian expression pattern (88). Furthermore, MyoD's timing and amplitude during myogenesis is dysregulated in animals lacking this CE region (86), suggesting Bmal1 may regulate myogenesis via circadian regulation of MyoD. Studies utilizing whole body Bmal1 KO animals have displayed inhibited muscle repair following toxin-induced muscle injury, largely due to the inability of SCs lacking Bmal1 to adequately proliferate and progress down the myogenic lineage (a myogenic function that relies on MyoD) (11, 12). However, given the models used thus far have been muscle and or whole body Bmal1 KO (11, 12), it is unclear if Bmal1 specifically within SCs regulates myogenic progression consequently influencing muscle repair.

As discussed, a systematic approach characterizing the circadian transcriptome of SC's over 24 h demonstrated that SC-specific molecular clock genes oscillate in a circadian fashion (17). At timepoints previously reflecting high (evening) versus low (morning) Bmal1 expression (17), Zhu and colleagues injured animals via cardiotoxin at both of these times of day (85). Animals injured in the evening (aligned with high SC-*Bmal1* expression) exhibited normal muscle regeneration, whereas animals injured in the morning (low SC-*Bmal1*expression) displayed deficits in muscle regeneration (85). To further elucidate how SC-specific Bmal1 effected muscle

regeneration, the same study induced muscle injury in SC-specific Bmal1 KO animals and observed that animals lacking Bmal1 in SCs could not adequality proliferate to accommodate the reparative needs of damaged muscle ultimately leading to blunted muscle regeneration. Indeed, this observation is in line with data from whole body Bmal1 KO animals (11, 12). Utilization of a SC-specific Bmal1 inducible depletion model provides new insights and confirms Bmal1's critical role in SC-mediated muscle regeneration (85). Additionally, in a second study by Zhu and colleagues (89), it was discovered that time-of-day differences in SC-mediated muscle repair hinges on SC time-of-day dependent communication to early-responsive neutrophils. This communication by SCs functions to prime the microenvironment for efficient muscle repair with evidence demonstrating this may be driven by cytokine CCL2 in a time-of-day fashion (89). This work identifies a unique communication link between SCs and neutrophils that regulates the time-of-day capacity of muscle repair following injury.

Under physiological conditions, injury typically occurs via high force eccentric contractions (15, 34, 90) versus the non-physiological injury induced by chemical toxins. As discussed earlier, Bmal1 plays a role in force-production (13, 52), and therefore injury occurring from high force eccentric contractions is likely to be affected by Bmal1's regulation on contractility. Additionally, as peak/trough human isometric torque aligns with concordant peaks/troughs in Bmal1 expression (8, 9), varying degrees of eccentric-force may induce different magnitudes of contractile-damage (67, 68). Thus, it is plausible that Bmal1 regulations on force-production at different times-of-day may dictate the degree of muscle damage sustained and thus the extent of muscle repair. In this regard, the role SC-Bmal1 may play in a contractile injury and repair setting may differ from prior work showcasing SC-Bmal1's role in muscle repair following *non-physiological* injury (85) (Fig 2.4). Future investigations should first evaluate if SC-Bmal1

effects force-production similar to past findings in muscle/whole body KO models (13, 52) and subsequently assess if such regulation on force has any effect on extents of muscle damage/repair following contractile injury.

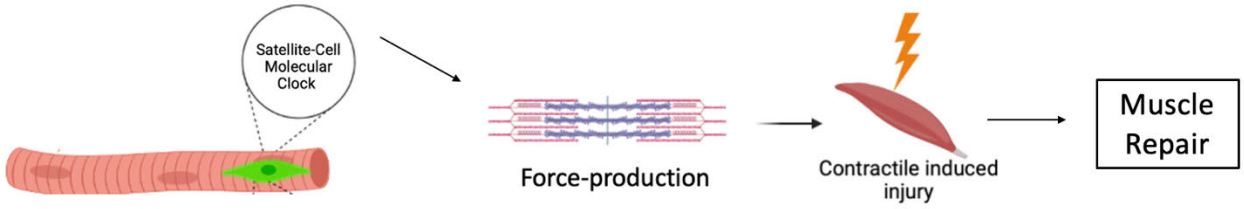

Figure 2.4: Proposed mechanisms of satellite cell molecular clock regulations on contractile injury induced muscle repair

Hypothetical logic-flow for satellite cell molecular clock sequential regulation of force production and thus the extent of contractile injury and subsequent repair

Chapter 3: Study-1

Kahn RE, Dinnunhan F, Meza G, Lieber RL, Lacham-Kaplan O, Hawley JA, & Dayanidhi S. (2024). Time-of-day mitochondrial respiration in glycolytic and oxidative skeletal muscle in the presence and following ablation of satellite cells. *Revised and resubmitting to MSSE.*

Time-of-day mitochondrial respiration in glycolytic and oxidative skeletal muscle in the presence and following ablation of satellite cells

Ryan E. Kahn[1,2], Fawzan Dinnunhan[1], Guadalupe Meza[2], Richard L. Lieber[2,3,4], Orly Lacham-Kaplan,[1] John A. Hawley[1*], Sudarshan Dayanidhi[2,3*]

[1]Exercise and Nutrition Research Program, The Mary MacKillop Institute for Health Research, Australian Catholic University, Melbourne, Australia

[2]Shirley Ryan AbilityLab, Chicago, IL, USA

[3]Feinberg School of Medicine, Northwestern University, Chicago, IL, USA

[4]Hines VA Medical Center, Maywood, IL, USA

Running Title: Time-of-day dependent mitochondrial respiration

*Corresponding Authors: SD and JAH

E-mail: sdayanidhi@sralab.org

john.hawley@acu.edu.au

3.1 Abstract

Endurance exercise capacity varies by time-of-day due to molecular clock time-of-day regulations on components of muscle physiology. Mitochondrial respiration, mainly responsible for the metabolic energy supply during submaximal endurance exercise, has been shown to vary by time-of-day and in animal models of muscle molecular clock disruption. Satellite cells (SCs) however, also house oscillatory molecular clocks with several clock and mitochondrial genes exhibiting diurnal oscillation. Given this diurnal nature of SCs and with evidence elsewhere demonstrating SC ablation leads to impaired endurance exercise capacity reliant on mitochondria, SCs may harbor regulations on mitochondrial function which may differ by time-of-day. Therefore, in this study, the primary aim was to assess if time-of-day mitochondrial function differs in the presence versus absence of SCs in oxidative (soleus) and glycolytic (TA) muscle. Utilizing a $Pax7^{CRE\text{-}ERT2/+;}$ $Rosa26^{DTA/+}$ mouse model capable of SC ablation (SC^{+}, SC^{-}), I conducted experiments in either the morning, afternoon, or evening. In both TA and SOL, no differences were observed in mitochondrial respiration across time-of-day in the presence versus absence of SCs. However, in glycolytic muscle (EDL), I observed that submaximal fatigue reliant on mitochondria energy was enhanced in the morning versus afternoon overlapping with peak/trough *Bmal1* and *CLOCK* gene expression (Morning-SC^{+}: 54 ± 5; Afternoon-SC^{+}: 36 ± 6 contractions until fatigue) ($p < 0.05$). Collectively, SCs are not a factor that influence time-of-day mitochondrial function and therefore time-of-day differences in submaximal fatigue are unlikely due to time-of-day regulations (SC, muscle, or otherwise) on mitochondrial respiration.

Keywords: muscle fatigue, muscle mitochondria, contractility, molecular clocks, satellite cells

3.2 Introduction

Endurance exercise capacity has recently been shown to be a function of time-of-day (25, 38-40). During prolonged, submaximal endurance exercise, muscle mitochondria are the primary source of cellular energy production that sustain contractile demands (28). Recently, evidence demonstrates mitochondria exhibit time-of-day rhythmicity in *ex vivo* maximal respiration (6, 10) due, in part, to regulation by the molecular clock, with ablation of molecular clock gene *Bmal1* decreasing both muscle mitochondrial content and respiration (13). However, recent work has shown SCs rhythmically express clock, contractile, and mitochondrial related genes over 24 hr (17) perhaps suggesting SCs may regulate mitochondrial function and thus, endurance exercise capacity according to time-of-day. Recently, I demonstrated maximal eccentric contractile function is altered in the presence/absence of SCs in the morning versus afternoon suggesting (91) that the diurnal SC transcriptome (17) may indeed exert an effect on the downstream relevant muscle physiology as well.

In a recent study, animals following SC ablation harbored impairments in submaximal endurance exercise capacity (49, 50), the bioenergetics of which are underpinned by mitochondrial energy production (28). The decrement in endurance exercise capacity was not accompanied by any change in mitochondrial abundance or muscle atrophy suggesting it was the function of mitochondria that was impaired during exercise however, respiration was not directly measured in $SC/^{+}SC^{-}$ animals in this study (49). As exercise-capacity is known to be a function of time-of-day in both humans and animals (25, 38-40, 92, 93), it is tempting to suggest that SCs impact mitochondrial respiration in a time-of-day dependent manner. In this context, the effects of SC presence/absence on mitochondrial respiration and if this relationship is time-of-day dependent has never been tested. Accordingly, the primary aim of the current study was to

determine time-of-day mitochondrial respiration (assessed by mitochondrial O_2 consumption) in the morning, afternoon, and evening, in the presence or absence of SCs. I hypothesized that variations in time-of-day mitochondrial respiration may depend on the presence of SCs.

3.3 Methods:

3.3.1 Animal info

$Pax7^{CRE\text{-}ERT2/+;}$ $Rosa26^{DTA/+}$ mice (n=43; male = 20; female = 23) 4-10 months of age and of mixed sex were used for these experiments (94, 95). All animal experiments were performed with the approval of the Northwestern University Institutional Animal Care and Use Committee (protocol number: IS000019422). Mice were euthanized via C02 inhalation followed by cervical dislocation. Mice were housed in groups of 2-5 animals per cage in a temperature/humidity-controlled environment on a 14:10 light-dark cycle (lights-on at 0600 h) and given *ad libitum* access to food/water. Prior to mitochondrial respiration experiments, all animals underwent an 8-12 h fast to avoid any confounding effects of diet/eating habits on mitochondrial respiration. Utilizing the Cre-lox system, inducible depletion of SCs was undertaken via five consecutive days of oral gavage of tamoxifen, while control (vehicle) animals received oral gavage of peanut oil (2mg in 100µl per day) (96, 97) followed by a minimum 14-day washout period (26.4 days ± 0.97 SEM). Prior literature has shown SC ablation is similar across hindlimb muscles (98) and as such, SC ablation in this study was quantified in the gastrocnemius. Animals were randomly assigned a treatment group (SC^--tamoxifen or SC^+-vehicle) and experimental timepoint (Morning-0700 h (ZT1), Afternoon-1500 h (ZT9), Evening-1900 h (ZT13); lights on at 0600 h (ZT0)). All experiments were performed after euthanasia at the assigned timepoints.

3.3.2 Gene expression

Immediately after euthanasia, quadriceps muscle was harvested and snap-frozen in liquid nitrogen-cooled isopentane for gene expression assays. Genes of interest were analyzed using the QX200 AutoDG Droplet Digital PCR system (Bio-Rad). Extracted RNA was analyzed for quality using Nanodrop-2000 and quantified using Qubit. Following this, an absorbance ratio of <1.8 was used to qualify the RNA and the quantification was used to equilibrate the samples to 1 ng/μL prior to ddPCR. A total of 5 μL of the equilibrated sample was aliquoted into the 96-well ddPCR plate along with 17 μL of a master mix (One-Step RT-ddPCR advanced kit for probes). The master mix also consisted of florescence labelled ddPCR primers (Bio-Rad) for the housekeeping gene Glyceraldehyde 3-phosphate dehydrogenase (*Gapdh*) and the gene of interest. Molecular clock genes of interest were *Bmal1, CLOCK, Cry1, Per2;* mitochondrial dynamics/morphology genes of interest were *Opa1, Fis1;* metabolic genes of interest were *Pdk4, PCG1a.* The plate was then placed into the AutoDG to generate up to 20000 droplets per well followed by reverse transcription. The plate was read using the QX200 droplet reader to visualize and yield exact gene concentration per μL of sample and was subsequently expressed relative to *Gapdh* concentration per well. For SC^+ and SC^- groups, all genes of interest across timepoints were normalized to the same, respective gene (represented as fold-change) for either Morning-SC+ or Morning-SC- groups. *Gapdh* was not altered between SC conditions or timepoints.

Time-of-day changes observed in molecular clock gene expression served as a guide for muscle physiology experimental timepoints as prior work has shown variation in muscle function is associated with time-of-day differences in clock gene expression (8, 9, 25, 39). These timepoints were also chosen for their general overlap with time-of-day expression of SC-specific core clock components in a much larger study (17)

3.3.3 Muscle Mitochondrial Respirometry

High resolution mitochondrial respirometry was performed using Oroboros O2K (Oroboros Instruments, Innsbruck, Austria), based on prior protocols (99, 100). Immediately following euthanasia, the soleus and tibialis anterior (TA) were dissected and placed in ice-cold BIOPS solution (2.77mM CaK_2EGTA, 7.23mM K_2EGTA, 5.7mM Na_2ATP, 6.56mM $MgCl_2$, 20mM taurine, 15mM Na_2Phosphocreatine, 20mM imidazole, 0.5mM DTT, and 50mM MES). The muscles were then further dissected under a microscope and mechanically separated in ice-cold BIOPS to obtain two replicates of 2-3 mg from each muscle. Following mechanical separation, muscles were chemically permeabilized with 50 μg/ml saponin for 30 min at 4°C and were subsequently washed for 10 min in mitochondrial respiration media [MiR05; 0.5mM EGTA, 3mM $MgCl_2$, 60mM K-lactobionate, 20mM taurine, 10mM KH_2PO_4, 20mM 4-(2-hydroxyethyl)-1-piperazineethanesulfonic acid, 110mM sucrose, 1g/L fatty acid-free bovine serum albumin]. Respirometry experiments on both samples from TA and soleus were run simultaneously and conducted at 37°C in hyperoxygenated (200–450μM O_2) conditions in MiRO5 to avoid any limitations/differences related to oxygen diffusion.

To assess maximal phosphorylation and electron transport chain capacity of complex-I and II mediated respiration I used a sequential substrate-uncoupler-inhibitor titrations (SUIT) respiration protocol. Specifically, I measured (final concentration in the O2k chamber are indicated in parentheses) 1) LEAK respiration (L) after TCA cycle stimulation with NADH-linked substrates pyruvate (5 mM) and malate (2 mM) to support electron flow through complex I (CI) of the electron transport chain (ETC); 2) CI-supported respiration (OXPHOS, $P_{CI(PM)}$; “State 3” respiration) after addition of adenosine diphosphate (ADP, 5 mM); 3) maximum CI-

supported respiration (OxPhos; P_{CI}) after addition of glutamate (10 mM); 4) maximum CI- and CII-supported respiration (OxPhos; P_{CI+II}) after addition of CII substrate succinate (10 mM); 5) uncoupled respiration, representing maximum ETC capacity (E_{CI+II}), after step-wise titration of the uncoupler carbonyl cyanide m-chlorophenyl hydrazine (CCCP; 0.5 mM); 6) maximum ETS capacity in the presence of CII substrate only (E_{CII}) after addition of CI-inhibitor rotenone (0.5mM); 7) residual, non-mitochondrial oxygen consumption (ROX) after inhibiting complex III (CIII) of the ETC with antimycin A (2.5mM). Prior to administration of succinate, cytochrome-c was administered to assess for over-permeabilization of the mitochondrial membrane. Any value higher than 15% following cytochrome-c administration was considered over-permeabilized and these data were not used. Maximum OxPhos and ETC capacity (P_{CI+II}, E_{CI+II}) were used for all statistical analyses. For all respirometry experiments, animals underwent an 8-12 h fast to account for potential differences in diurnal substrate availability.

3.3.4 Mitochondrial Activity Assays

Immediately after euthanasia, the TA from the contralateral limb was flash frozen in liquid nitrogen-cooled isopentane and stored in -80°C. Muscles were powdered using liquid nitrogen-cooled mortar and pestle, then homogenized in 0.5 mL of Zheng buffer (210mmol/L man- nitol, 70mmol/L sucrose, 5mmol/L 4-[2-hydroxyethyl]-1- piperazineethanesulfonic acid [HEPES] and 1mmol/L ethylene glycol-bis(b-aminoethyl ether)-N,N,N’,N’- tetraacetic acid [EGTA] [pH 7.2]) (101, 102). Homogenization was performed on ice by using glass-on-glass conical tissue grinders undergoing 16 strokes at 500 rpm. Homogenized tissue was subsequently centrifuged at 600g at 4°C for 10 min. Supernatant protein concentration was ascertained using the Pierce™ bicinchoninic acid protein assay kit per manufacturer’s instructions (Thermo Fisher

Scientific, Waltham, MA, USA) (101). Based on protein concentrations, aliquots of equal protein concentrations were made to perform citrate synthase (CS) and electron-transport-chain Complex-I (ETC-C-I) enzymatic activity assays.

For the CS assay, to enzymatically assess the reaction in the TCA Cycle that mediates the transition from acetyl coenzyme A (acetyl-coA) to citrate, tris buffer (pH 8.0) was used with 12.5 mmol/L acetyl coenzyme A. To catalyze the reaction from acetyl-coA to citrate via citrate synthase, 5 mmol/L oxaloacetic acid was administered to initiate the actions of citrate synthase and the subsequent absorbance rate of the reactionary byproduct 5,50-dithiobis–(2- nitrobenzoic acid) was measured every 15 s for 3 min to determine the rate of citrate synthase activity (48, 101). Assays were carried out on 10µg of protein per well, in triplicates in a 96 well-plate at a wavelength of 412 nm.

To assess ETC Complex-I activity, 2 mmol/L of NADH was used as substrate to be oxidized by Complex-I and 5 mmol/L of ubiquinone (Coenzyme-Q) was administered to facilitate the passing of electrons from Complex-I to Complex-III. The rate of reduction in absorbance in NADH fluorescence over 3-min was used as a surrogate for the rate of Complex-I's oxidation of NADH to NAD^+ and thus its maximal capacity of electron flux. To assess the test's specificity to Complex-I, 1 mmol/L of rotenone was administered. All assays used 30ug of protein per well, in triplicates in a 96 well-plate at a wavelength of 340nm.

Mitochondrial copy number was carried out as previously described (101). In brief, following DNA purification, DNA concentration and purity was assessed spectrophotometrically. I used primers for a mitochondrial gene (Cox1), and a nuclear gene (Ribosomal L13a) (Integrated DNA Technologies, Coralvile, IL) with Terra qPCR Direct TB Green (Takara Bio Inc., Mountain View, CA, USA) to perform Real-time PCR to measure

mitochondrial DNA to genomic DNA ratio. The forward and reverse primers of mitochondrial and nuclear genes used in this assay were as follows: mtDNA COX1-F 5'- AGA TGT AGA CAC CCG AGC CT -3', mtDNA COX1-R 5'- GGC TCA TAA TAT GGC GGG GG -3'; Ribosomal L13a-F 5'- TGC TCA CAG ACT CTC AGG -3', Ribosomal L13a-R 5'- AAG CCT TCC TCT TTC CAC AGG -3'. To calculate mitochondrial copy number, Pfaffl's model was utilized to assess the difference in threshold cycle between mitochondrial/nuclear gene pairs and expressed in arbitrary unit (103).

3.3.5 *Ex vivo* Contractile Experiments

Immediately after euthanasia, the extensor digitorum longus (EDL) was isolated via tying 5.0 silk sutures to the proximal/distal tendons, while doused in Ringer's solution (mM: 137 NaCl, 5 KCl, 1 NaH_2PO_4, 24 $NaHCO_3$, 2 $CaCl_2$, 1 $MgSO_4$, and 11 glucose containing 10 mg/l curare with a pH of 7.5). For *ex vivo* contractile measurements, the EDL was mounted between a force transducer (Aurora 300C) and motor in a custom bath filled with oxygenated Ringer's solution at 37°C with platinum electrodes straddling the muscle as previously described (104-106).

Muscle stimulation parameters were based on prior work (104-106). Briefly, after the EDL was mounted and allowed to stabilize for 5 min, optimal muscle length (L_o) and voltage were determined through a series of twitch contractions. Force and length from each contraction were acquired using a custom LabVIEW program. Raw contractile force was converted to Newtons (N) and expressed as specific force (N/cm^2) by normalizing to EDL physiological cross-sectional area (PCSA) (104-106).

A force frequency curve (300ms per contraction, 3 min rest between contractions; 10, 20, 30, 40, 50, 60, 70, 100, 110Hz) was constructed to identify maximal tetanic force (P_o). Following this, the frequency reflective of ~50% P_o (~25Hz) was used for 300ms sub-maximal fatiguing contractions at intervals similar to previous reports (107-109). The fatigue protocol started at 50% P_o and ended at 15% P_o. The first 10 contractions were separated by 10s each, followed by the next 10 contractions separated by 7s with all remaining contractions administered at 5s intervals until cessation (15% P_o). The number of contractions needed to reach 15% P_o from 50% P_o was defined as the fatigue index.

I validated that this submaximal fatigue protocol relied on mitochondria for contractile-energetic needs by inhibiting mitochondria (110). In a subset of mice (n=3), immediately after completion of force-frequency contractions, Ringer's solution was replaced with Ringer's containing 10mM of Oligomycin (an inhibitor of mitochondrial ATP synthase). Muscle was allowed to rest in this solution for 10 min (110). Maximal force and submaximal fatigue were compared between only-Ringer's and Ringer's with Oligomycin. After validating that the submaximal fatigue protocol indeed relied on mitochondria, I then performed submaximal fatigue-experiments on the EDL of Morning-SC^+ and Afternoon-SC^+ animals.

3.3.6 Immunohistochemistry

Gastrocnemius muscle was flash frozen in liquid nitrogen-cooled isopentane, stored at -80°C, and transferred to a -25°C cryostat for sectioning and subsequent immunohistochemical staining. In brief, muscle was allowed to equilibrate for 1 h in the cryostat before sectioning, embedded in a cryomold and subsequently flash-frozen in liquid nitrogen-cooled isopentane for ten seconds and allowed to re-equilibrate for 30 min in the cryostat (111). Muscle sections were

cut at 10 micrometers and following sectioning, slides were allowed to air dry for 1hr and were subsequently stored at -80^{o}C. Briefly, after thawing, slides were fixed in 4% PFA and incubated in 3% H_20_2 to block endogenous peroxidases and washed with PBS. A heat-induced epitope retrieval step (slides steamed for 30 min in a pressure cooker in a Citrate buffer bath) was performed and slides were permeabilized in 1% Triton-X thereafter. Following this, slides were blocked for 1h in 1% BSA mouse-on-mouse blocking buffer and incubated in primary antibody solution overnight. The following day, slides were incubated for 90 min in a biotinylated secondary antibody, washed, and incubated in secondary antibody solution for 1hr. Slides were then incubated in an amplification solution for 20 minutes, washed, mounted with Vectashield with DAPI, and cover-slipped. (112, 113). Primary antibodies used were anti-Pax7 [mouse IgG1, 1:100 DSHB, concentrate], anti-laminin (rabbit IgG, 1:500, Sigma-Aldrich, L9393]. Secondary antibody for Pax7 were goat anti- mouse IgG1 biotin-SP-conjugated (1:1,000, Jackson Immuno Research, 115-065-205), Streptavidin-horseradish peroxidase (SA-HRP) (1:500, Invitrogen, S-911), SuperBoost Tyramide reagent Alexa Fluor 594 (1:500, Thermo Fisher, B40957), while for laminin were Alexa Fluor 488 goat anti-rabbit IgG (H + L) (1:250, Invitrogen, A-11034). Slides were imaged at 20x and entire cross-section images were analyzed for myofiber cross-sectional area (CSA) and SC abundance. Cross-sectional area and SC quantification were carried out via blinded-automated analyses using MuscleJ (114).

3.3.7 Statistical Analysis

Comparisons of gene expression, mitochondrial respiration, and activity assays across time-of-day in either SC^{+} or SC^{-} groups were analyzed by a one-way ANOVA. Comparisons of *ex vivo* contractility between morning and afternoon groups were analyzed via unpaired t-tests.

All IHC was analyzed via unpaired t-tests. Specific statistical tests are indicated in figure legends. All statistical analysis were performed using Prism 9.0 (GraphPad, San Diego, CA). All data in the results are reported as means ± standard error of mean (SEM).

3.4 Results

3.4.1 Gene expression

Gene expression was carried out to assess muscle mRNA expression for specific clock, mitochondrial, and metabolic genes to expose any alterations according to time-of-day in the presence or following ablation of SCs. *Bmal1*, *CLOCK*, and *Per2* all exhibited significant time-of-day changes in gene expression while *Cry1* did not (Fig 1A-1D) ($p < 0.0001$), ($p < 0.001$), ($p < 0.01$), ($p < 0.05$). *Opa1* exhibited a trend toward significance ($p = 0.09$) in Morning-SC^+ animals (Fig 1E) and was significantly higher in Morning-SC^- animals compared to Afternoon-SC^- (Fig 1M) ($p < 0.05$). I report no significant findings in *Fis1*, *Pdk4*, *PGC1a* gene expression.

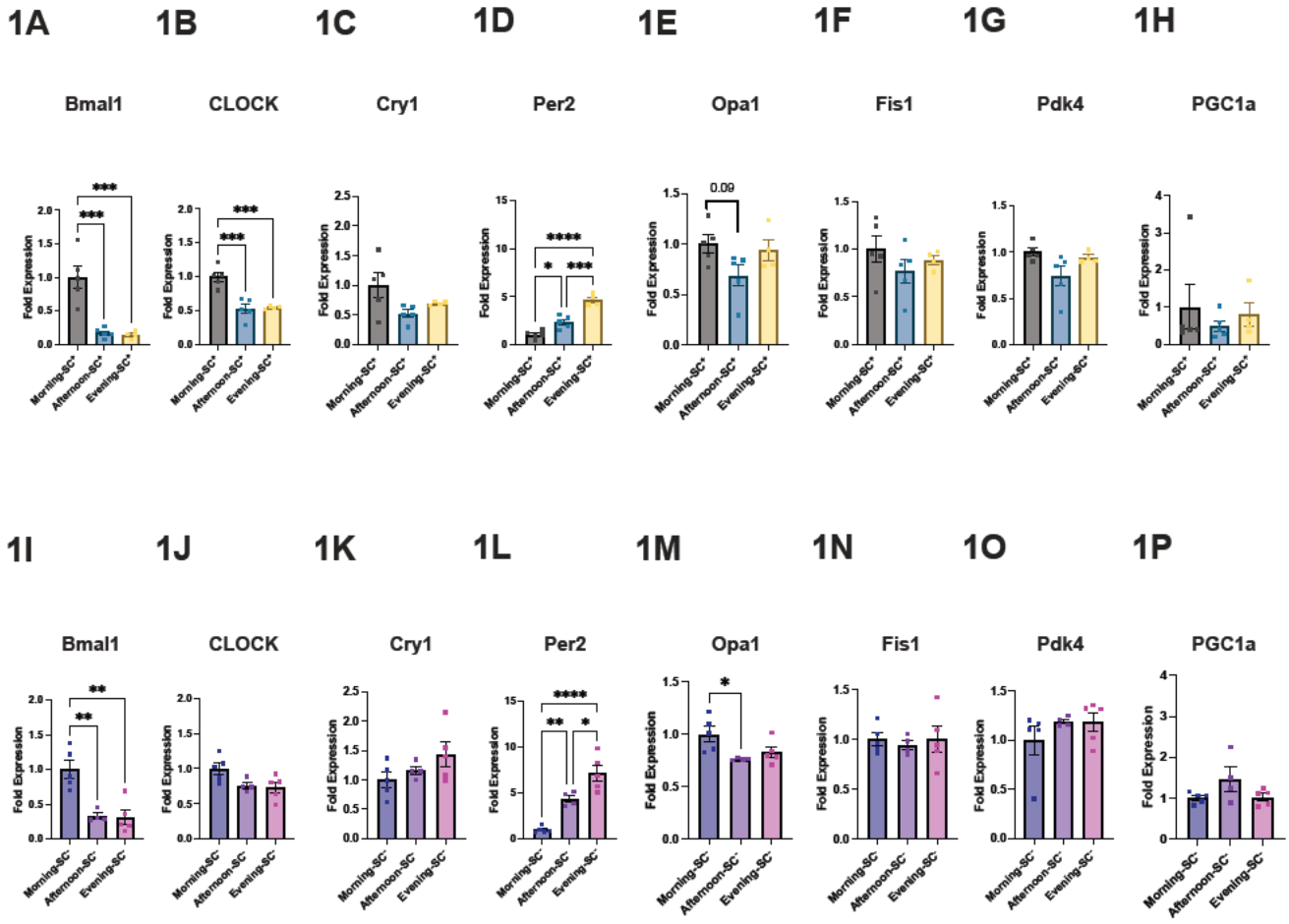

Figure 3.1: Gene expression of muscle molecular clock and mitochondrial genes across time-of-day and satellite cell groups

*1A-1D, 1I-IL) Muscle molecular clock gene expression (Bmal1, CLOCK, Per2, Cry1). 1E-1F, 1M-1N) Expression of mitochondrial fusion (Opa1) and fission (Fis1) genes. 1G-1H, 1O-1P) Expression of metabolic genes (Pdk4 and Pgc1a). All gene expression data is of the quadriceps. All data in units of fold-expression. All data shown as mean ± s.e.m. All groups analyzed via one-way ANOVAs (*p < 0.05), (***p < 0.005), (****p < 0.001) (n=4-5 per group).*

3.4.2 Mitochondrial respiration, activity assays and mitochondrial DNA copy number

No time-of-day differences were noted in mitochondrial respiration in the SOL or TA in the presence or absence of SCs (Fig 2A-2D, Table 1). In TA muscle, citrate synthase activity, a marker of mitochondrial content, did not vary by time-of-day in the presence or absence of SCs (Morning-SC^+: 81 ± 18; Afternoon-SC^+: 37 ± 14; Evening-SC^+: 47 ± 14; Morning-SC^-: 55 ± 16; Afternoon-SC^-: 55 ± 19; Evening-SC^-: 45 ± 15 nmol/min/mg protein) (Fig 3B, 3F). Maximal ETC Complex-I activity exhibited no statistical differences across time-of-day in either SC^+ or SC^- groups (ETC Complex-I activity: Morning-SC^+: 45 ± 8; Afternoon-SC^+: 61 ± 9; Evening-SC^+: 37 ± 14; Morning-SC^-: 52 ± 15; Afternoon-SC^-: 61 ± 12; Evening-SC^-: 58 ± 10 nmol/min/mg) ($p > 0.05$) (Fig 3C, 3G). Mitochondrial DNA copy number (mtDNA) demonstrated no differences across time-of-day in either SC^+ or SC^- groups (mtDNA Copy number: Morning-SC^+: 14 ± 4; Afternoon-SC^+: 11 ± 2; Evening-SC^+: 13 ± 4; Morning-SC^-: 23 ± 7; Afternoon-SC^-: 8 ± 2; Evening-SC^-: 10 ± 2, all units reported as mitochondrial copy number) (Fig 3D, 3H) ($p > 0.05$).

	Leak (Pyruvate, Malate)	**OxPhos; $P_{CI(PM)}$ (ADP)**	**OxPhos; P_{CI} (Glutamate)**	**OxPhos; P_{CI+II} (Succinate)**	**ETC; E_{CI+II} (CCCP)**	**ETC; E_{CII} (Rotenone)**	**ROX; (Antimycin- A)**
Soleus Morning-SC^+	16.6 ± 1.8	103.6 ± 8.9	120.4 ± 10.2	173.1 ± 13.3	168.3 ± 12.2	87.8 ± 3.8	8.2 ± 0.9
Soleus Afternoon-SC^+	16.3 ± 1.4	106.2 ± 14.1	121.1 ± 16.0	185.1 ± 16.4	188.3 ± 16.1	95.7 ± 7.2	8.1 ± 0.6
Soleus Evening-SC^+	12.3 ± 2.9	108.4 ± 4.2	116.1 ± 7.2	147.4 ± 12.3	140.2 ± 14.2	69.7 ± 8.3	8.1 ± 0.9

Soleus Morning-SC$^-$	16.0 ± 1.0	102.2 ± 7.5	110.2 ± 7.4	173.0 ± 11.5	185.2 ± 19.0	103.7 ± 8.7	8.1 ± 1.0
Soleus Afternoon-SC$^-$	16.3 ± 2.0	119.1 ± 9.8	131.2 ± 11.8	183.3 ± 9.5	186.6 ± 10.0	100.9 ± 9.9	9.4 ± 1.1
Soleus Evening-SC$^-$	15.8 ± 1.5	111.3 ± 4.3	121.9 ± 5.5	174.3 ± 14.0	171.9 ± 15.9	88.6 ± 9.3	8.3 ± 0.6
TA Morning-SC$^+$	11.4 ± 1.7	71.0 ± 9.3	77.2 ± 6.4	134.6 ± 9.2	139.2 ± 9.3	69.7 ± 6.8	4.9 ± 0.3
TA Afternoon-SC$^+$	6.9 ± 0.6	55.7 ± 3.1	67.2 ± 2.8	101.5 ± 4.8	110.6 ± 7.9	60.6 ± 2.7	2.9 ± 1.5
TA Evening-SC$^+$	6.8 ± 1.2	68.4 ± 9.2	80.3 ± 11.8	117.3 ± 16.3	126.3 ± 17.1	68.5 ± 7.3	3.0 ± 0.7
TA Morning-SC$^-$	9.2 ± 0.6	67.7 ± 2.7	81.4 ± 4.4	126.5 ± 8.0	136.3 ± 12.0	68.1 ± 5.0	3.6 ± 0.4
TA Afternoon-SC$^-$	7.0 ± 1.2	60.2 ± 7.1	77.9 ± 7.0	113.1 ± 10.8	119.2 ± 13.6	65.8 ± 5.0	3.7 ± 0.5
TA Evening-SC$^-$	6.7 ± 1.4	56.6 ± 3.9	78.9 ± 5.8	110.1 ± 7.0	130.5 ± 3.6	63.0 ± 4.9	3.7 ± 1.5

3.

Table 3.1: All mitochondrial respiration data

T1) All mitochondrial oxygen consumption values across all states, muscles, groups, and timepoints (pmol O_2/s/mg). All data shown as mean ± s.e.m.

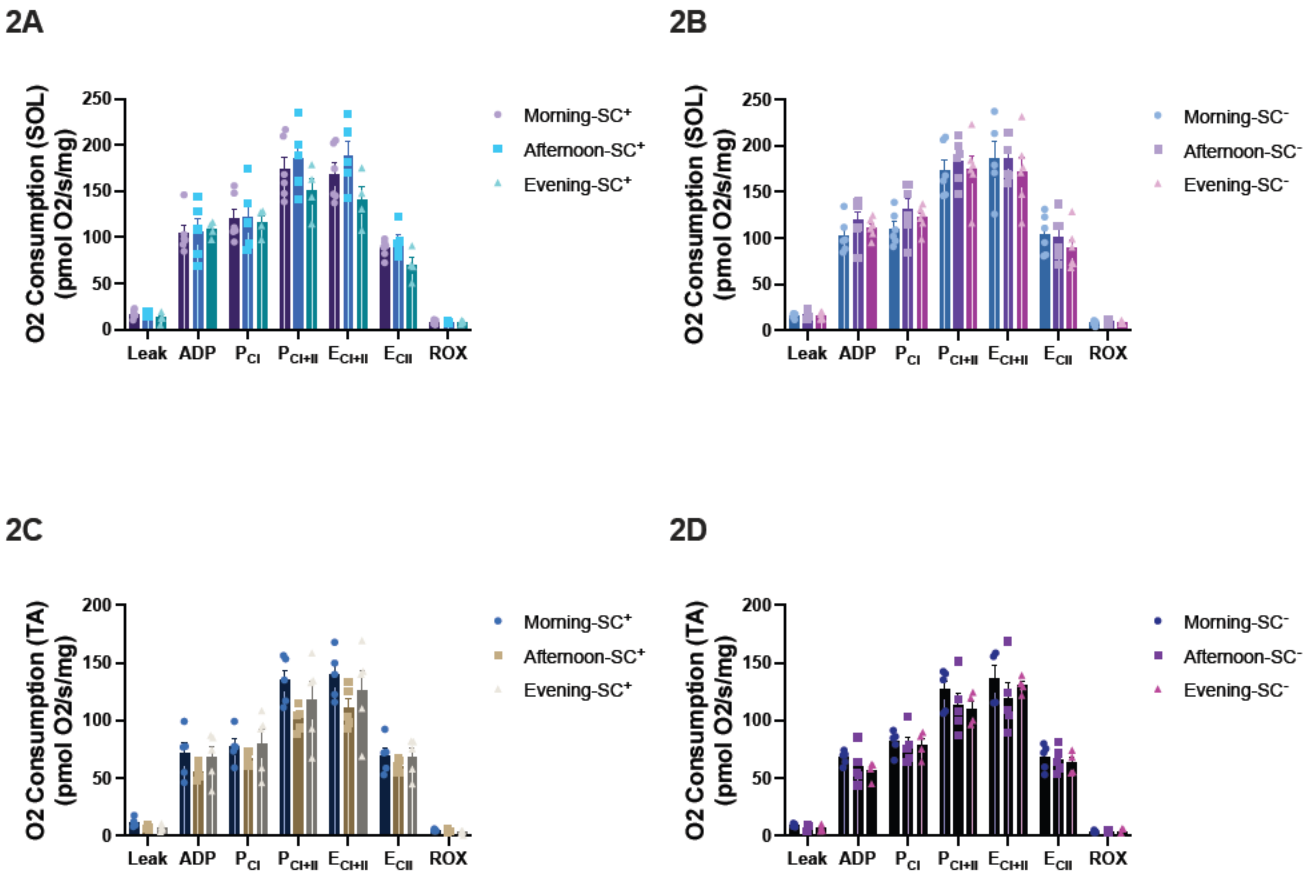

Figure 3.2: Mitochondrial respiration in the soleus and TA across time-of-day in the presence and absence of SCs

A-B) Mitochondrial respiration across all states of the soleus in A) SC^+ and B) SC^- animals. C-D) Mitochondrial respiration across all states of the TA in A) SC^+ and B) SC^- animals. All groups compared via one-way ANVOA (n=4-7 per group).

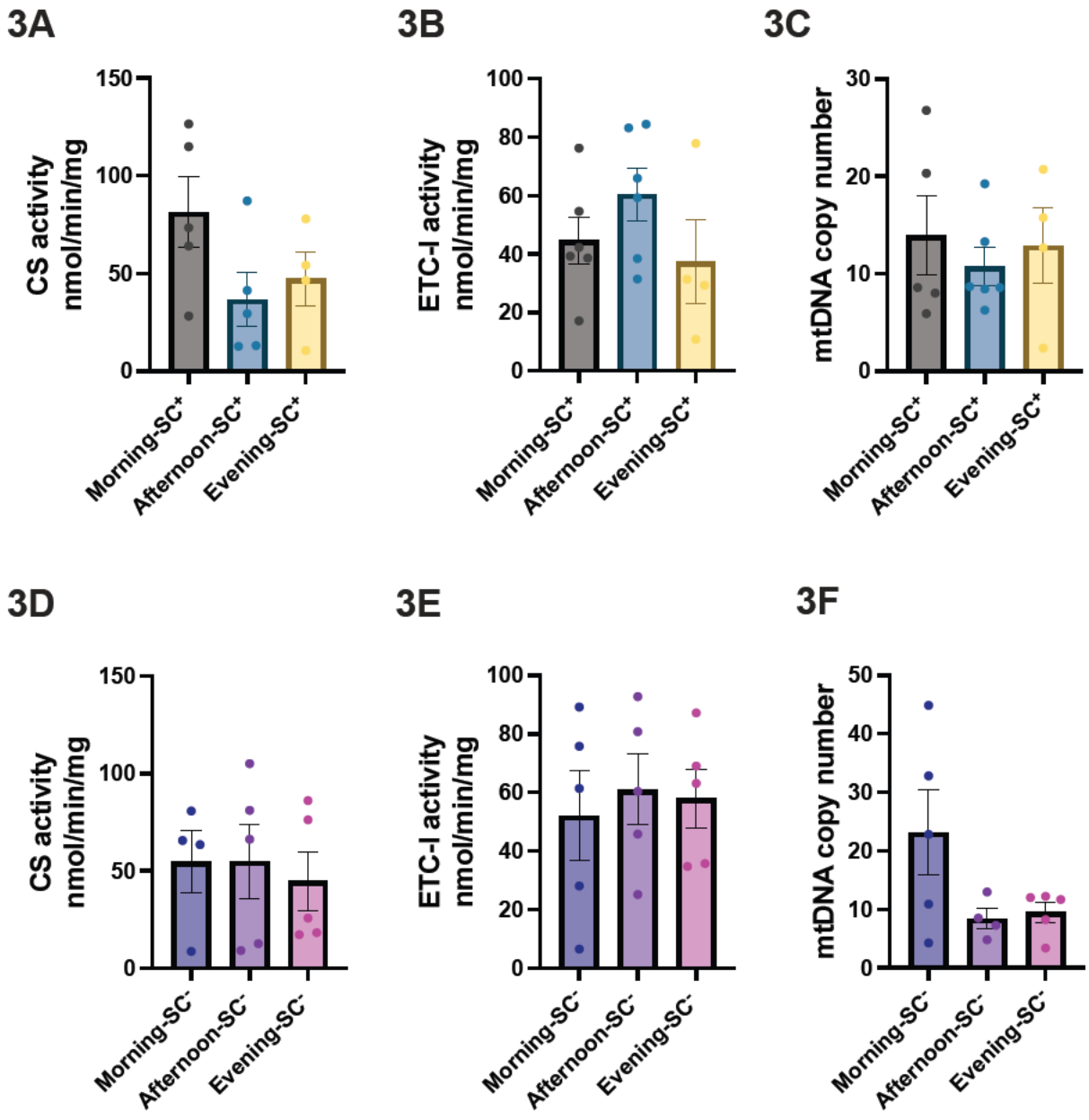

Figure 3.3: Maximal mitochondrial oxidative phosphorylation, citrate synthase activity, Complex-I, and mitochondrial DNA copy number across time-of-day and satellite cell groups in glycolytic muscle

A) Maximal oxidative phosphorylation (pmol O_2/s/mg) B) Citrate synthase activity (nmol/min/mg) C) State 3 complex-I (nmol/min/mg) and D) Mitochondrial DNA copy number

across time of day in either $SC^{+/-}$ groups All data shown as mean ± s.e.m. Groups were compared via one-way ANOVAs (n=4-5 per group).

3.4.3 *Ex vivo* submaximal contractile fatigue

Before assessing whether time-of-day differences in mitochondrial respiration impacted submaximal contractile fatigue (reliant on mitochondrial-energy), I first validated that the fatigue protocol indeed relied on mitochondria. Force-frequency curves were generated on untreated mice to identify the frequency corresponding to of 50% P_o (Fig 4A). Maximal tetanic force measured immediately before and after 10 min of incubation with Oligomycin, an inhibitor of mitochondrial ATP synthase, revealed that force declined by ~13% (87% P_o) ($p < 0.01$). During the fatiguing protocol (representative trace in Fig 4B) when mitochondria were inhibited with Oligomycin, muscle fatigued ~50% more rapidly compared to control animals (Ringers: 39 ± 1 contractions; Ringers+Oligomycin: 19 ± 2 contractions, $p < 0.005$) (Fig 4C).

Next, using the novel protocol validated above (Fig 4), I assessed whether differences in mitochondrial respiration impacted submaximal contractile fatigue profiles. Prior to submaximal fatiguing contractions, I measured baseline tetanic specific force at 100Hz and 25Hz in morning and afternoon animals to assess if any baseline time-of-day differences in force existed before assessing rates of contractile fatigue. Maximal tetanic specific force at 100Hz was similar between Morning-SC^+ and Afternoon-SC^+ animals (Morning-SC^+: 25 ± 2; Afternoon-SC^+: 25 ± 4 N/cm^2) (Fig 5A). Specific force at 25Hz prior to fatigue trials was also similarly ~50% P_o for both Morning-SC^+ and Afternoon-SC^+ mice (Morning-SC^+: 13 ± 1; Afternoon-SC^+: 12 ± 3 N/cm^2) (Fig 5A). However, during fatiguing contractions, Morning-SC^+ animals were more

fatigue-resistant as they required ~35% more contractions to fatigue compared to Afternoon-SC^{+} animals (Morning-SC^{+}: 54 ± 5; Afternoon-SC^{+}: 36 ± 6 contractions) ($p < 0.05$) (Fig 5B).

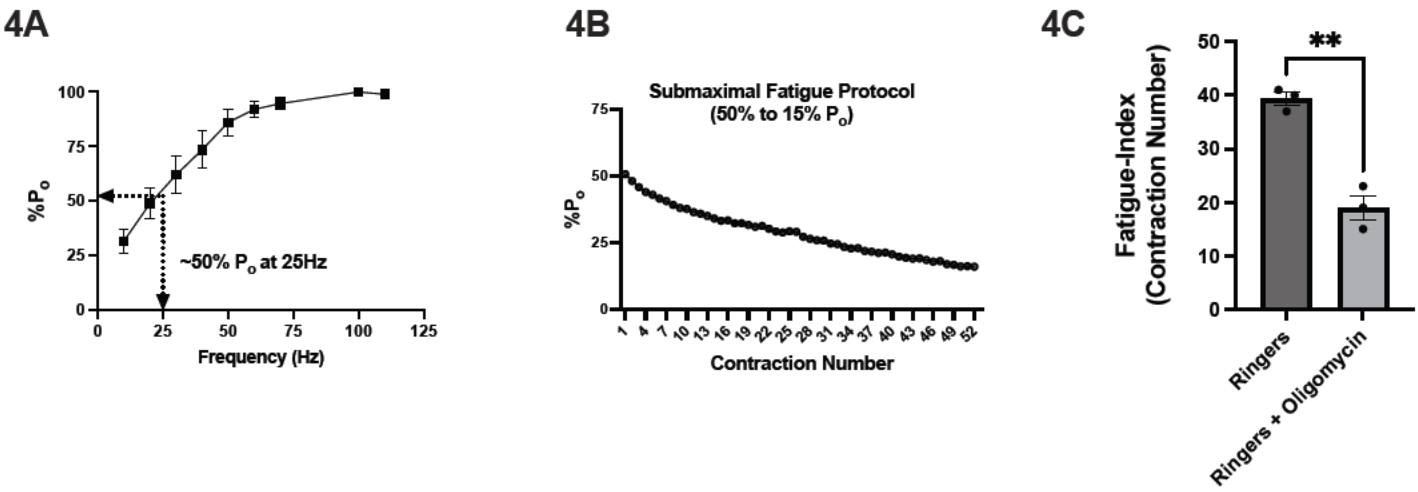

Figure 3.4: Validation of a novel contractile submaximal-fatigue protocol reliant on mitochondria in glycolytic muscle

*A) Force frequency stimulation curve showing maximal tetanic specific force (P_o). The lines indicate 25Hz frequency stimulation resulted in 50% P_o. B) Representative figure showing ex vivo fatiguing protocol from 50% P_o to 15% P_o. C) Comparison of number of contractions until fatigue between control (Ringers) versus Ringers+Oligomycin incubated muscles. Fatigue-index indicates number of contractions until fatigue (defined as 50% P_o to 15% P_o). All data shown as mean ± s.e.m. EDL muscles were used for these experiments. All groups analyzed using unpaired t-tests (**p<0.01), (***p<0.001) (n=3 per group).*

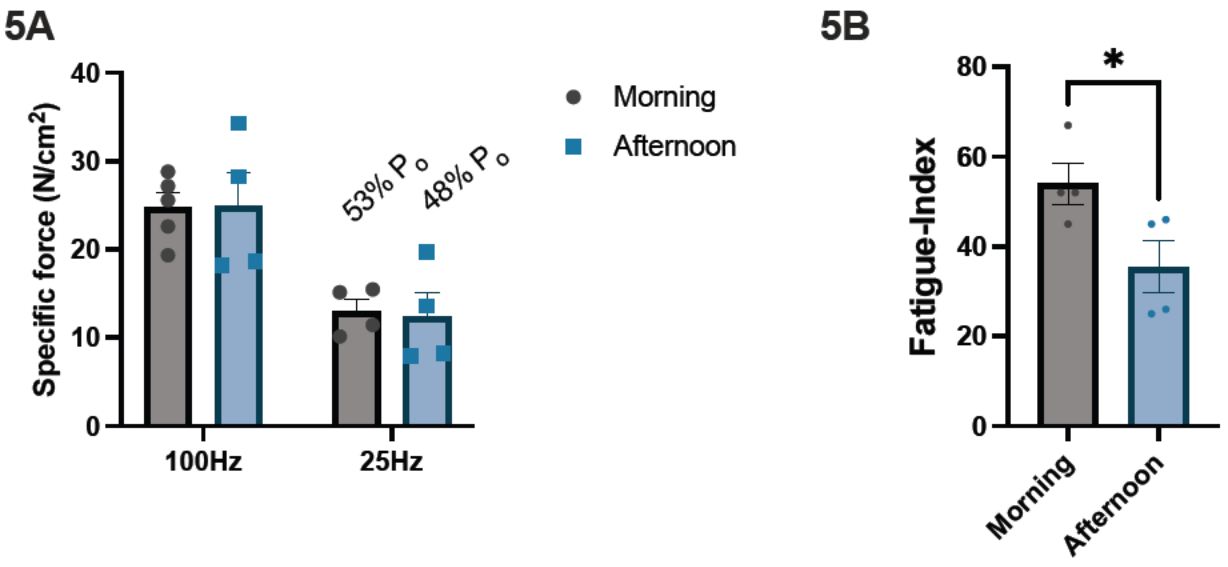

Figure 3.5: Fatigue-resistance profiles of Morning-SC$^+$ and Afternoon-SC$^+$ animals in glycolytic muscle

*A) Specific force at 100Hz and 25Hz in Morning-SC$^+$ and Afternoon-SC$^+$ animals B) Fatigue index in Morning-SC$^+$ and Afternoon-SC$^+$ animals. EDL muscles were used for these experiments. Superscript in 5A denotes specific force at 25Hz as percent P_o. All data shown as mean ±s.e.m. All groups analyzed using unpaired t-tests (*p<0.05) (n=3-5 per group).*

3.4.4 Immunohistochemistry

Tamoxifen treatment induced an ~80% reduction in SCs (Pax7$^+$/DAPI+ cells (SC$^+$: 7 ± 2; SC$^-$: 1 ± 2 SCs/100fibers, $p < 0.05$) (Fig 6A, 6B). Average myofiber area was similar between SC$^+$ and SC$^-$ groups (SC$^+$: 1954 ± 155; SC$^-$: 2218 ± 288 μm^2) (average number of fibers used for calculations: SC$^+$: 2693 ± 185; SC$^-$: 3424 ± 918) ($p > 0.05$) (Fig 6C).

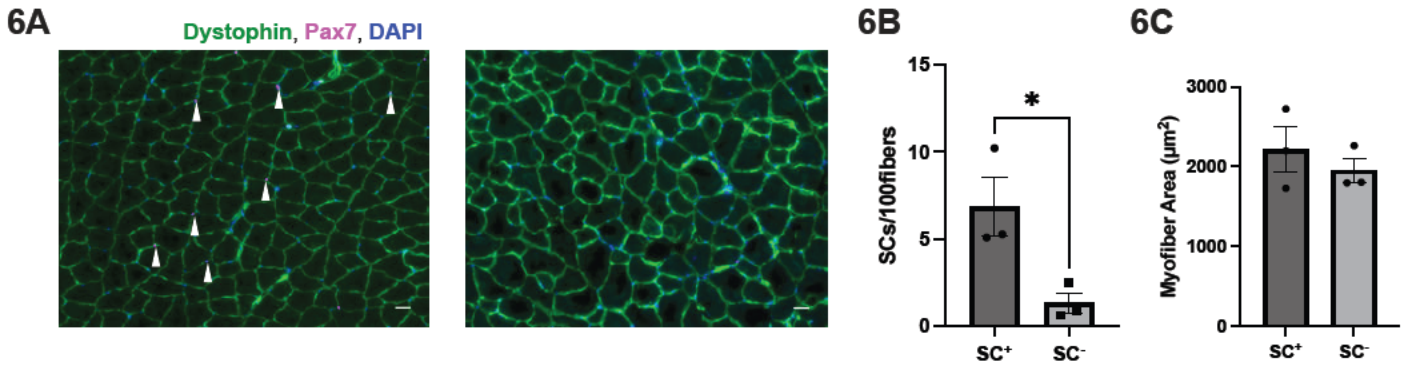

Figure 3.6: Satellite cell ablation and myofiber area

A) Representative images of muscle cross-sections labeled for laminin and Pax7 showing the presence of SCs and their absence (right) (scalebar set to 100 µm). B) Ablation of $Pax7^{+}$ satellite cells (SC) following tamoxifen administration. C) Myofiber area in SC^{+} versus SC^{-} animals (μm^2). All IHC was carried out on the gastrocnemius and auto quantified using MuscleJ. All data shown as mean ± s.e.m. All groups analyzed using unpaired t-tests ($p<0.05$) (n=3 per group).*

3.5 Discussion

In this study, I found that SCs are not a factor that influence mitochondrial respiration according to time-of-day. At a peak and trough in *Bmal1* and *CLOCK* molecular clock gene expression, I measured mitochondrial-dependent submaximal fatigue and found that glycolytic muscle (EDL) was ~35% more fatigue resistant in the morning versus afternoon. Collectively, SCs do not influence diurnal mitochondrial function and therefore time-of-day differences noted in submaximal fatigue are unlikely due to time-of-day regulations (SC, muscle, or otherwise) on mitochondrial respiration.

As molecular clocks reside in SCs (17) and SC ablation has been shown to negatively impact endurance exercise capacity heavily reliant on mitochondria (49, 50), it is unknown whether SCs exert diurnal influence over mitochondrial function. Several metabolic, contractile, and mitochondrial genes related to exercise-performance within SCs display an oscillatory expression profile (17) suggesting SCs exert time-of-day dependent downstream regulations on exercise performance. However, direct assessment of the muscle physiology pertinent to exercise (i.e. force production, metabolism) by time-of-day in the presence/absence of SCs is lacking. I have recently reported SC ablation alters maximum eccentric specific force according to time-of-day (91) adding support to the view that the diurnal SC transcriptome (17) exerts effects on the corresponding muscle physiology at the functional level as well. Although not specific to time-of-day, a recent study observed that SC ablation negatively impacted endurance exercise performance while mitochondrial content and muscle size were preserved (49). Given the results show no effects of SC ablation on respiration and markers of mitochondrial fusion/fission (*Fis1, Opa1*) were similar, the decrement in performance noted in SC absence from past studies (49, 50) is likely not due to an impairment in mitochondrial respiration but, perhaps altered muscle fatiguability.

Although in this study I show that mitochondrial function is unaffected by the presence/absence of SCs at different times of day, mitochondrial-dependent submaximal fatigue did exhibit variation with time-of-day. These findings indicate time-of-day regulations (SC, muscle, or otherwise) on the contractile kinetics of submaximal fatigue rather than direct influence on mitochondria may underpin differences noted in this work. In this regard, I have previously shown that SCs regulate force production via modulation of calcium availability specifically in the morning and thus a similar mechanism may be at play in this work as well

(91). In line with this, enhanced fatigue resistance in the morning versus afternoon coincided with peak *Bmal1* and *CLOCK* gene expression which are known regulators of calcium handling genes critical to E-C coupling (26). Interestingly, while *submaximal* fatigue differed by time-of-day, *maximal* force production did not differ by time-of-day potentially indicating different nodes of metabolism are subject to divergent time-of-day regulations. Supportive of this, participants exercising for 60 minutes at 50% of their maximal power output in the morning vs evening displayed no differences in blood lactate accumulation (surrogate of glycolytic flux) whereas their submaximal %VO2 sustained during the prolonged exercise trial indeed differed by time-of-day (25). In these contexts, the findings of enhanced submaximal fatigue resistance in the morning agree with the results of exercise studies that found both humans and mice display markers of enhanced fatigue-resistance during endurance-exercise in the morning (25, 38).

Interestingly, a recent study reported that *ex vivo* fatigue induced by maximal tetanic contractions was not shown to vary with time-of-day (115). However, as mentioned previously, the metabolism that underpins *maximal* versus *submaximal* fatigue are distinct from each other (28, 33) and evidence has shown these nodes of metabolism may be under separate time-of-day regulations (25). In this regard, a previous report showed that while inhibiting mitochondria reduced force-production maximally (also reported in this work here to be a ~13% reduction), rates of fatigue induced my maximal contractions in the soleus and EDL were similar (116). This suggests mitochondria may play a permissible role in *ex vivo* whole muscle fatigue induced by *maximal* contractions and is therefore why I sought to use a novel submaximal fatigue protocol that relied on mitochondrial-derived energy. In this context, the mechanism by which mitochondrial dependent submaximal fatigue differs by time-of-day may lie at the intersect of mitochondrial energy deliverance to contractile units during submaximal contractions inductive

of fatigue. This is partially supported by the fact that I observe time-of-day differences in mitochondrial-dependent contractile fatigue however, in mitochondrial respiration experiments where the ATP produced is not utilized to produce contractile forces, no differences are seen.

3.6 Conclusion

In conclusion, I report SC presence/absence does not affect time-of-day mitochondrial respiration. In line with peak, trough *Bmal1* and *CLOCK* gene expression, mitochondrial-dependent submaximal fatigue showed ~35% greater fatigue-resistance in the morning versus afternoon. Collectively, SCs are not a factor that influence time-of-day mitochondrial function and therefore time-of-day differences in submaximal fatigue I observe may not be due to SC time-of-day regulations on mitochondrial respiration.

Limitations

This study has several technical limitations I would like to address to provide clarity and discuss potential confounds. The transgenic mouse model (Pax7TDA) that inducibly depletes satellite cells relies on the Cre-lox system which is accomplished via oral gavage of tamoxifen. However, tamoxifen may have unintended metabolic effects on various organ-systems and therefore tamoxifen treatment is always followed up by a washout period to avoid any unintended effects of tamoxifen. Therefore, in-line with past works, I performed all experimentation following a minimum washout period of two weeks (average washout period 26.4 days ± 0.97 days SEM) (49, 50, 64, 91, 94, 95, 98, 117-119). Additionally, all experiments were carried out after “lights-on” and therefore, generalizability of these findings to the active phase may be limited. Lastly,

animals fasting for the 8-12 hours were not monitored nor were any physical activity measures monitored at different times of day perhaps limiting my interpretations of the findings.

Acknowledgements

This work was supported, in part, by a Novo Nordisk Foundation Challenge Grant (NNF14OC0011493) to J.A.H, National Institutes of Health grant HD094602 to S.D. This work was supported in part by Research Career Scientist Award Number IK6 RX003351 from the United States (U.S.) Department of Veterans Affairs Rehabilitation R&D (Rehab RD) Service. Graphical abstract was created with Biorender.com.

I thank Michael Hogan and Leonardo Nogueira (University of California, San Diego) for their insights and help developing a submaximal contractile-fatigue protocol reliant on mitochondria for energy. I also thank Gretchen Meyer (Washington University in St. Louis) for sharing her Pax7 immunohistochemistry protocol. I thank Leonidas Karagounis for helpful discussions as well.

Data Availability Statement

All data used within the results and to create figures are included in the material of this manuscript. Additional analysis and files can be provided upon request.

Competing Interests

The authors declare no competing interests.

Author Contributions

RK, SD, OLK, JAH contributed to conceptualization and preparation of this manuscript. RK performed all physiology and IHC experimentation. GM performed activity assay experiments. OLK and FD performed gene expression experiments. RLL contributed in helping develop the novel submaximal contractile fatigue protocol used in this study. RK, SD, OLK, JAH, RLL edited and revised the manuscript. All authors approved of its content.

Chapter 4, Linking Chapter: Study 1 & Study 2

The results from study-1 (described in chapter 3) revealed that SCs are not a factor that influence mitochondrial respiration according to time-of-day. At a peak and trough in *Bmal1* and *CLOCK* molecular clock gene expression, I measured mitochondrial-dependent submaximal fatigue and found that glycolytic muscle (EDL) was ~35% more fatigue resistant in the morning versus afternoon. Given the evidence provided in study-1 (chapter-3), SCs do not influence diurnal mitochondrial function and therefore time-of-day differences noted in submaximal fatigue are unlikely due to SC time-of-day regulations on mitochondrial respiration.

The findings from this first study may suggest an underappreciated role SCs play in influencing skeletal muscle contractility by time-of-day however, cannot provide direct evidence to demonstrate that SCs regulate force-production by time-of-day. Therefore, in the next study (described in chapter-5), the influence of SCs on force-production was directly evaluated at different times of the day. For consistency and in line with the patterns of diurnal contractility observed in morning versus afternoon groups in study-1, the experiments in study-2 were conducted at these same timepoints. Previous studies have reported that human isometric torque varies with the time-of-day exhibiting a trough in the morning compared to a peak observed in the afternoon (8). This fluctuation in muscle isometric torque has been attributed, in part, to the muscle molecular clock as changes in *Bmal1* expression mirror these strength oscillations (9). Additionally, experiments utilizing molecular clock KO animal models report alterations in *ex vivo* force production strongly suggesting that molecular clocks have a regulatory role in force contractility (13, 14, 52). However, whether the SC-molecular clock exerts an influence on force-production is largely still unknown. Accordingly, the experiments described in study-2 assessed contractile function in the presence and absence of SCs in the morning and afternoon.

Chapter 5: Study-2

Publication Statement:

The content of Chapter 5 is from an original research article published on the date of 1 April 2024 in *American Journal of Physiology-Cell Physiology*.

Kahn, R. E., Lieber, R. L., Dinnunhan, F., Lacham-Kaplan, O., Dayanidhi, S., & Hawley, J. A. (2024). Satellite cells differentially regulate *ex vivo* force production according to time-of-day. *American Journal of Physiology-Cell Physiology* https://doi.org/10.1152/ajpcell.00157.2024

Time-of-day effects on *ex vivo* muscle contractility following short-term satellite cell ablation

Ryan E. Kahn[1,2], Richard L. Lieber[2,3,4], Guadalupe Meza[2], Fawzan Dinnunhan, Orly Lacham-Kaplan[1], Sudarshan Dayanidhi[2,3*], John A. Hawley[1*]

[1]Exercise and Nutrition Research Program, The Mary MacKillop Institute for Health Research, Australian Catholic University, Melbourne, Australia

[2]Shirley Ryan AbilityLab, Chicago, IL, USA

[3]Feinberg School of Medicine, Northwestern University, Chicago, IL, USA

[4]Hines VA Medical Center, Maywood, IL, USA

Running Title: Time-of-day variation in force production in SC presence versus absence

*Corresponding Authors: SD and JAH

E-mail: sdayanidhi@sralab.org

john.hawley@acu.edu.au

Supplemental Material Available at

URL: https://figshare.com/s/0943bf2cc5a9a69e012e

DOI: https://doi.org/10.6084/m9.figshare.25514272

5.1 Abstract

Muscle isometric torque fluctuates according to time-of-day with such variation owed to the influence of circadian molecular clock genes. Satellite cells (SC), the muscle stem cell population, also express molecular clock genes with several contractile related genes oscillating in a rythmic pattern. Currently, limited evidence exists regarding the relationship between SCs and contractility, although long-term SC ablation alters muscle contractile function. Whether there are acute alterations in contractility following SC ablation and with respect to the time-of-day is unknown. I investigated whether short-term SC ablation affected contractile function at two times of day, and whether any such alterations lead to different extents of eccentric contraction-induced injury. Utilizing an established mouse model to deplete SCs, I characterized muscle clock gene expression and *ex vivo* contractility at two times-of-day (morning 0700 h and afternoon, 1500 h). Morning-SC^{+} animals demonstrated ~25-30% reductions in tetanic/eccentric specific forces and, after eccentric injury, exhibited ~30% less force-loss and ~50% less dystrophin^{negative} fibers *versus* SC^{-} counterparts; no differences were noted between Afternoon groups (Morning-SC^{+}: -5.63 ± 0.61, Morning-SC^{-}: -7.93 ± 0.61; N/cm^2; $p < 0.05$) (Morning-SC^{+}: 32 ± 2.1, Morning-SC^{-}: 64 ± 10.2; dystrophin^{negative} fibers; $p < 0.05$). As Ca^{++} kinetics underpin force-generation, I also evaluated caffeine-induced contracture-force as an indirect marker of Ca^{++} availability and found similar force reductions in Morning-SC^{+} vs SC^{-} mice. I conclude that force-production is reduced in the presence of SCs in the morning but not the afternoon, suggesting that SCs may have a time-of-day influence over contractile-function.

Keywords: Muscle stem cells, eccentric contractions, contractility, molecular clocks, contractile injury

News and Noteworthy

Muscle isometric torque fluctuates according to time-of-day with such variation owed to molecular clock regulation. Satellite cells have recently demonstrated diurnal characteristics related to muscle physiology. In this work, I found that force-production was reduced in the presence versus absence of SCs in the morning but, not afternoon. Morning-SC+ animals, producing lower force, sustained lesser degrees of injury versus SC- counterparts. One potential mechanism underpinning lower forces produced appears to be lower calcium availability.

5. 2 Introduction

Skeletal muscle comprises 40-50% of body mass in mammals and plays vital roles in contractile function and locomotion (30, 120, 121). Recent evidence demonstrates that muscles have circadian molecular clocks residing within cell nuclei, whose gene expression oscillates daily (26). The rhythmicity of molecular clocks regulates numerous processes in muscle such that numerous physiological and metabolic events are time-of-day dependent (7, 23, 24). In this regard, muscle isometric torque differs with respect to time-of-day (8) with the mechanism underpinning this variation linked to the molecular clock. Alterations to force production in several clock-gene knockout mouse models provides further support for time-of-day regulations (13, 14, 52). Physiologically, different levels of maximal force induce varying degrees of injury (67, 68), and consequently, diurnal changes in force-production may also lead to varying degrees of injury and repair according to time-of-day. Recent evidence in support of this contention is that the extent of muscle injury and repair following major injury (cardiotoxin) varies according to time-of-day (85).

Satellite cells (SC), resident muscle stem cells responsible for muscle repair, also house molecular clocks that rhythmically expresses clock-genes over 24 h (17). Further characterization of the quiescent SC transcriptome demonstrates several contractile related genes are rhythmically expressed (17). However, it is unclear whether rhythmically expressed SC-specific clock genes and contractile related genes impact muscle contractile function (64, 97). Alterations in *ex vivo* whole muscle contractile function have been reported after long-term SC-ablation in an overload-model of hypertrophy (64), although such alterations may be secondary to changes in muscle morphology (i.e., increased fibrosis) rather than being directly attributable

to the absence of SCs. Whether SCs directly affect contractile function in the short-term remains unknown.

Utilizing an established mouse model to deplete SCs, I investigated whether short-term SC ablation affects muscle force production at two different times of day (0700h Morning-SC^{+}, -SC^{-} and 1500h Afternoon-SC^{+}, -SC^{-}), and, if such differences exist, whether this alters contractile injury-induced force-loss and loss of cytoskeletal protein (dystrophin).

5.3 Methods:

5.3.1 Animals

$Pax7^{CreERT2/+}$; $Rosa26^{DTA/+}$ mice (n=24), ages 4-6 months of mixed sex (Jackson Laboratories, Bar Harbor, ME, stock numbers 017763 and 010527, respectively) were used for these experiments (97, 98, 122, 123). Mice had *ad libitum* access to food/water and were housed on a 14:10 light-dark cycle (lights-on at 0600h). Morning experiments were undertaken at 0700h (1 h into the light-phase) and afternoon experiments carried out at 1500h (9 h into the light-phase). Inducible depletion of SCs was accomplished through Cre-Lox mediated $Pax7^{+}$ cell ablation via five consecutive days of oral gavage of either tamoxifen (2mg/ml) or vehicle (peanut oil) followed by a 10-day washout period, similar to prior studies (119). Experiments were performed immediately after euthanasia at each timepoint.

5.3.2 Muscle Isolation & Experimental Apparatus

Immediately after euthanasia, 5.0 silk sutures were tied to proximal and distal EDL tendons, dissected and mounted between a force transducer (Aurora 300C, Aurora Scientific, Ontario, Canada) and length motor in a custom bath of Ringer's solution (137mM NaCl, 5mM

KCl, 1mM NaH_2PO_4, 24mM $NaHCO_3$, 2mM $CaCl_2$, 1mM $MgSO_4$, and 11 mM glucose containing 10 mg/L curare, pH 7.5) at 37°C with platinum electrodes straddling the muscle as previously described (104, 105, 124). Force, length, and time records were recorded on both an oscilloscope and a custom LabVIEW program.

5.3.3 Isometric tetanic and caffeine specific forces

All contractile forces were normalized to physiological cross-sectional area (PCSA). A total of three maximal isometric tetanic contractions were administered at 100Hz, 400ms duration, 9-12V, and the maximal value of the three was used similar to previous protocols (104, 105, 124). Each contraction was separated by 3 min rest. Caffeine contracture force was induced to estimate maximal unstimulated Ca^{++} induced force via caffeine acting directly on the sarcoplasmic reticulum (SR) RyR1 receptor (57, 59, 125). Muscle tetanic tension was evaluated first in Ringer's and after 3 min, replaced with Ringer's containing 50mM caffeine. For caffeine contracture, the muscle was not stimulated but tension was allowed to rise to a plateau over a 30-min time period until it peaked. Peak caffeine contracture force was recorded and subsequently expressed in units of specific force (N/cm^2).

5.3.4 Eccentric Contraction

To evaluate maximal eccentric specific force, muscle was stimulated isometrically for 200 ms, then lengthened by 15% of L_f at a velocity of 2 L_f/s. Muscle was stimulated for a total of 400 ms. A single bout of 10 injurious eccentric contractions was performed with 3 min rest between contractions to avoid the confounding effects of fatigue (105, 124). A maximum isometric tetanic contraction was administered 3 min prior and 5 min following the ten eccentric

contractions to quantify the extent of isometric force-loss, widely used as an indirect marker of injury (126-128). Following the post-eccentric tetanic contraction, muscle rested at L_o for 30 minutes before being dismounted, snap-frozen, and stored in -80 degrees Celsius (total time from first eccentric contraction to dismounting/snap-freezing ~65 minutes). Linear regression was used to assess the relationship between maximum eccentric force and isometric tetanic force-loss following injury.

5.3.5 Gene Expression

Genes of interest were analyzed using the QX200 AutoDG Droplet Digital PCR system (Bio-Rad). Muscle RNA extraction was performed as previously described (129, 130) and was analyzed for quality using Nanodrop-2000 and quantified using Qubit. An absorbance ratio of <1.8 was used to qualify the RNA and the quantification was used to equilibrate the samples to 1 ng/µL prior to ddPCR.

A total of 5 µL of the equilibrated sample was aliquoted into the 96-well ddPCR plate along with 17 µL of a master mix (One-Step RT-ddPCR advanced kit for probes). The master mix also consisted of florescence labelled ddPCR primers (Bio-Rad) for the housekeeping gene Glyceraldehyde 3-phosphate dehydrogenase (*Gapdh*) and the gene of interest *(BMAL1, CLOCK, CRY1, PER2).* The plate was then placed into the AutoDG to generate up to 20,000 droplets per well followed by reverse transcription. The plate was read using the QX200 droplet reader to visualize exact gene copy numbers per µL of relative samples.

5.3.6 Immunohistochemistry (IHC)

Flash frozen EDL muscles, stored at -80ºC, were transferred to a -25 ºC cryostat to section for immunohistochemical staining of SCs and myofiber perimeter (described in detail in supplemental methods).

5.3.7 Statistical analyses

Individual groups were analyzed using unpaired t-tests. Simple linear regression was used to analyze the relationship between tetanic and caffeine specific forces, as well as eccentric force and isometric tetanic force-loss. Gene expression of muscle molecular clock genes were analyzed by two-way ANOVA for main effects of time-of-day and treatment. Specific statistical tests are indicated throughout the results as well as in figure legends. All statistical analysis were performed using Prism 9.0 (GraphPad, San Diego, CA). All data in the results are reported as means ± standard error of mean (SEM). Significance level (α) was set to 0.05 for all parametric tests.

5.4 Results

5.4.1 Gene Expression

The pattern of muscle clock gene expression from morning to afternoon was similar in SC^+ animals compared to SC^-. A main effect of time-of-day was observed in Cry1 and Per2 genes ($p < 0.05$) (Fig 5.1C-D). Muscle clock gene expression was unaltered by SC ablation at either timepoint compared to SC^+ animals (Fig 5.1A-D).

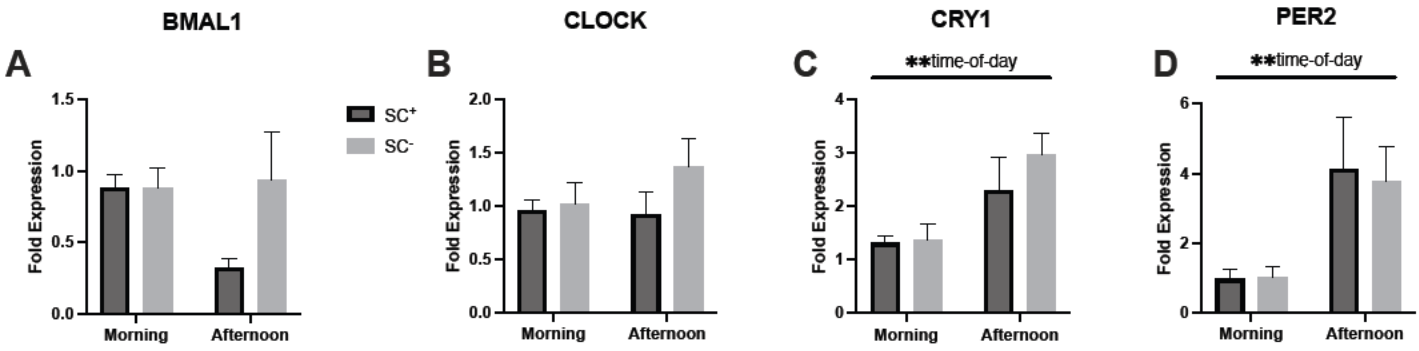

Figure 5.1: Muscle molecular clock gene expression

*A-D) Gene expression of muscle molecular clock components BMAL1, CLOCK, CRY1, PER2 (respectively) in morning and afternoon animals represented in units of change in fold expression All data shown as mean ±s.e.m. SC ablation and myofiber area compared through an unpaired t-tests and clock gene expression compared through two-way-ANOVA for main effects of time-of-day and treatment (*p<0.05), (n=5 per group)*

5.4.2 Eccentric specific force and contractile-injury following ten eccentric contractions

Although eccentric force in Morning-SC^+ was reduced compared to Afternoon-SC^+ animals, I note that such differences did not reach statistical significance (Morning-SC^+: 19.88 ± 1.42, Afternoon-SC^+: 25.56 ± 2.80 all values in N/cm^2) ($p = 0.09$). Eccentric specific force of Morning-SC^+ animals was reduced compared to SC^- counterparts, while no differences were observed between afternoon groups (Morning-SC^+: 19.88 ± 1.42, Morning-SC^-: 27.81 ± 1.89, Afternoon-SC^+: 25.56 ± 2.80, Afternoon-SC^-: 25.26 ± 2.88 all values in N/cm^2) ($p < 0.05$) (Fig 5.2A-F). Tetanic force-loss and dystrophin^{negative} fibers (131, 132) were used to determine the

extent of injury across groups (Fig 5.2C-D, 5.2G-H, Fig. 5.S.2). Morning-SC^{+} animals exhibited reduced force-loss and lesser amounts of dystrophin^{negative} fibers following 10 eccentric contractions compared to Morning-SC^{-} counterparts (Tetanic force-loss: Morning-SC^{+}: -5.63 ± 0.61, Morning-SC^{-}: -7.93 ± 0.61; N/cm^2) (Dystrophin^{negative} fibers: Morning-SC^{+}: 32 ± 2.1, Morning-SC^{-}: 64 ± 10.2) ($p < 0.05$) (Fig 5.2C-D). No differences in force-loss or dystrophin^{negative} fibers were observed between afternoon groups (Tetanic force-loss: Afternoon-SC^{+}: -6.81 ± 0.39, Afternoon-SC^{-}: -6.01 ± 0.4; N/cm^2) (Dystrophin^{negative} fibers: Afternoon-SC^{+}: 32 ± 5.0, Afternoon-SC^{-}: 32.7 ± 10.7) ($p > 0.05$) (Fig 5.2G-2H). An overall negative association was found between force-loss and maximal eccentric force (Overall $r^2 = 0.39$, $p < 0.01$) (Fig 5.3A).

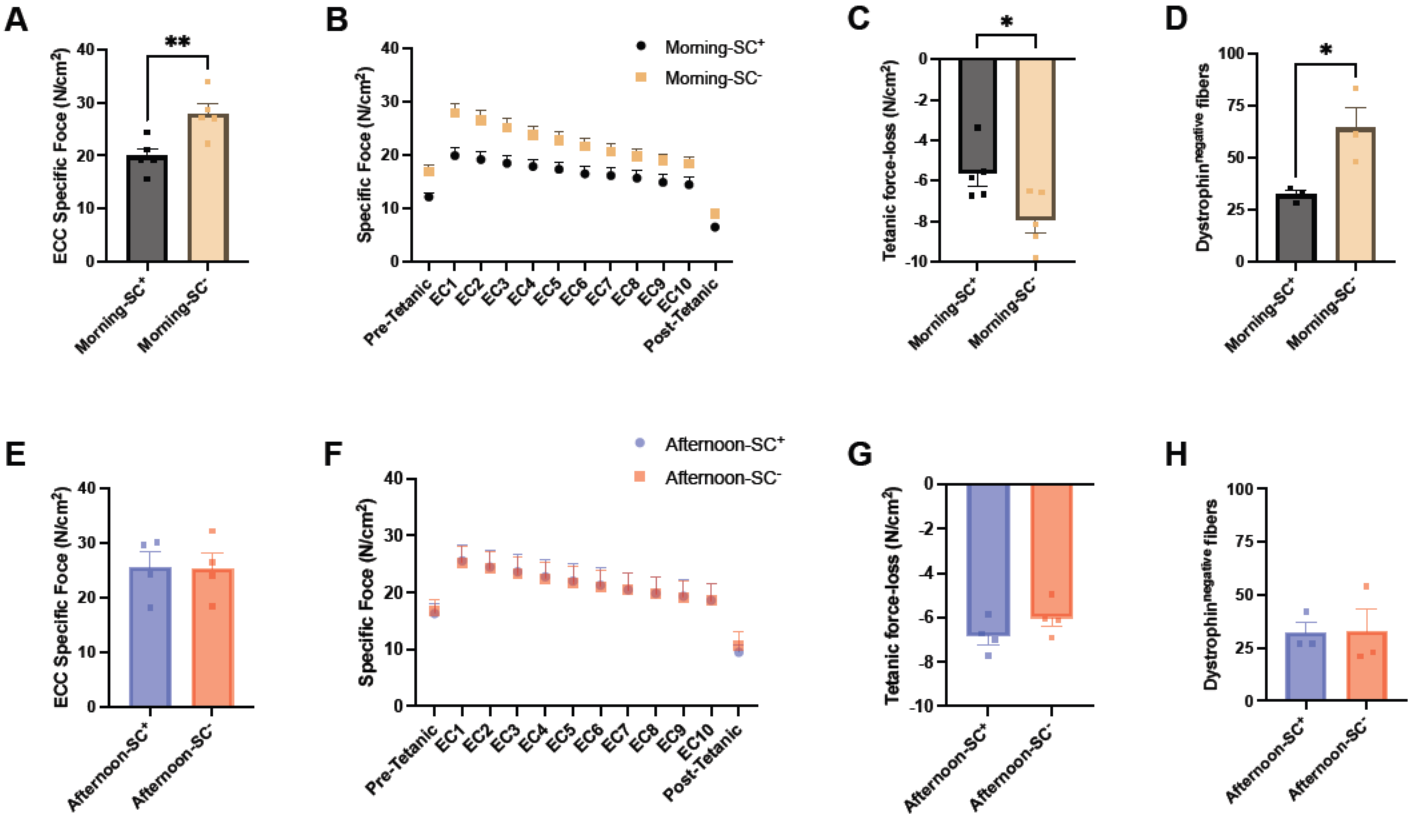

Figure 5.2: Eccentric specific force and contractile injury in Morning and Afternoon groups

*A, E) Eccentric specific forces of morning and afternoon groups (N/cm^2). B, F) Representative figure of experimental contractile-injury protocol consisting of a pre-eccentric tetanic, 10 eccentric contractions. C, G) Extents of tetanic force-loss in morning and afternoon groups (N/cm^2). D, H) Dystrophin^{negative} fibers in morning and afternoon groups. All data shown as mean ± s.e.m. All groups compared through an unpaired t-tests (*p<0.05) (**p<0.01), (n=4-5 per group)*

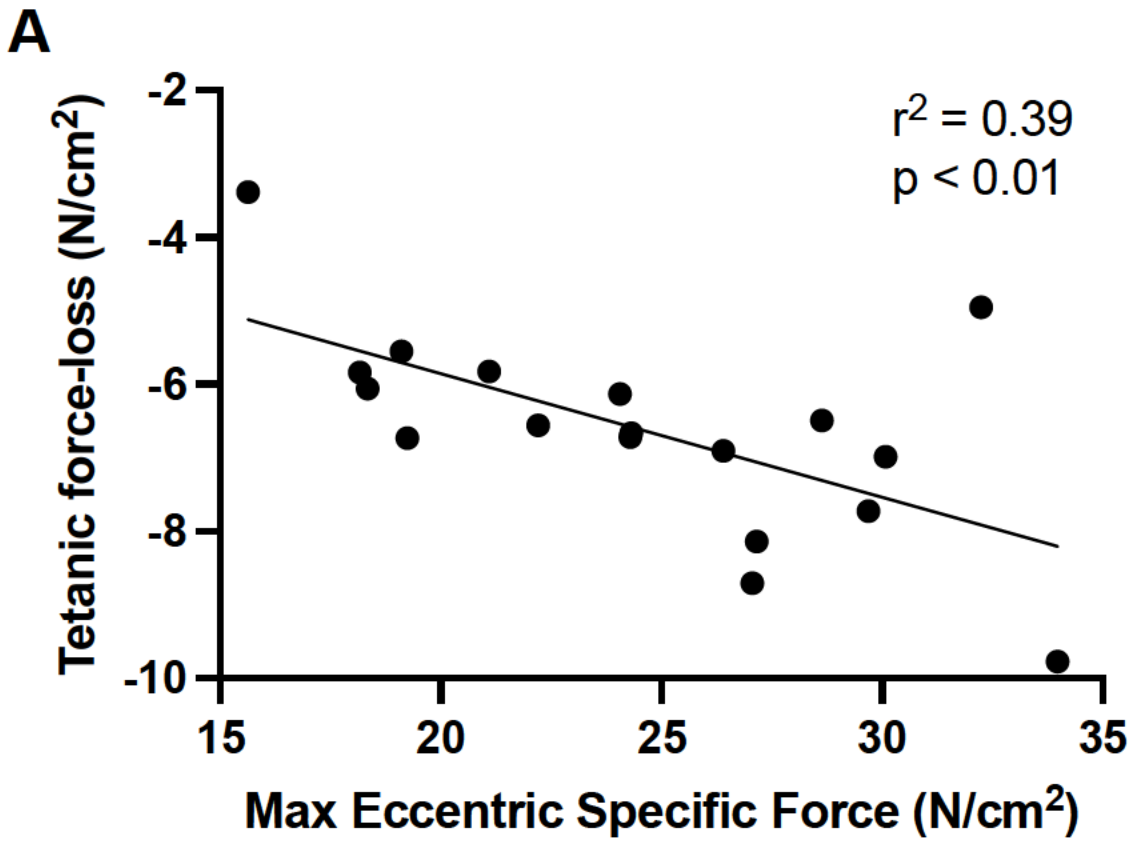

Figure 5.3: Extent of contractile force-loss is a function of maximum eccentric specific force

*A linear regression between max eccentric force and tetanic force-loss. All data shown are raw data points (**p<0.01), (n=18)*

5.4.3 Isometric tetanic and caffeine specific forces

Tetanic specific force of Morning-SC^+ animals was reduced compared to SC^- animals (Morning-SC^+: 18.66 ± 2.12, Morning-SC^-: 24.3 ± 1.07; N/cm^2) ($p < 0.05$) (Fig 5.4A), while no differences were observed between afternoon groups (Afternoon-SC^+: 23.22 ± 1.53, Afternoon-SC^-: 21.45 ± 1.40; N/cm^2). Caffeine-induced contracture force, reflective of maximal Ca^{++} release and/or availability to contractile units, was reduced in Morning-SC^+ mice compared to SC^- counterparts (Morning-SC^+: 4.23 ± 0.24, Morning-SC^-: 5.059 ± 0.16, N/cm^2, n=6, $p < 0.05$) (Fig. 5.4B). Caffeine-contracture force was significantly correlated with maximal tetanic force ($r^2 = 0.95$, $p = 0.001$) (Fig 5.4C). Maximum tetanic force measured immediately prior to measuring caffeine forces confirmed initial findings of reduced forces in Morning-SC^+ compared to SC^- animals (Morning-SC^+: 24.57 ± 1.10, Morning-SC^-: 29.41 ± 0.56, N/cm^2, n=6, $p < 0.05$).

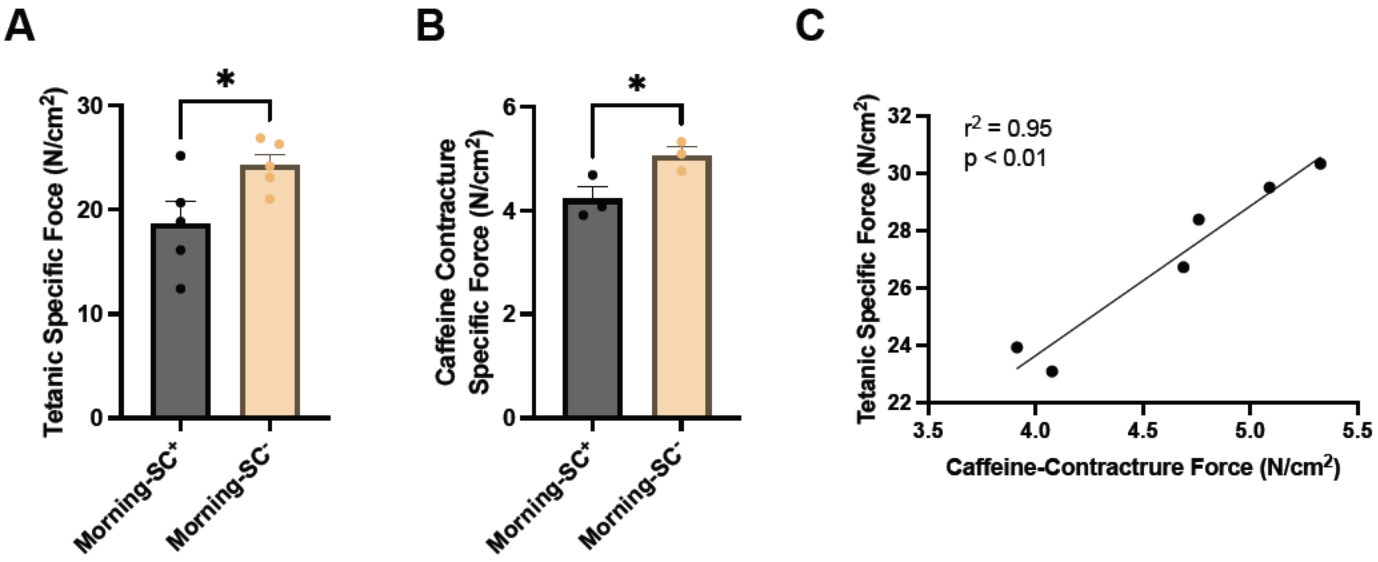

Figure 5.4: Tetanic and caffeine contracture specific forces in Morning-SC$^+$ versus Morning-SC$^-$ animals

*A) Tetanic specific forces of morning groups (N/cm^2). B) Caffeine contracture specific forces of Morning-SC$^-$ vs Morning-SC$^+$. C) Linear regression between maximal tetanic force and caffeine-contracture force. All data shown as mean ± s.e.m. All groups compared through an unpaired t-tests (*p<0.05) (n=4-5 per group) (caffeine data: n=3 per group)*

5.4.4 Satellite Cell Ablation and Myofiber Characteristics

Pax7 abundance was significantly reduced (75%) in the tamoxifen treated group (Total SCs: SC$^+$ 36.3 ± 4.66 vs SC$^-$ 12.66 ± 3.71) ($p < 0.05$) (Fig 5.S.1A). Figure 5.S.1C and 5.S.1D are a representative image of SC ablation, respectively. Myofiber area was not different between SC$^+$ and SC$^-$ animals (SC$^+$ 1,528.57 ± 148.63 vs SC$^-$ 1,501.54 ±128.79; units in μm^2) (Fig 5.S.1B).

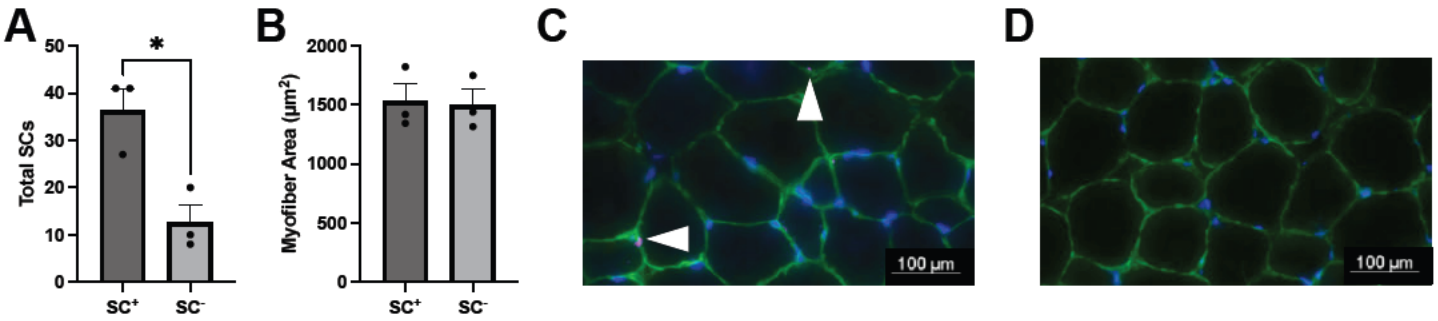

Figure 5.S.1: Satellite cell ablation

*A) Quantification of SC ablation expressed as total number of SCs per whole cross-section (around 700 fibers per biological replicate). B) Average myofiber area of the EDL from SC^+ vs SC^- animals. C) Representative image from a SC^+ animal; arrows denoting SC residing around individual fibers. All values reported as number of total SCs per cross-section (~700 fibers/section). All data shown as mean ± s.e.m. All groups compared through an unpaired t-tests (*p<0.05) (**p<0.01), (n=3 per group).*

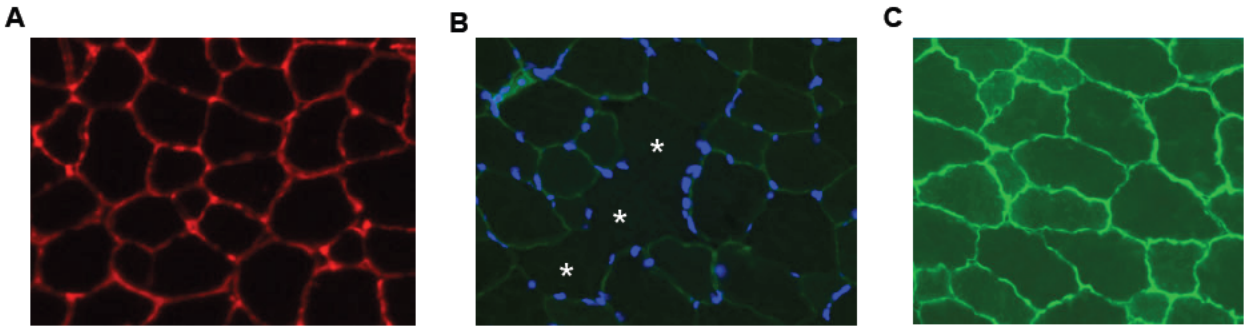

Figure 5.S.2: Laminin and dystrophin immunohistochemical representative images

A) Representative image of laminin presence in a damaged cross-section. B) Representative image from the same muscle as figure 2A showing dystrophin-negative fibers with nuclei following eccentric injury. C) Representative image of dystrophin-presence in uninjured muscle

5.5 Discussion

I used an established mouse model to deplete SCs to characterize muscle clock gene expression and *ex vivo* skeletal muscle force-production in the morning or afternoon in the presence and absence of SCs (Morning-SC^+, -SC^- Afternoon-SC^+, -SC^-). Morning-SC^+ animals demonstrated reduced tetanic and eccentric specific force compared to SC^- animals, although no differences were observed between Afternoon SC^+/SC^- groups. Additionally, Morning-SC^+ animals, who produced lower forces, exhibited lower levels of contractile injury-induced force-loss and cytoskeletal protein loss (less $dystrophin^{negative}$ fibers) versus SC^- counterparts, but no such differences were noted between afternoon groups for these outcomes. To identify possible mechanisms for the lower forces observed in Morning-SC^+ animals, I assessed caffeine-induced contracture-force (a surrogate for maximal Ca^{++} availability to contractile units) and found Morning-SC^+ harbored lower forces vs SC^- counterparts. Collectively, these data suggest contractile function was influenced by SCs according to time-of-day.

Mounting evidence suggests force-production varies with respect to time of day (8), which may, in part, be explained by clock-gene regulation of contractile function. In this regard, *Per*, *BMAL1*, and *Clock*-mutant animals have alterations (reductions/increases) in *ex vivo* force production (13, 14, 52). Additionally, SC molecular clock-genes and contractile related genes demonstrate a 24 h rhythmic expression pattern (17, 26), although how such oscillations effect muscle contractility is unclear. Currently, there is limited evidence to suggest SCs play a role in

contractile function as few studies have assessed baseline contractile function in whole-muscle preparations following SC ablation (63, 64, 97). In a recent report, Bachman et al. (2018) reported reduced force in pre-pubertal SC^- mice, although in mature mice, such force differences were not observed (63). Fry et al. (2014) examined the long-term effects of SC depletion following an overload-model of hypertrophy and found that whole muscle contractile function was reduced in SC^- mice, which they attributed to excess ECM accumulation (64). In the present study I assessed whole muscle force in the presence or absence of SC's and with respect to time-of-day after short-term (10-14 day) SC ablation. I found that SCs differentially regulated contractile properties according to time-of-day following short-term ablation, with Morning-SC^+ animals displaying lower forces compared to SC^- animals.

Eccentric contractions produce the greatest contractile force and consequently lead to greater contractile-induced muscle damage/injury compared to concentric or isometric contractions (127, 133-135). As different eccentric forces can induce varying levels of injury (67, 68), I evaluated if time and SC dependent differences in force observed in morning groups would lead to differences in two markers of contractile injury; force-loss and loss of cytoskeletal protein dystrophin. Post-injury force-loss and loss of various cytoskeletal proteins such as dystrophin have been widely used as markers for muscle damage across a variety of contractile injury models (15, 36, 67, 127, 131-133, 136-138). After administration of an injury protocol (105, 124), I found that Morning- SC^+ animals exhibited reduced force-loss and lower amounts of dystrophin^{negative} fibers post-injury compared to Morning- SC^- counterparts, with no differences in these markers between Afternoon SC^+/SC^- animals. These results support previous reports (67, 68) that higher forces lead to higher force-losses reflective of greater magnitudes of injury with past data suggesting that time-of-day SC influence may be a secondary influence underlying this

observation. Further support for this hypothesis comes from recent evidence in mice demonstrating that the magnitude of injury and repair following major muscle-injury (cardiotoxin) differs according to the time-of-day injury is sustained (85). Although higher sample sizes are probably required to detect statistical significance, I observed lower eccentric force in Morning-SC^{+} versus Afternoon-SC^{+} animals ($p = 0.09$). This may be relevant for future studies that determine if human muscle repair following eccentric contractions differs by time-of-day similar to toxin-induced injury-repair models reported in animals (85). A recent study highlighted that the time-of-day muscle injury occurs at influenced the early SC/neutrophil communication which consequently influenced the efficacy of muscle repair long-term in mice (89). Such mechanisms may also be at play in humans following eccentric damage and require further investigation.

As the maximal force production and extent of contractile injury was reduced in Morning SC^{+} versus Morning-SC^{-} animals, I sought to determine a potential mechanism to explain such reductions in baseline force. In this regard, evidence has shown molecular clocks harbor a connection to Ca^{++} related contractile proteins and signaling pathways (13, 26, 56, 139). Interactions between Ca^{++} and contractile proteins can induce post-translational modifications (i.e., phosphorylation) capable of altering force-production (26) and previous evidence has demonstrated post-translational modifications differ according to exercise-timing (38). Although I did not directly measure any contractile protein phosphorylation kinetics, given the critical role Ca^{++} plays in force-generation, I evaluated caffeine-induced contracture-forces, as an indirect measure of maximal Ca^{++} availability, between morning groups. Similar to past findings in tetanic/eccentric force, I observed a reduction in caffeine-contracture force in Morning-SC^{+} compared to SC^{-} counterparts, suggesting lower tetanic/eccentric forces in Morning-SC^{+} animals

may be due to a reduced volume of Ca^{++} available to contractile units. While the measure of Ca^{++} was indirect, I note that a similar approach has previously been reported as a valid surrogate measure for the evaluation of Ca^{++} volume (57, 59, 125). Additionally, linear regression analyses revealed a strong association ($r^2 = 0.95$, $p < 0.01$) between caffeine-contracture force and maximal tetanic force.

While the observation that SCs may regulate contractile function via Ca^{++} kinetics by time-of-day is most intriguing, I recognize that more work is needed to establish this connection. Mechanistically, one report has shown that increases in Ca^{++} following electrical stimulation in single fibers led to concordant increases in Ca^{++} levels within SCs as well (51). Additionally, the means by which changes in Ca^{++} levels were communicated was through SC filopodial protrusion attachments to muscle (51). SC protrusions have previously been shown to have a "sensing" capability that is in-tuned with homeostatic and injury cues within muscle (140-143). Supportive of this relationship, SCs lacking filopodial protrusions did not experience such increases in Ca^{++} following electrical stimulation (51). This combined evidence suggests SC protrusions are mechanically in-tuned and responsive to contractile stimuli which may be "how" SCs regulate Ca^{++} levels within muscle. Supportive of this claim, a recent report inducibly depleted SC-protrusions and found that expression of Ca^{++} related elements involved in E-C coupling were dysregulated and force production was reduced compared to control mice following injury as well (141).

5.6 Conclusion

In conclusion, I report reduced *ex vivo* force-production in the presence of SCs in the morning but not in the afternoon. Furthermore, morning-SC^+ animals demonstrating reduced

force-production also experienced lesser extents of injury induced force-loss and dystrophin^{negative} fibers. One potential mechanism underpinning lower maximal forces observed in Morning-SC^{+} animals may be lower Ca^{++} availability for force generation. While I attribute time-of-day findings to be regulated, in part, by time-sensitive molecular clocks within SCs, the model of inducible depletion ablates the entire SC and is not confined to molecular clocks. Accordingly, I cannot rule out the possibility that another cellular mechanism in SCs outside of the molecular clock may be contributing to differences in force production. Taken collectively, the results from the current study suggest that SC time-of-day characteristics may be an important consideration in future experiments that investigate the mechanisms underpinning the diurnal nature of contractile function.

Acknowledgements

This work was supported, in part, by a Novo Nordisk Foundation Challenge Grant (NNF14OC0011493) to J.A.H, National Institutes of Health grant HD094602 to S.D. This work was supported in part by Research Career Scientist Award Number IK6 RX003351 from the United States (U.S.) Department of Veterans Affairs Rehabilitation R&D (Rehab RD) Service. Graphical abstract was created with Biorender.com.

Data Availability Statement

All data used within the results and to create figures are included in the material of this manuscript. Additional analysis and files can be provided upon request.

Competing Interests

The authors declare no competing interests.

Author Contributions

RK, RLL, SD, OLK, JAH all contributed to preparation of this manuscript and approve of its contents.

5.7 Supplemental Methods

Stimulation Parameters

Stimulation parameters were adopted from previous studies (104, 124). Five minutes after mounting, twitches were imposed on the muscle to define optimal muscle fiber length (L_o) and voltage. Muscle length was measured after optimizing twitches and fiber length was calculated using a fiber length-to-muscle length ratio of 0.51 for the EDL (144). A custom LabVIEW program recorded force, length, time data from each contraction. Force was recorded in volts and converted to Newtons (N). Force in newtons was converted into specific force (force normalized to physiological cross-sectional area (PCSA)). PCSA was calculated using the following equation (145):

$$PCSA = M / [L_o \times (L_f / L_o) \times \rho\ ]$$

where M is mass, L_o is optimal muscle length, L_f is optimal fiber length, and ρ is fiber density assumed to be 1.056 g/cm^3 for skeletal muscle (146).

After experimentation, muscle was unmounted, blotted dry, weighed, and flash frozen in liquid nitrogen-cooled isopentane for storage at -80°C.

Immunohistochemistry (IHC)

Flash frozen EDL muscles, stored at -80ºC, were transferred to a -25 ºC cryostat to section for immunohistochemical staining. In brief, muscle mid-belly was cut perpendicular to the fiber orientation, embedded in a cryomold, and quickly flash frozen (ten seconds) in liquid nitrogen-cooled isopentane to rapidly freeze the cryomold. Muscle sections were cut at 10 µm

thickness. For IHC staining assays, slides were fixed in 4% PFA, then incubated in 3% H_20_2 to block endogenous peroxidases and washed with PBS. After this, an epitope retrieval step (slides steamed for 30 min in a pressure cooker in a citra buffer bath) was performed and slides were permeabilized. Slides were blocked for 1hr in 1%BSA mouse-on-mouse blocking buffer and were then incubated in the primary antibody solution overnight. The next day, slides were incubated for 90 min sin a biotinylated secondary antibody, washed, and incubated in secondary antibody solution for 1hr. Following this incubation, slides were incubated in an amplification solution for 20 minutes, washed, mounted with Vectashield with DAPI, and cover-slipped. (112, 113). Primary antibody details were as follows: anti-Pax7 [mouse IgG1, 1:100 DSHB, concentrate], anti-laminin (rabbit IgG, 1:500, Sigma-Aldrich, L9393], anti-dystrophin (rabbit IgG, 1:100, Abcam, ab15277]. Secondary antibody details for Pax7 were: goat anti- mouse IgG1 biotin-SP-conjugated (1:1,000, Jackson Immuno Research, 115-065-205), Streptavidin-horseradish peroxidase (SA-HRP) (1:500, Invitrogen, S-911), SuperBoost Tyramide reagent Alexa Fluor 594 (1:500, Thermo Fisher, B40957). Secondary details for laminin and dystrophin were: Alexa Fluor 488 goat anti-rabbit IgG (H þ L) (1:250, Invitrogen, A-11034)

Slides were imaged at 20x and whole tilescan cross-section images were analyzed for cross-sectional area (CSA) and SC abundance, Cross-sectional area and SC quantification were carried out via a blinded-automated analysis using MuscleJ (114). Dystrophin negative fibers were quantified by hand on ImageJ as fibers lacking dystrophin borders.

Chapter 6, Linking Chapter: Study-2, Review Paper, Study-3

In the second study undertaken for this thesis (Chapter 5), it was found that SCs differentially regulated force-production according to time-of-day. Specifically, SC presence had reduced force production in the morning, whereas this was not observed in the afternoon. It has been previously shown that high versus low forces produced during eccentric contractions results in proportional degrees of contractile injury (67, 68). Accordingly, study-2 employed an established *ex vivo* eccentric injury model (104, 124) to determine whether this phenomenon was applicable in the contexts of the differences in observed forces. Morning-SC^{+} animals that produced lower eccentric forces exhibited lesser degrees of injury (force-loss and $dystrophin^{negative}$ fibers) versus SC^{-} counterparts. No differences in eccentric force were observed in afternoon groups with both SC^{+} and SC^{-} groups demonstrating similar extents of injury. Mechanistically, additional evidence from study-2 revealed differences in force-production noted between morning groups were due to lower Ca^{++} availability for contractile units. Collectively, this demonstrates that SCs play a regulatory role in force-production according to time-of-day. Such regulation may be important in the context of high force induced contractile injuries. Additionally, these findings suggest muscle repair following contractile injury may be a function of SC-molecular clock regulation on the eccentric forces inductive of the injury. However, given the terminal nature of the *ex vivo* contractile injury model employed in study-2, measurements of muscle repair were not possible.

Therefore, in a third study (described in chapter 8), a SC-specific Bmal1 KO mouse model was utilized to assess the effects of the SC-molecular clock on muscle repair following *in vivo* contractile injury. As study-2 demonstrated SCs' time-of-day influence on contractile function was a critical determinant of the magnitude of injury sustained, SC-Bmal1 KO animals were firstly

assessed for any baseline differences in contractile function prior to undergoing *in vivo* eccentric contractile injury. Following these assessments and subsequent contractile injury, markers for muscle damage, neutrophil infiltration, SC-myogenic progression, and muscle repair were assessed at 24 h, 72 h, and 7 days post injury. Previous work utilizing the same mouse model has shown that SC-Bmal1 KO mice exhibit blunted SC-proliferation following cardiotoxin injury and consequently muscle failed to fully regenerate (85). However, as the model used in that study involved non-physiological injury (85), it is unclear if the same effects will occur when injury is sustained through eccentric muscle contractions. This evidence in association with the evidence from study-2 (altered extents of injury due to SC time-of-day modulations of force-production) necessitates evaluation of how SC-molecular clocks influence repair following contractile-injury. Chapter 7 discusses how SC-molecular clocks regulate muscle regeneration following *non-physiological* models of muscle injury (chapter 7). Chapter 8 details the experimental study that assessed muscle repair following *in vivo contractile* injury in SC-Bmal1 KO animals.

Chapter 7: Review paper

Publication Statement:

The content of Chapter 7 is from an original research article published on the date of 3 May 2023 in *American Journal of Physiology-Cell Physiology*.

Kahn, R. E., Dayanidhi, S., Lacham-Kaplan, O., & Hawley, J. A. (2023). Molecular clocks, satellite cells, and skeletal muscle regeneration. *American Journal of Physiology-Cell Physiology*. https://doi.org/10.1152/ajpcell.00073.2023

Molecular clocks, satellite cells, and skeletal muscle regeneration

Ryan E. Kahn[1,2], Sudarshan Dayanidhi[2,3], Orly Lacham-Kaplan[1] John A. Hawley[1]

[1]Exercise and Nutrition Research Program, The Mary MacKillop Institute for Health Research, Australian Catholic University, Melbourne, Australia

[2]Shirley Ryan AbilityLab, Chicago, IL, USA

[3]Feinberg School of Medicine, Northwestern University, Chicago, IL, USA

Running Title: Molecular Clocks Role in Muscle Regeneration

Keywords: Muscle stem cells, myogenic regulatory factors, circadian rhythms, cell cycle, myogenesis

Corresponding Author: John A, Hawley, Ph.D.

Exercise & Nutrition Research Program

The Mary MacKillop Institute for Health Research

Australian Catholic University

Melbourne

Australia

E-mail: john.hawley@acu.edu.au

7.1 Abstract

Skeletal muscle comprises approximately 50% of individual body mass and plays vital roles in locomotion, heat production, and whole-body metabolic homeostasis. This tissue exhibits a robust circadian rhythmicity which is under control of the suprachiasmatic nucleus (SCN) region of the hypothalamus. The SCN acts as a 'central' coordinator of circadian rhythms, while cell-autonomous 'peripheral' clocks are located within almost all other tissues/organs in the body. Synchronization of peripheral clocks in muscle (and other tissues) together with the central clock is crucial to ensure temporally coordinated physiology across all organ systems. By virtue of its mass, human skeletal muscle contains the largest collection of peripheral clocks, but within muscle resides a local stem cell population, satellite cells (SC's), which have their own functional molecular clock, independent of the numerous muscle clocks. Skeletal muscle has a daily turnover rate of 1-2%, so the regenerative capacity of this tissue is important for whole-body homeostasis/repair and depends on successful SC myogenic progression (i.e., proliferation, differentiation, and fusion). Emerging evidence suggests SC-mediated muscle regeneration may, in part, be regulated by molecular clocks involved in SC-specific diurnal transcription. Here I provide insight on molecular clock regulation of muscle regeneration/repair and provide a novel perspective on the interplay between SC-specific molecular clocks, myogenic programs, and cell cycle kinetics that underpin myogenic progression.

New & Noteworthy

Insights into molecular clock regulation of muscle regeneration/repair and perspectives on the interplay between SC-specific molecular clocks, myogenic programs, and cell cycle kinetics that underpin myogenic progression.

7.2 Circadian Biology: A primer

The circadian clock is a highly conserved autonomous timekeeping system of biological oscillators that aligns behavioral patterns with the rotation of the earth's light-dark cycle, supporting bodily functions in almost all tissues and organs by anticipating and coordinating the required metabolic programs needed for whole-body cellular homeostasis (3, 18). The rhythmicity of molecular clocks manifests as time-dependent regulation of downstream processes commonly referred to as diurnal events. Many physiological and metabolic activities are time-of-day dependent including sleep-wake cycles, feeding-fasting cycles, core and skin temperature, and levels of circulating hormones and metabolites. Within the cell, circadian regulation is underpinned by autonomous cell type-specific peripheral molecular clocks. Key features of molecular clocks include an input pathway that receives environmental (e.g., photopic signals) or physiological (e.g., timing of meals or exercise) cues and subsequently transmits them to the central oscillator (1) which maintains circadian time, generates daily rhythm, and communicates these rhythms to coordinate various metabolic, physiological, and behavioral processes (18-20).

The master or "central" circadian clock is in the brain's hypothalamus, within the suprachiasmatic nucleus (SCN) and contains ~20,000 neurons that oscillate with a roughly 24 hr rhythm (2, 20). As such, the SCN clock functions autonomously, independent of external input, but can be reset or 'phase shifted' in response to environmental cues ("zeitgebers" or time givers), most notably photopic signals such as light or dark (2, 22). Synchronization of peripheral clocks in other organs and tissues together with the central clock is crucial to ensure temporally coordinated physiology across all organ systems. Indeed, circadian disruption or misalignment between central and peripheral clocks predisposes to a variety of chronic metabolic disorders including obesity, insulin resistance, type 2 diabetes, and cardiovascular disease (7). Fundamental

to the circadian clock network are core transcription factors, circadian locomotor output cycles kaput (CLOCK), and brain and muscle arnt-1 like protein-1 'BMAL1' (147). These factors orchestrate transcription of multiple clock-controlled genes by binding to E-box sites within the promoter of circadian responsive genes (148), synchronizing transcription of their own repressors, period (PER) and cryptochrome (CRY) family members, and generating a tightly self-regulated feedback loop (Figure 7.1). Specifically, increased transcription of *per* and *cry* genes leads to translation and accumulation of the PER and CRY proteins outside of the nucleus. These circadian repressors then translocate into the nucleus to inhibit CLOCK:BMAL1-driven transcription of *per*, *cry*, and numerous other clock-controlled genes (Figure 7.1). The degradation of PER and CRY alleviates transcriptional repression and permits CLOCK:BMAL1-mediated transcription to proceed once more, underpinning cyclical circadian gene expression (148)

While the relationship between the circadian clock and energy metabolism has been extensively studied in organs such as the liver (1, 149, 150), only recently has the role of the clock in skeletal muscle received widespread attention. It is now appreciated that skeletal muscle molecular clocks have regulatory roles in glucose, lipid and protein metabolism (151-153), exercise capacity, muscle function, (8, 25, 39, 52, 92) and gene expression (7, 23, 26, 139, 152, 154). Within skeletal muscle resides a local stem cell population, satellite cells (SC), which have their own functional molecular clock independent of the muscle (myonuclei) clocks (17). SC molecular clocks are involved in SC-specific diurnal transcription as well as SC-mediated muscle regeneration (17, 85). Recently, studies utilizing clock-disrupted mouse models have reported that muscle molecular clocks interact with cell cycle components to facilitate myogenesis during injury (i.e., toxin, freeze injuries) (83, 84). However, the role of the SC-specific molecular clock in muscle repair/regeneration remains largely unknown and has not been investigated in

physiological models of muscle injury, or humans. Here I provide a brief synopsis of how SC myogenic regulatory factors (MRFs) guide the cell cycle, consider how the molecular clock is involved in these myogenic processes, and how core-clock components interact with the cell cycle and SC/myogenic factors during myogenesis following muscle damage/injury. I propose that SC-derived myogenic regulatory factors and the SC-molecular clock act in harmony with the cell cycle to regulate the time-course of myogenic progression following injury.

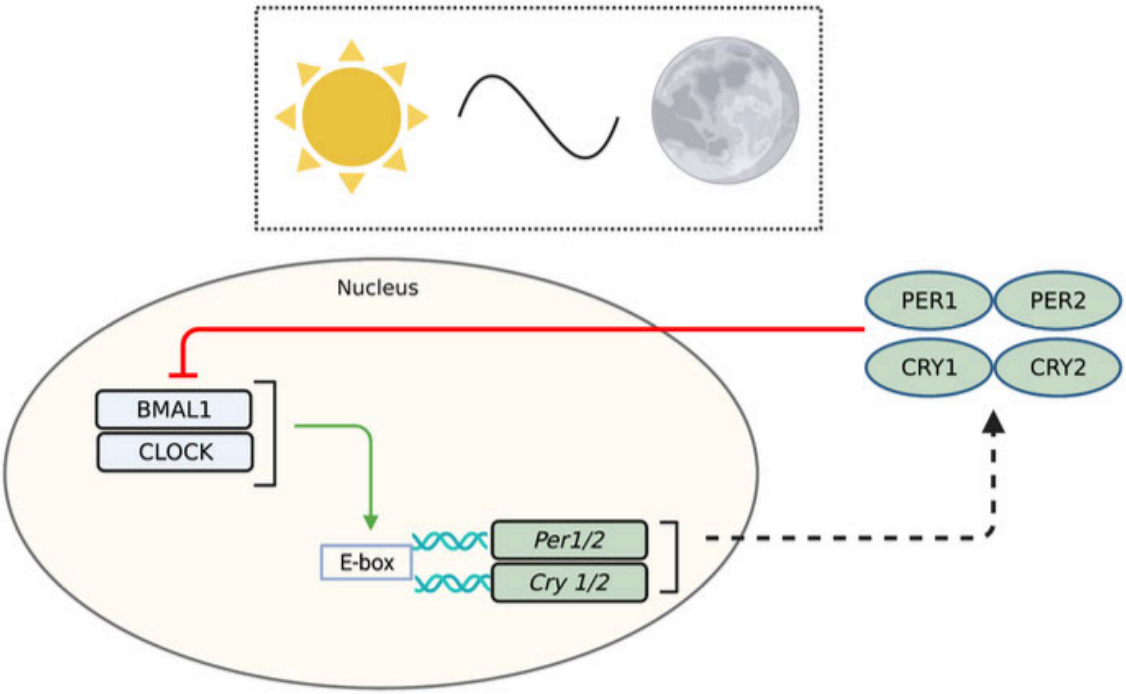

Figure 7.1: Simplified Model of the Core Molecular Clock

BMAL1 and CLOCK bind to the E-box region of clock genes Per1/2, Cry1/2 inducing their expression and exit of the nucleus. Per1/2 and Cry1/2 translocate back into the nucleus to bind to the E-box region of BMAL1 and CLOCK, repressing their transcription of Per1/2, Cry1/2. This

transcriptional/translational feedback loop dictates the oscillations of molecular clock output generating "circadian rhythms." Transcript is signified by lower-case and italics. Protein is signified by capital and non-italics.

7.3 Satellite Cells, Myogenic Regulatory Factors, Cell Cycle and Molecular Clocks: Timely Regulators of Myogenesis?

Individual muscle cells are post-mitotic and retain the muscle stem cell population, SCs, for reversible entry/exit of the cell cycle (16, 155). Upon activation, SCs proceed down a myogenic lineage ultimately donating nuclei to the host-fiber to maintain cellular homeostasis and/or facilitate repair/regeneration (16, 155, 156). In adulthood, the majority of SCs are quiescent unless activated for reparative/regenerative needs (157, 158). Upon muscle damage SCs exit their basal quiescence state, enter the cell cycle, and subsequently proliferate/differentiate and fuse to host myofibers (15, 75, 159, 160). This complex process, termed the myogenic program, is facilitated by SCs undergoing a highly conserved expression pattern of the myogenic regulatory factors, Pax7, Myf5, MyoD, Mrf4 and Myogenin (69, 75, 161).

The progression of myogenesis is underpinned by SC myogenic regulatory factors (MRFs) acting on the cell cycle, predominantly MyoD that activates proliferative cell cycle machinery, with Myogenin promoting differentiative cell cycle activity (76, 162, 163). Consequently, any modifications/actions to either MRFs or cell cycle machinery will alter the time-course of myogenesis following acute injury (164-170). Specific molecular clock components (discussed subsequently) induce diurnal MRF expression in an upstream manner while also binding to several downstream MRF target genes (i.e., titin) to induce rhythmic expression of these dual clock-myogenic targets (55, 88). As MRFs act on cell cycle machinery to drive myogenesis, diurnal

expression of MRFs play a regulatory role in determining when these actions in the cell cycle occur. Molecular clocks, however, not only influence cell cycle activity through MRFs, but have direct interactions with cell cycle machinery (83, 84). This suggests the molecular clock has multiple nodes (i.e., actions on MRFs or cell cycle to influence SC proliferation, differentiation, fusion, and muscle gene expression) within the myogenic program capable of modifying the timelines that occur during repair/regeneration. The diurnal gene expression of SC specific molecular clocks (17) is likely to impact SC-MRF activity and downstream actions on the cell cycle (Figure 7.2). Although not well established in muscle/SCs, other lines of evidence (i.e., zebrafish cell lines, bacterial cells, plant cells, murine liver cells) provide support that the cell cycle and molecular clock communicate with each other (171-177). Checkpoint genes and molecular clocks harbor regulatory feedback with these regulatory nodes acting as 'gating' features to modulate cell cycle progression (171-177). In the following section I dissect the results of studies in muscle/SC's that have explored the cellular interplay between SC/muscle clock genes (BMAL1, CLOCK, Per, Cry), myogenic components, cell cycle kinetics, and how disruptions to the molecular clock have the capacity to alter the myogenic program during muscle repair/regeneration.

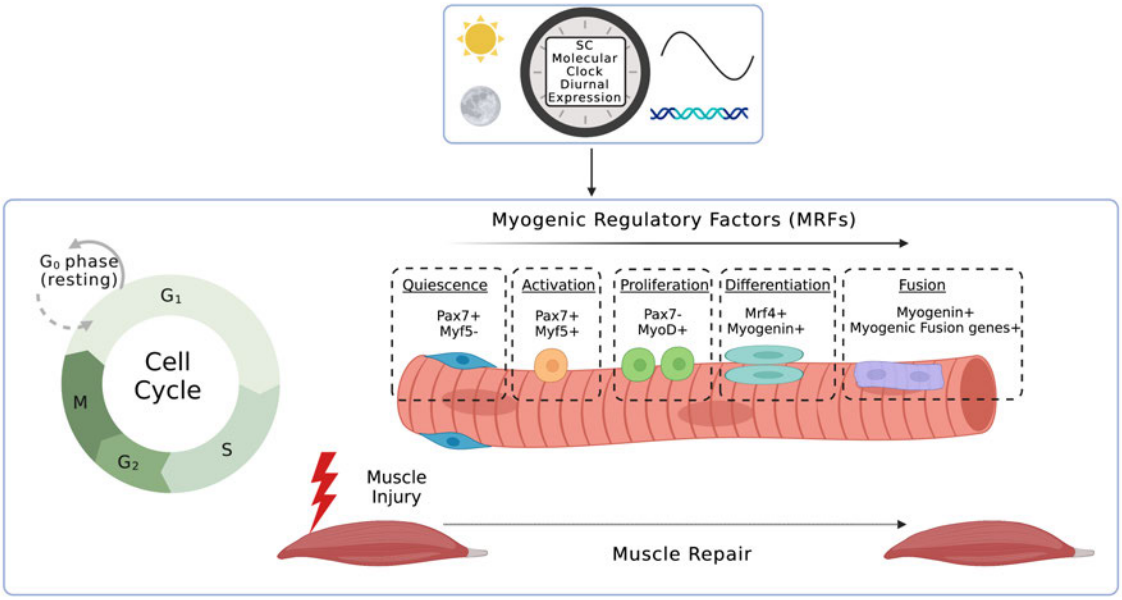

Figure 7.2: SCs, MRFs, Clocks, and the Cell Cycle During Myogenesis

Graphical representation of likely intracellular nodes and components within the cell cycle and myogenic regulatory factors (MRFs) that the SC-molecular clock may regulate during myogenic progression. Growing evidence suggests myogenic regulatory factors, mainly responsible for driving myogenic progression, are under circadian control. Evidence elsewhere shows cell cycle components are also under molecular clock control. This graphical figure displays a suggestive regulation the SC-molecular clock may have over myogenic regulator factors and cell cycle components to guide myogenesis on a time-dependent basis.

7.4 Molecular Clock Regulation of Skeletal Muscle Regeneration: The Satellite Cell-Specific Molecular Clock

7.4.1 The role of molecular clocks in SC-mediated muscle regeneration: BMAL1, CLOCK

7.4.1.1 The role of BMAL1 in the early stages of SC activation

Approximately 15% of total mRNA transcripts involved in skeletal muscle growth, proliferation, and differentiation are regulated by the molecular clock (13, 178). Specifically, BMAL1 promotes myogenic progenitor cell (MPC) proliferation and differentiation through diurnal transcriptional patterns on components of Wnt signaling pathways (12) (Figure 7.3). Wnt signaling in the myofiber/SC node is crucial for maintaining quiescence as well as ushering myogenic progression during muscle regeneration (179, 180). Upon freeze/toxin injuries to muscle of BMAL1-null mice, SCs exhibited impaired expansion/proliferation and ultimately blunted repair/regeneration (11, 12). Further, Wnt signaling components in wildtype myoblasts display robust circadian expression patterns, whereas BMAL1-null myoblasts do not, implicating BMAL1 as a crucial player regulating circadian rhythmicity of Wnt signaling (54). These observations highlight the important role of BMAL1 in myogenesis and suggest that lack of BMAL1 may remove circadian influence on Wnt signaling that appears to be obligatory for SC transitioning from quiescence to proliferative stages. In this context, the interactions between BMAL1 and Wnt signaling may be one mechanism by which SCs time their exit from quiescence and initial myogenic progression during muscle repair/regeneration (Figure 7.3). BMAL1's actions on cell signaling involved in quiescence is likely time-dependent and evidence of SC-specific BMAL1 circadian behavior could underpin how the molecular clock regulates SC quiescence.

Recently, other studies have reported that the expression of SC-specific BMAL1 oscillates on a ~24 h cycle with peak gene expression occurring at ZT16 (zeitgeber hour 16) in mice (17). The diurnal nature of SC specific BMAL1 offers support for the roles it plays in regulating SC quiescence, whether through Wnt or other mechanisms. To elucidate if peak diurnal BMAL1

expression in SCs effects rates of muscle regeneration, Zhu et al. (26) induced muscle injury using cardiotoxin injections at the same timepoint (ZT16/active-phase) to previously observed peak SC-BMAL1 gene expression, and at ZT4 (inactive-phase; lower BMAL1 gene expression than ZT16) in wildtype mice (85). Animals injured at ZT16 exhibited enhanced muscle repair compared to animals at ZT4, evidenced by greater average myofiber size and higher frequency of larger fibers 7 days post injury (85). This data suggests that if muscle is injured during the inactive-phase when SC-specific BMAL1 gene expression is low, SCs myogenic progression may be altered, and repair/regeneration may be attenuated. One possible rationale for altered myogenic progression during times of low SC BMAL1 expression could be due to Rev-erbα's inhibitory effect on SC-mediated myogenesis as animals lacking Rev-erbα experienced enhanced myogenic capacity in vitro and in situ (181). However, these animals were 8-10 weeks of age i.e., skeletally immature, and therefore extrapolating these findings to contexts of adult myogenesis may be difficult. Results from other studies show that BMAL1 induces diurnal transcription of Rev-erbα and upon expression, Rev-erbα inhibits BMAL1 expression (1). As Rev-erbα transcriptionally represses BMAL1, it is possible that altered myogenic progression observed at ZT4 in Zhu et al (2022) could be underpinned by a time-specific function of Rev-erbα to suppress myogenesis through limiting BMAL1 expression resulting in limited SC progression.

7.4.1.2 Role of BMAL1 in proliferation and regulation of MyoD

BMAL1's role during regeneration was further explored in that study by utilizing a SC-specific BMAL1 KO mouse model (85). Following toxin injury, SCs of these mice could not adequately mount an expansive/proliferative response and consequently had impaired regeneration evidenced by smaller myofiber sizes after 7 and 14 days injury compared to wildtype injured muscles at the

same time points. During quiescence, SCs mainly derive cellular energy for homeostatic requirements from oxidative sources, whereas proliferative activities are fueled by glycolytic sources to meet energetic demands (182-184). As such the impaired myogenic responses may stem from the inability of these SC's to energetically transition from mitochondrial to glycolytic metabolism (85). The transitioning of intracellular energetics within SCs is fundamental for the sequential expression of MRFs throughout myogenesis (76, 162, 163, 182). As SCs from SC-BMAL1 KO mice cannot transition into glycolysis, it is likely that BMAL1 circadian input is required for SC transitions between energetic states and thus, appropriate, and successive expression of MRFs supporting proliferative demands. Indeed, SC specific BMAL1 modulation of SC proliferation is likely mediated through timely actions on MRFs such as MyoD and Myogenin, who exhibit circadian expression rhythmicity (13, 55). Further evidence in support of an MRF/clock connection is that BMAL1-KO and CLOCK-mutant animals display blunted oscillatory expression patterns of MyoD, confirming the myogenic gene's circadian nature (13). Furthermore, BMAL1 is largely responsible for MyoD's circadian-oscillatory expression during early phases of myogenesis (88). Hence, BMAL1's timely regulation of MyoD expression could be one mechanism by which the molecular clock ensures the correct timeline for SC proliferation with respect to the overarching time-course of myogenic progression during muscle regeneration.

The relationship between MRF's and molecular clock components also reveals that MyoD, BMAL1, and CLOCK can form a transcriptional feedback-loop complex (55). In this positive feedback loop, BMAL1/CLOCK induces MyoD expression, with MyoD then binding BMAL1/CLOCK to amplify expression patterns of these two clock genes. This positive feedback transcriptional complex functions to synergistically bind shared muscle targets and collectively

modulate their expression patterns thereby rendering these genes as dual myogenic/molecular-clock targets (54, 55).

Collectively, BMAL1 and CLOCK influence SC myogenic progression through modulations of MyoD expression on a diurnal basis, with lack of these clock components leading to impaired myogenic progression and muscle repair. However, the precise mechanisms regulating how and when MyoD and/or other MRFs and clock components communicate with each other to guide appropriate timing of SC-mediated myogenesis is unknown. Furthermore, most investigations aimed at dissecting the relationships between BMAL1 and MRFs have focused exclusively on MyoD, and future work should aim to uncover how, and if molecular clocks interact with other MRF's such as Myf5, Mrf4, and Myogenin.

7.4.2 The molecular clock's role on SC-mediated muscle regeneration: Cry

7.4.2.1 Cry2 regulates differentiation via timely actions on the cell cycle gene, Cyclin D1

The results of recent investigations utilizing whole-body Cry1 and Cry2 KO mice demonstrate that Cry clock genes influence SC-derived myoblast differentiation/fusion through alterations in cell cycle progression (84) (Figure 7.3). Following chemical muscle injury, Cry1 KO mice undergo accelerated muscle regeneration. In contrast, regeneration in Cry2 KO mice is impaired, as evidenced by decreased embryonic-MHC content, an indicator of fewer fibers undergoing active regeneration. Cry2 KO animals also presented with defects in differentiative/fusion *in vitro* while Cry2 KD cell lines revealed that Myogenin is suppressed in the absence of Cry2. These defects in differentiation and regeneration processes in Cry2 KO animals and cell lines were attributed to a detrimental and premature exit from the cell cycle due to inhibited Cyclin D1 expression (84). Cyclin D1 is a known cell cycle 'check point' gene regulating transitions from G1 to S phase

during SC differentiation (76, 163). Taken collectively, current evidence suggests that Cry clock genes may regulate myogenic progression through downstream actions on SC cell cycle components and/or check-point genes. Furthermore, depending on when and what components of the SC-cell cycle Cry acts on, SC-mediated muscle repair may be either accelerated or impaired. This phenomena of modulating the timeline of myogenesis may be a unique quality of skeletal muscle and/or SC-specific molecular clocks and probably hinges on circadian expression patterns of Cyclin D1 and other cell cycle regulators (Figure 7.3). In line with this notion, Cyclin D1 exhibits circadian expression patterns throughout the day, whereas Cry2 KO mice have reduced rhythmic expression patterns (84). These data establish Cry2 as an upstream modulator responsible for circadian regulation over cell-cycle kinetics during differentiation (Figure 7.3).

7.4.2.2 Cry2's rhythmic expression of Tmem176b is required for appropriate myoblast fusion

Cry2's regulation of the cell cycle during myogenesis extends beyond differentiation, with observations of a circadian influence over SC-derived myoblast fusion showing that the myogenic fusion gene, Tmem176b, is expressed on a diurnal basis in muscle, with a lack of Cry2 leading to impaired expression patterns and incomplete myoblast fusion (84) (Figure 7.3). The dual influence of Cry on SC-derived myoblast differentiation and fusion provides insight into how the molecular clock in muscle and, potentially SCs effect the timeline of myogenic progression during muscle repair (84). However, since Cry2 modulates Cyclin D1 activity, impairments in fusion may stem from decreased myogenic differentiation. Cry clock genes modulating roles in differentiation and fusion are likely linked by their actions on the cell cycle during myogenesis following injury although further work is warranted to uncover the precise mechanisms underpinning such actions.

Future work involving SC-specific ablation of Cry clock genes will uncover the cascade of events that constitute Cry's downstream regulation on SC cell cycle kinetics that underpin clock control over differentiation and fusion timelines during myogenic progression.

7.4.3 The molecular clock's role on SC-mediated muscle regeneration: Per

7.4.3.1 Per1 and Per2 influence over quiescence, time-dependent rates of myogenic progression, and differentiation/fusion

Recently, it was reported that Per1 and Per 2 regulate the circadian expression of IGF2 (Insulin-like Growth Factor 2, a major regulator of muscle anabolism) in an upstream fashion, with the absence of Per1, 2 leading to the loss of rhythmic expression patterns in IGF2 (83). IGF2 KD *in vitro* or absence of IGF2 after injury to muscles of Pax7-specific IGF2 ablated animals led to impaired differentiation and fusion. These data suggest that Per1 and Per2 modulate myogenic progression through downstream circadian regulation of IGF2 (Figure 7.3). Results from other studies have demonstrated that IGF2 binds to the same receptor as IGF1 (upstream activator of mTORC1 anabolic signaling) and can mimic IGF1's actions in activating mTORC1 pathways, major drivers of muscle anabolism during hypertrophy, repair/regeneration (185, 186). Unlike mTORC1 in muscle, SC specific mTORC1 have distinct roles in regulating SC quiescence (187-190). Upon muscle injury, SCs of non-injured muscles receive systemic ligands that act on SC-specific mTORC1 machinery to shift cell cycle state from G-0 to G-Alert (187, 188). Although both G-states are quiescent, upon injury, SCs in G-Alert are activated more rapidly and exhibit faster regenerative capacity (187). Within the context of the clock gene *Per* and in light of the importance of mTORC1 in SCs, it is plausible that SC-specific Per1, 2 circadian regulation over IGF2 extends downstream to mTORC1 signaling within SCs. This would suggest Per1, 2 may function to prime SCs to more readily be activated based on time of day following muscle injury.

This view of enhanced SC "readiness" to initiate myogenesis is supported by reports that myogenic progression occurs at different rates when muscle is injured at different times of day (83, 85), and offers support that SC exit of quiescence and subsequent rates of myogenic progression are under circadian influence. Furthermore, other clock genes (i.e., Cry) have been shown to exert downstream regulation over IGF isoforms in several tissue types (191). Further work is required to determine whether the IGF family may be a shared downstream target gene family that multiple clock genes act on to modulate cell cycle progression and thus, myogenesis.

Recently, chemical injury to muscles of Per 1, Per 2, and Per 1/2 KO and wildtype animals were undertaken to determine how Per clock genes influence myogenesis following injury. Four days post-injury, Per 1, Per 2, and Per 1/2 KO mice displayed greater rates of proliferating SCs compared to wildtype mice. However, this observation may merely reflect delayed cell-cycle entry as the wildtype mice had already progressed past proliferative stages. Such a delay in proliferation in Per KO animals may, in part, be the reason why muscle regeneration was ultimately delayed post-injury. (83). To further investigate the mechanisms underpinning impairments in myogenic progression, Per KO myoblasts were utilized and shown to have reduced rates of differentiative and fusion, presumably due to altered cell cycle kinetics during proliferation. *In vitro* work utilizing Per 1/2 KD cell lines confirm that Per 1/2's influence over differentiative/fusion processes originates from their actions on the cell cycle during proliferative stages of myogenesis. (83). Given the evidence presented, the regulation of proliferation by Per 1, 2 may be bimodal through their modulations of SC "readiness" to initiate activation/progression during quiescence and via downstream actions on cell cycle components that facilitate proliferation. Specific approaches to alter Per clock genes within SCs will help elucidate what specific SC intracellular interactions underpin clock-gene regulation over SC-mediated myogenic progression.

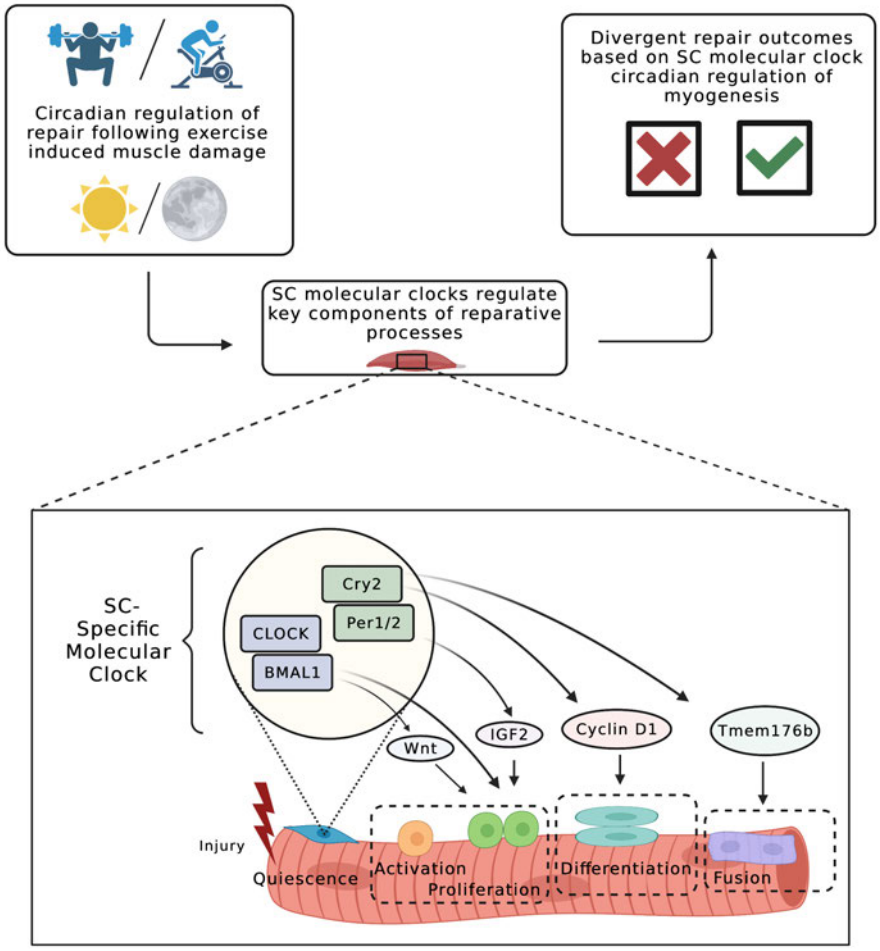

Figure 7.3: Circadian Regulation over Satellite Cell-Mediated Muscle Regeneration.

Schematic of circadian regulations on muscle repair following hypothetical exercise induced muscle damage underpinned by SC-molecular clock actions on components driving repair (activation/proliferation/differentiation/fusion) during myogenic progression. Time-appropriate actions by SC-molecular clocks on such regulated components may ultimately lead to divergent outcomes of repair.

7.5 Applications and Summary

The investigations reviewed have, for the most part, utilized non-physiological models of muscle injury in cell lines and/or rodents. Moving forward, human studies of exercise-induced damage/injury in association with time-course serial tissue (i.e., muscle) sampling will be required to evaluate the precise timelines and major regulatory nodes that clocks act on within SCs during skeletal muscle repair/regeneration in a physiological context. A plethora of human studies have utilized different variations of eccentric (lengthening) contractions to induce muscle injury/damage and have observed SC-mediated reparative events. However, the role of SC and/or muscle clocks in these contexts has not been adequately addressed (15, 74, 133, 136, 192-199). Future studies identifying time of day SC-clock regulatory functions over muscle injury and regeneration could provide information regarding the optimal time of day to undertake strenuous muscle damaging activities (i.e., eccentric exercise) so as to avoid possible increased injury-risks and/or inadequate abilities of SC-mediated regeneration at certain times of day (as observed in animal models from Zhu and colleagues). Additionally, as protein intake has been shown to enhance the SC response following muscle-damage, the timing of protein intake following exercise sessions to diurnal peaks of SC molecular clock expression may augment the SC-mediated reparative response as well as accelerate the overall timeline of repair (200, 201). Such insights would greatly impact the fields of performance and rehabilitation by aiding in the design of training/rehabilitation sessions and post-exercise feeding strategies which may serve as injury-preventative measures and augment repair outcomes/timelines.

In summary, I highlight the important role of BMAL1 in the early stages of SC activation and proliferation, with Per dictating the amount of time SCs spend in cell cycle proliferative stages. Per may also harbor a secondary function in regulating the optimal time-of-day SCs exit

quiescence after muscle injury, although further work is required to confirm this hypothesis. Differentiation and fusion appear to be a Per/Cry dual modulated event as both clock proteins act on cell cycle machinery responsible for facilitating these later stages of myogenesis. Taken collectively, I propose that molecular clock components of SCs influence myogenic progression during muscle repair/regeneration via regulation of MRFs and cell cycle machinery in a time-dependent fashion. Future work should aim to decouple the discreet contributions to repair/regeneration from muscle and SC molecular clocks as well as the interplay between them.

Acknowledgements

The writing of this review was, in part, supported by a Novo Nordisk Foundation Challenge Grant (NNF14OC0011493) to J.A.H.

All figures were created with Biorender.com.

Competing Interests

The authors declare no competing interests.

Author Contributions

RK, JAH, SD, OLK all contributed to preparations of this manuscript.

Chapter 8: study-3

Kahn RE, Zhu P, Roy I, Peek C, Hawley JA, & Dayanidhi S. (2024). Ablation of satellite cell-specific clock gene, *Bmal1*, alters force production, muscle damage, and repair following contractile injury. *Submitted to FASEB.*

Ablation of satellite cell-specific clock gene, *Bmal1*, alters force production, muscle damage, and repair following contractile injury

Ryan E. Kahn[1,2], Pei Zhu[5,6], Ishan Roy[2,3], Clara Peek[5,6], John A. Hawley[1*], Sudarshan Dayanidhi[2,3*]

[1]Exercise and Nutrition Research Program, The Mary MacKillop Institute for Health Research, Australian Catholic University, Melbourne, Australia

[2]Shirley Ryan AbilityLab, Chicago, IL, USA

[3]Feinberg School of Medicine, Northwestern University, Chicago, IL, USA

[5]Department of Biochemistry and Molecular Genetics, Northwestern University Feinberg School of Medicine, Chicago, IL, USA

[6]Department of Medicine, Division of Endocrinology, Metabolism, and Molecular Medicine, Northwestern University Feinberg School of Medicine, Chicago, IL, USA

Running Title: Contractile induced injury, repair, and myogenic progression following satellite cell *Bmal1* ablation

*Corresponding Authors: SD and JAH

E-mail: sdayanidhi@sralab.org

john.hawley@acu.edu.au

8.1 Abstract

Following injury, skeletal muscle undergoes repair via satellite cell (SC)-mediated myogenic progression. In SCs, circadian molecular clock gene, *Bmal1,* is necessary for appropriate myogenic progression and repair with evidence that muscle molecular clocks also affect force production. Utilizing a mouse model allowing for inducible depletion of *Bmal1* within SCs, I assessed contractile function, SC myogenic progression, muscle damage, and repair following eccentric contractile-induced injury. At baseline, SC-*Bmal1*^{iKO} animals displayed a ~20-25% reduction in normalized force production (*ex vivo* and *in vivo*) compared to control SC-*Bmal1*^{Cntrl} and SC-*Bmal1*^{iKO} control untreated littermates ($P < 0.05$). Following contractile injury, SC-*Bmal1*^{iKO} animals exhibited reduced signs of muscle damage and repair post injury (Dystrophin^{negative} fibers 24 h: SC-*Bmal1*^{Cntrl} 199 ± 41; SC-*Bmal1*^{iKO} 36 ± 13, $P < 0.05$) (eMHC^{+} fibers 7 day: SC-*Bmal1*^{Cntrl} 217.8 ± 115.5; SC-*Bmal1*^{iKO} 27.8 ± 17.3; Centralized nuclei 7 day: SC-*Bmal1*^{Cntrl} 160.7 ± 70.5; SC-*Bmal1*^{iKO} 46.2 ± 15.7). SC-*Bmal1*^{iKO} animals also showed reduced neutrophil infiltration, further indicating these animals had experienced less injury (Neutrophil content 24 h: SC-*Bmal1*^{Cntrl} 2.4 ± 0.4; SC-*Bmal1*^{iKO} 0.4 ± 0.2, % area fraction, $P < 0.05$). SCs from SC-*Bmal1*^{iKO} animals activated and proliferated at an earlier timepoint (24 h) in-line with these animals having experienced lesser necrosis and neutrophil-infiltration. SC-*Bmal1*^{iKO} animals displayed greater SC activation/proliferation at an earlier timepoint and had an unexplained increase in activation 7 days post injury. Collectively, these data suggest SC-*Bmal1* plays a regulatory role in force-production, influencing the magnitude of muscle damage/repair with altered SC myogenic progression following contractile-induced muscle injury.

8.2. Introduction

Molecular clocks reside in all cells and regulate numerous physiological processes in a circadian fashion (1, 202). Specifically, a transcriptional/translational feedback loop consisting of rhythmic expression of *Per/Cry* and CLOCK/ Bmal1 collectively underpin circadian rhythmicity (1, 202). Recent evidence demonstrates molecular clocks play a regulatory role in skeletal muscle repair from injury (78, 81, 82, 203, 204). In skeletal muscles, satellite cells (SCs) are the resident muscle stem cell population that lie quiescent sandwiched between the basal lamina and muscle membrane. Following injury, SCs proceed down a myogenic lineage via activation, proliferation, differentiation, and eventually fuse to the host myofiber to facilitate muscle repair (15, 16). SCs express molecular clock genes as well as several contractile and myogenesis related genes that oscillate over a 24 h cycle (17).

Molecular clocks play a critical role in muscle repair as myogenic progression and the magnitude of repair are impaired in Per1/2, Cry1/2, Bmal1 muscle-specific and whole-body knockout (KO) animals following injury (11, 83, 84). However, these studies have used either muscle or whole-body clock-gene ablation/KO methods, and the specific role of the SC molecular clock during muscle repair remains unclear. A previous study assessed the time-of-day capacity of SC-mediated repair following cardiotoxin-induced injury and reported blunted repair in the morning versus the evening (85). Such observations are likely underpinned by divergent time-of-day capacities of the SC-molecular clock. To directly assess the role of SC-molecular clocks in repair, the same study utilized an inducible depletion model capable of SC-specific *Bmal1* ablation. SCs lacking *Bmal1* did not proliferate sufficiently following cardiotoxin-injury, leading to blunted muscle repair (85). SC activation and proliferation hinges on the myogenic regulatory factor, MyoD (76), a clock-controlled gene (13, 26, 55). *Bmal1* binds to the core-

enhancer (CE) region of MyoD and ablation of the CE disrupts its diurnal expression and amplitude/timing during myogenic progression, ultimately leading to blunted myogenesis (86, 88), at least in embryonic muscle. While whole body Bmal1 KO models alter MyoD's response during SC proliferation (11, 12), evidence that SC-*Bmal1* affects MyoD is lacking.

Prior evidence has also shown *Bmal1* regulates contractile-force production in animal models (13, 52, 53, 205). As higher forces typically lead to greater magnitudes of muscle damage (67, 68), *Bmal1's* regulation on force production may lead to varying magnitudes of damage and subsequent repair. However, it is unknown if SC-specific, *Bmal1,* affects force production and if there any subsequent effects on contractile-induced injury and repair. Recent work has shown that SC ablation alters time-of-day muscle contractility, with the overall extent of contractile injury being associated with the magnitude of eccentric force (91). These results suggest that SC molecular clocks may regulate force-production, which may subsequently determine the extent of contractile injury. Accordingly in the present study, I hypothesized that SC-*Bmal1* would alter force-production characteristics and the extent of contractile-injury, muscle damage, and subsequent muscle repair. Given the role of *Bmal1* in myogenic progression, I also postulated that in response to physiological contractile injury, SC-*Bmal1* ablation would dysregulate myogenic progression. Utilizing a mouse model capable of SC-specific inducible depletion of molecular clock gene, *Bmal1*, I assessed baseline contractile function, and following *in vivo* eccentric contractile injury, muscle damage, SC myogenic progression, and muscle repair.

8.3. Methods

8.3.1 Animals

All animal experiments were undertaken after approval by the Northwestern University Institutional Animal Care and Use Committee. A previously established mouse model was utilized in this study for inducible depletion of SC-specific clock gene, *Bmal1* (85). To generate these mice, *Pax7CreER* mice were crossed with a *flox-stop-flox-tdTomato* mouse line (PMID: 20023653 – Jackson Labs, stock # 007905). Second generation *Pax7CreER/tdTomato* mice were then crossed with either SC-*Bmal1*$^{fx/fx}$ or SC-*Bmal1*$^{+/+}$ mouse lines to generate *Pax7CreER/tdTomato/Bmal1*$^{fx/fx}$ (SC-*Bmal1*^{iKO}) capable of inducible depletion or *Pax7CreER/tdTomato/Bmal1*$^{+/+}$ control mice (SC-*Bmal1*^{Cntrl}). Additionally, since the *tdTomato* is only expressed in the presence of *Pax7CreER* expression, this induces fluorescent labeling of SCs in this mouse model after treatment by tamoxifen (85). Genotyping (TransnetYX, Cordova, TN) was performed on all mice to ensure appropriate gene construct. In experimental mice (SC-*Bmal1*^{iKO}), *Bmal1* within SCs is floxed to allow for inducible depletion utilizing the Cre-Lox system, resulting in a >80% loss of *Bmal1* in SCs after treatment by tamoxifen (85). Both groups were treated with tamoxifen (2 mg in 100μL per day) via oral gavage for five consecutive days with a ten-day washout period. This leads to *Bmal1* ablation and *tdTomato* expression in SCs of SC-*Bmal1*^{iKO} animals while only *tdTomato* expression in SCs of SC-*Bmal1*^{Cntrl} mice. Both male and female animals between 12-16 months of age were used for all experiments (n=38, male = 19, female = 19). Animals were housed in a 14:10 light-dark cycle and fed *ad libitum* food. All *in vivo/ex vivo* experiments were performed between 1000-1200 h (ZT4-ZT6).

8.3.2 Baseline *in vivo* contractile characteristics

In vivo maximal tetanic and eccentric torque of the dorsiflexors were assessed in SC-*Bmal1*^{Cntrl}, SC-*Bmal1*^{iKO}, and SC-*Bmal1*$^{iKO\ Cntrl}$ (untreated) animals for baseline contractile

function measures. *In vivo* muscle contractility of the dorsiflexors was undertaken according to previous methods (Aurora Scientific, 3-in-1 contractile apparatus, 1300A Whole Animal Muscle Test System, Ontario, CA) (206). In brief, after general anesthesia, the left hindlimb was shaved, ankle fixed at 90^0 and inserted onto a foot-plate attached to a torque motor, capable of bi-direction torque measurement. Two needle-electrodes were placed percutaneously in the region of the peroneal nerve to selectively stimulate the dorsiflexors and twitch contractions (3-6 mA, 100Hz) were administered thereafter to optimize voltage and electrode placement (207). Dorsiflexor and plantar flexor torque were simultaneously evaluated throughout all contractions to ensure plantar flexors were not co-contracting. 500 ms maximal tetanic contractions separated by 3 min rest were administered to determine maximal isometric torque. One eccentric contraction was administered to determine maximal eccentric torque by a 300 ms maximal tetanus followed by a lengthening ramp of 50 ms that rotated the foot into 38^o of plantarflexion approximately at 200 degrees/s (starting foot position, -19 degrees; ending foot position, +19 degrees) (206). Optimal stimulation frequency was determined during pilot torque-frequency curves and all subsequent experimental tetanic and eccentric contractions were administered at 120Hz. All contractile torque data was normalized to mouse body mass (BW) and expressed as Nm/kg BW (57, 207, 208).

8.3.3 *In vivo* eccentric contractile injury

In vivo eccentric contractile injury in the dorsiflexors was induced via 200 electrically-stimulated eccentric contractions, with each contraction separated by 10 s rest (209). Maximal tetanic torque was assessed three min before and after the injury bout as an indirect measure of mechanical injury (torque-deficit in maximal tetanic torque) (67, 127, 135, 209-213). Total work

was calculated by the sum of work per contraction ((torque x angular displacement)/BW) across all 200 eccentric contractions per mouse. Following the injury protocol, mice were returned to their housing, allowed to recover and euthanized 24 h, 72 h, or 7 d post-injury (n=3-5/group). TA muscles were harvested to evaluate the injury, cellular responses, and repair processes at these the timepoints.

8.3.4 *Ex vivo* baseline contractile characteristics

Ex vivo tetanic and eccentric specific forces were assessed using the EDL of SC-*Bmal1*^{Cntrl} and SC-*Bmal1*^{iKO} animals (91). In brief, the left hindlimb was stabilized with pins, 5-0 silk sutures were tied to the proximal and distal tendons of the EDL and transferred to a bath containing Ringer's solution at 37° C (137mM NaCl, 5mM KCl, 1mM NaH_2PO_4, 24mM $NaHCO_3$, 2mM $CaCl_2$, 1mM $MgSO_4$, and 11 mM glucose containing 10 mg/L curare, pH 7.5). The proximal end of the muscle was sutured to a force-transducer (Aurora 300C, Aurora Scientific, Ontario, Canada) and the distal tendon sutured to a length-motor with platinum electrodes straddling the muscle end-to-end (124). A custom LabVIEW program recorded force, length, and time data from each contraction. Twitch contractions were used to optimize muscle length/voltage and fiber length was subsequently calculated using a standard fiber-length-to-muscle-length ratio of 0.51 for the EDL (144). Three 300 ms maximal tetanic contractions were used to determine maximal tetanic force (the highest of the three used as the tetanic force value). A single eccentric contraction was administered to determine maximal eccentric force and consisted of a 200 ms tetanus followed by a 100 ms lengthening ramp. The eccentric portion of the contraction consisted of muscle lengthening by 15% of L_f at a strain-rate of 2 L_f/s. All contractile data were measured in volts (V), converted to Newtons (N) based on a calibration

curve, and normalized to calculated physiological cross-sectional area (PCSA), and expressed as specific force (N/cm^2).

Time-to-peak tension (TPT) was assessed from the maximal tetanic contractions to evaluate differences in contractile kinetics. TPT was calculated as the time from baseline to the first data point of the maximal tetanic force plateau on the ascending limb of the force trace for each muscle. Half relaxation time (HRT) was calculated as the time from the last data point on the tetanic force plateau to the time that reflected half maximum tetanic force on the descending limb of the force trace.

8.3.5 Histology and Immunohistochemistry

TA muscle was flash frozen in liquid nitrogen-cooled isopentane immediately after euthanasia and stored at -80°C. Muscles were transferred to a -25°C cryostat and allowed to equilibrate for one hour prior to sectioning. In brief, the muscle mid-belly was cut perpendicular to the orientation of the fibers, embedded in a cryomold and flash frozen (10 s) in liquid nitrogen-cooled isopentane (214). Molds were then allowed to equilibrate in the cryostat for 30 min before sectioning. Sections were cut at 10 μm thickness. Slides were air-dried for one hour following sectioning and stored at -80°C until experimental procedures.

Prior to all staining, slides were thawed at room temperature for one hour. Hematoxylin & eosin (H&E) histological staining consisted of sequentially dipping slides into baths of the following: 1% glutaraldehyde, PBS, hematoxylin, tap water, alcoholic acid, tap water, ammonia water, DI water, alcoholic eosin, 70% ETOH, 80% ETOH, 95% ETOH, 100% ETOH (2x), Xylene (2x). Following staining, slides were coverslipped and stored at -20 ºC until imaging.

For immunohistochemistry (IHC), slides were thawed for 1 h prior to staining and a hydrophobic barrier was drawn around sections and allowed to dry for 20 min. Sections were washed in PBS, fixed in 4% paraformaldehyde (103), rehydrated with PBS washes, and were blocked in 1%BSA mouse-on-mouse blocking buffer for . Following blocking, primary antibody cocktails were made in 1%BSA and incubated overnight at -4 ^{o}C. The next day, sections were washed with PBS and incubated in a secondary antibody cocktail made in PBS. Sections were then washed with PBS, mounted using Vectashield with (Vectashield, H-1200) or without DAPI (Vectashield, H-1000), as appropriate, coverslipped, and stored at -20 ^{o}C until imaging (113, 214). Primary and secondary antibody details were as follows: Primary antibodies: anti-laminin (rabbit, IgG, 1:500, Sigma, L9393), anti-dystrophin (rabbit, IgG, 1:100, Abcam, ab15277), anti-MYH3 (eMHC) (mouse, IgG1, 1:50, DSHB, F1-652), anti-Ly-6G/C (rat, 1:30, BD Biosciences, lot # 553123), anti-Ki67 (rabbit, IgG, 1:200, Abcam, ab15580), anti-MyoD (mouse, IgG2b, 1:50, Santa Cruz Biotechnologies, sc-377460), anti-SC71 (mouse, IgG1, 1:50, DHSB, lot # 2147165), anti-BF-F3 (mouse, IgM, 1:100, DHSB, lot # 2266724). Secondary antibodies: Alexa Flour 488 goat anti-rabbit IgG (H+L) (1:250, Invitrogen, A-11034), Alexa Flour 488 goat anti-mouse IgG1 (1:250, Invitrogen, A21121), Alexa Flour 488 goat anti-mouse IgG2b (1:250, Jackson ImmunoResearch Laboratories, 115-545-207), Alex Flour 594 goat anti-rat IgG (H+L) (1:250, Invitrogen, A-11007), goat anti-mouse IgM (1:250, Invitrogen, A-21426).

8.3.6 Image acquisition and quantification

Images were taken at 10 x and 20 x magnification depending on the IHC protocol and whole tile-scan images were acquired (entire cross-section). For quantification of myofiber necrosis H&E images were used. “Necrosing fibers” were defined as fibers that had nuclei

covering the entire fiber. Based on Dystrophin IHC, fibers that were missing myofiber borders but had nuclei surrounding the remaining outline of the border (and inside the fiber in many cases) were classified as Dystrophin^{negative} fibers. In a subset of images, locations of these fibers were validated by finding the specific Dystrophin^{negative} fiber using fiber-borders, i.e., laminin-stained sections from a different slide of the same muscle. Ly6+ content was calculated as area-fraction of the total cross-sectional area using ImageJ. The number of eMHC+ positive fibers and fibers with centralized nuclei were manually quantified using ImageJ. As noted, tdTomato is expressed in the presence of *Pax7Cre* in this mouse model (85) and therefore all staining of SCs were accomplished via use of the tdTomato/Pax7/DAPI construct. Total tdTomato+ cell (SC) abundance in uninjured sections, tdTomato+/Ki67+/DAPI, and tdTomato+/MyoD+/DAPI cells were manually quantified in ImageJ and expressed as cells/100 fibers. Fiber-type quantification was performed using an automated muscle-analysis software MuscleJ (114).

8.3.7 Statistics

Individual groups were compared using unpaired t-tests for all contractile data. All IHC group data were analyzed using two-way ANOVAs with main effects of time and treatment, with post-hoc Sidak's multiple comparison tests. Simple linear regressions were also used to analyze relationships between selected variables. Statistical analyses were performed using Prism 9.0 (GraphPad, San Diego, CA) and reported throughout as mean ± standard error of mean (SEM).

8.4. Results

8.4.1 Baseline *in vivo* and *ex vivo* contractile characteristics are lower after *Bmal1* ablation in satellite cells

Baseline *in vivo* eccentric dorsiflexor torque was significantly lower (~20%) in SC-*Bmal1*^{iKO} compared to both SC-*Bmal1*^{Cntrl} and littermate-untreated control *SC-Bmal1*$^{iKO\ Cntrl}$ animals (SC-*Bmal1*^{iKO} 84 ± 5 Nm/kg BW; SC-*Bmal1*^{Cntrl} 105 ± 8 Nm/kg BW; SC-*Bmal1*$^{iKO\ Cntrl}$ 110 ± 4 Nm/kg BW) ($p < 0.05$) (Fig 8.1A). No differences were observed in tetanic torque. *Ex vivo* tetanic, eccentric specific forces were also reduced ~ 20%, ~ 26% respectively in EDL of SC-*Bmal1*^{iKO} versus control animals (tetanic specific force: SC-*Bmal1*^{Cntrl} 21 ± 1 N/cm^2; SC-*Bmal1*^{iKO} 16 ± 1 N/cm^2; eccentric specific force: SC-*Bmal1*^{Cntrl} 31 ± 2 N/cm^2; SC-*Bmal1*^{iKO} 23 ± 1 N/cm^2) ($p < 0.05$) (Fig 8.1B). There were no differences in tetanic TPT, HRT, fiber-type proportions (Fig 8.1C-D), or myofiber area.

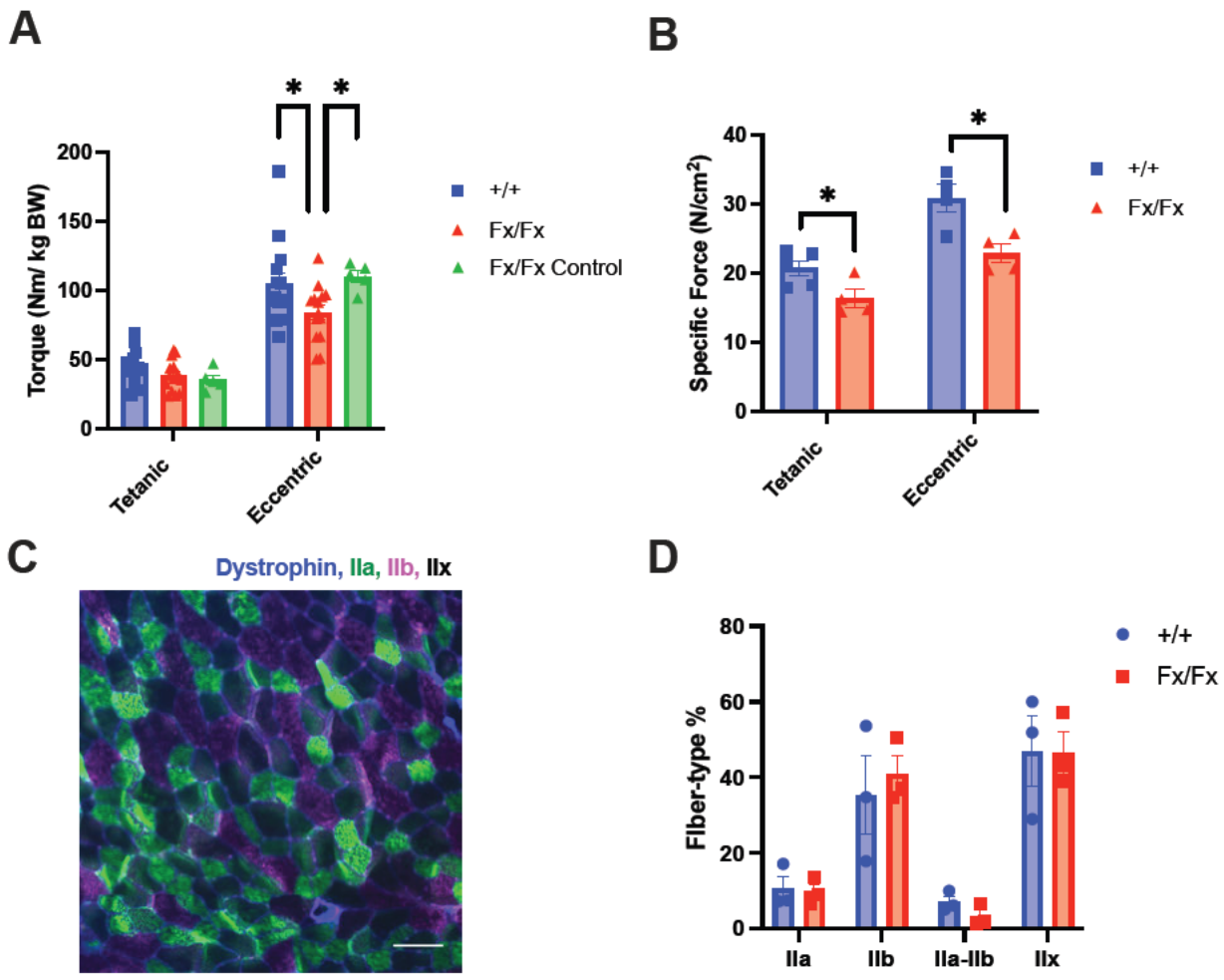

Figure 8.1: Force production is reduced in SC-Bmal1^{iKO} animals

1A) In vivo tetanic and eccentric torque of the dorsiflexors of all groups (Nm/kg BW) (SC-Bmal1^{Cntrl} and SC-Bmal1^{iKO} n=14-15, SC-Bmal1$^{iKO\ Cntrl}$ n=4-5). 1B) Ex vivo tetanic and eccentric specific forces of the EDL for Cntrl and iKO animals (N/cm^2) (n=4-5). 1C) Representative image of fiber-type distribution in the TA (blue: dystrophin; green: IIa; Magenta: IIb; Green/Magenta: IIa-IIb; Unlabeled: IIx) (scale bar set to 100 µm). 1D) Fiber-type distribution of TA muscle from Cntrl and iKO animals (n=3). All data shown as mean ± s.e.m.

*Contractile data groups were compared using unpaired t-tests. Fiber-type data groups compared using two-way ANOVA (*p<0.05).*

8.4.2 *In vivo* contractile injury

Figure 8.2A shows a representative trace of eccentric dorsiflexor torque over 200 eccentric contractions, which declines throughout the protocol indicative of contractile injury. Immediately following contractile injury, torque was decreased by a similar magnitude from maximal tetanic torque values between groups (SC-*Bmal1*^{Cntrl} 21 ± 2 (47% reduction); SC-*Bmal1*^{iKO} 19 ± 2.6 (49% reduction), units expressed as Nm/kg BW) (Fig 8.2B). Total work performed during the contractions were ~20% lower in SC-*Bmal1*^{iKO} compared to control animals (SC-*Bmal1*^{Cntrl} 12.5 ± 1.2 J/g; SC-*Bmal1*^{iKO} 9.9 ± 0.6 J/g; p = 0.06, Fig 8.2C).

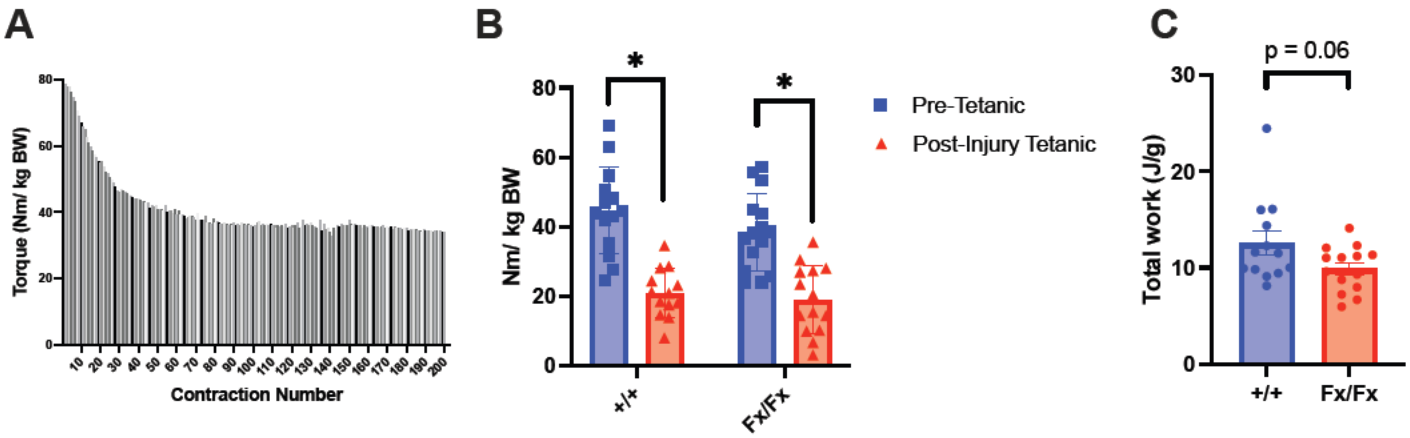

Figure 8.2: In vivo eccentric contractile injury

2A) A representative trace from a single animal of all 200 eccentric contractions (torque in units of Nm/ kg BW). 2B) Pre-injury torque versus post-injury torque values following 200 eccentric contractions in both groups (n=14-15). 1C) Total work performed in both groups throughout

200 eccentric contractions (n=14-15). All data shown as mean ± s.e.m. Groups were compared using paired t-tests for torque deficit data and unpaired t-tests for total work data ($p < 0.05$).*

8.4.3 SC-*Bmal1*^{iKO} animals exhibit less fiber necrosis and dystrophin^{negative} fibers following contractile muscle injury

Figures 8.3A-B, 8.3D-E are representative images of H&E and dystrophin-stained cross-sections showing uninjured and 24 h post-injury necrosing (H&E) and dystrophin^{negative} fibers, respectively. There was both a main effect for post-injury time and an interaction effect in necrosing as well as dystrophin^{negative} fibers, and a main effect of treatment for dystrophin^{negative} fibers. SC-*Bmal1*^{Cntrl} mice demonstrated greater necrosing fibers and dystrophin^{negative} fibers at 24 h versus 72 h and 7 days (Sidak's multiple comparisons, Fig 8.3C, 8.3F). However, there were no differences within SC-*Bmal1*^{iKO} groups between 24 h, 72 h, and 7 days. SC-*Bmal1*^{iKO} animals demonstrated ~62% less necrosing fibers and ~82% less dystrophin^{negative} fibers compared to SC-*Bmal1*^{Cntrl} animals 24 h post-injury (Sidak's multiple comparisons, 24 h: Necrosing fibers: SC-*Bmal1*^{Cntrl} 87 ± 18; SC-*Bmal1*^{iKO} 33 ± 15, Dystrophin^{negative} fibers: SC-*Bmal1*^{Cntrl} 199 ± 41; SC-*Bmal1*^{iKO} 36 ± 13). While these were higher in the SC-*Bmal1*^{iKO} at 72 h, they were not significantly different (Necrosing fibers at 72 h: SC-*Bmal1*^{Cntrl} 39 ± 14; SC-*Bmal1*^{iKO} 46 ± 14, Dystrophin^{negative} fibers at 72 h: SC-*Bmal1*^{Cntrl} 25 ± 11; SC-*Bmal1*^{iKO} 68 ± 19) (Fig 8.3C, 8.3F).

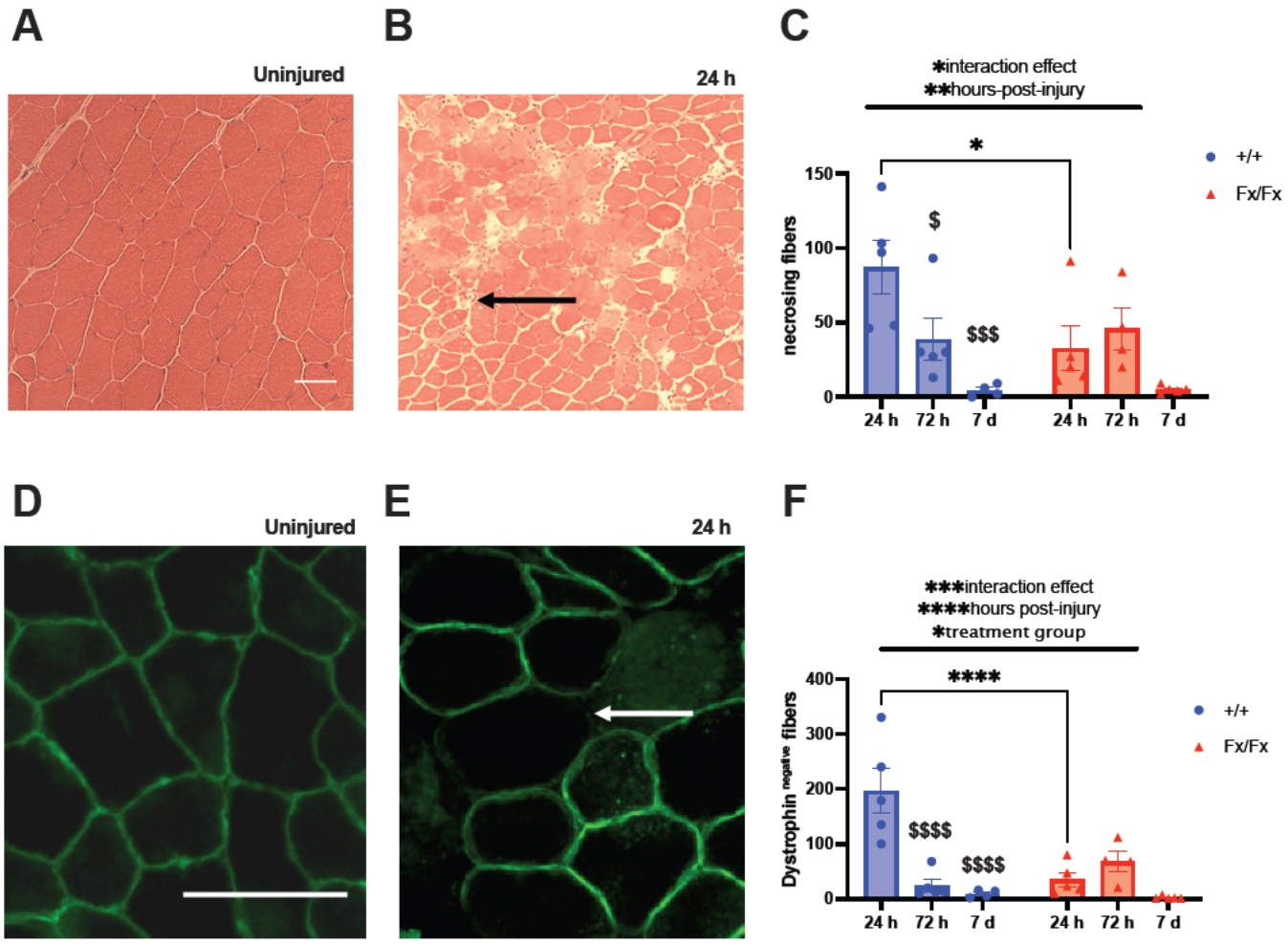

Figure 8.3: SC-Bmal1^{iKO} animals demonstrate less necrosing fibers and dystrophin^{negative} fibers compared to control animals

4A-B, 4D-E) Representative images of H&E and dystrophin-stained cross-sections showing uninjured and 24 h post-injury necrosing and dystrophin^{negative} fibers, respectively (arrow indicates necrosing fiber and dystrophin^{negative} fiber, respectively). 4C) Number of necrosing fibers in either group across all timepoints (n=4-5). 4F) Number of dystrophin^{negative} fibers in either group across all timepoints (n=4-5). Scale bar for all images set to 100 µm.

All data shown as mean ± s.e.m. Groups were compared using two-way ANOVA for main effects of hours-post-injury and treatment-group with post-hoc Sidak's multiple comparison tests (, refer to results for Cntrl versus iKO comparisons and,* ***$,*** *refer to results for intra-group significance) (p < 0.05*) (p < 0.005**) (p < 0.001***) (p < 0.0001****).*

8.4.4 SC-*Bmal1*^{iKO} animals exhibit reduced signs of muscle repair following contractile muscle injury

Figure 8.4A and 8.4C are representative images showing a cross-section stained for laminin (blue)/eMHC+(green) and an H&E cross-section reflective of centralized nuclei fibers, respectively, 7 d post-injury. In both eMHC+ fibers and fibers containing centralized nuclei, using a two-way ANOVA, a main effect of time post-injury and an interaction effect were observed. SC-*Bmal1*^{Cntrl} mice revealed a greater number of fibers containing centralized nuclei and eMHC+ fibers at 7 d versus 24 h and 72 h (Fig 8.4B, 8.4D, Sidak's multiple comparisons). However, no differences were noted across timepoints within SC-*Bmal1*^{iKO} groups in eMHC+ fibers or centralized nuclei. Muscle repair (measured as eMHC+ fibers and fibers containing centralized nuclei) was lower in SC-*Bmal1*^{iKO} compared to SC-*Bmal1*^{Cntrl} animals with ~87% fewer eMHC+ fibers and 71% fewer fibers containing centralized nuclei at 7 d post injury (eMHC^{+} fibers 7 day: SC-*Bmal1*^{Cntrl} 217.8 ± 115.5; SC-*Bmal1*^{iKO} 27.8 ± 17.3; Centralized nuclei 7 day: SC-*Bmal1*^{Cntrl} 160.7 ± 70.5; SC-*Bmal1*^{iKO} 46.2 ± 15.7, Sidak's post-hoc multiple comparisons).

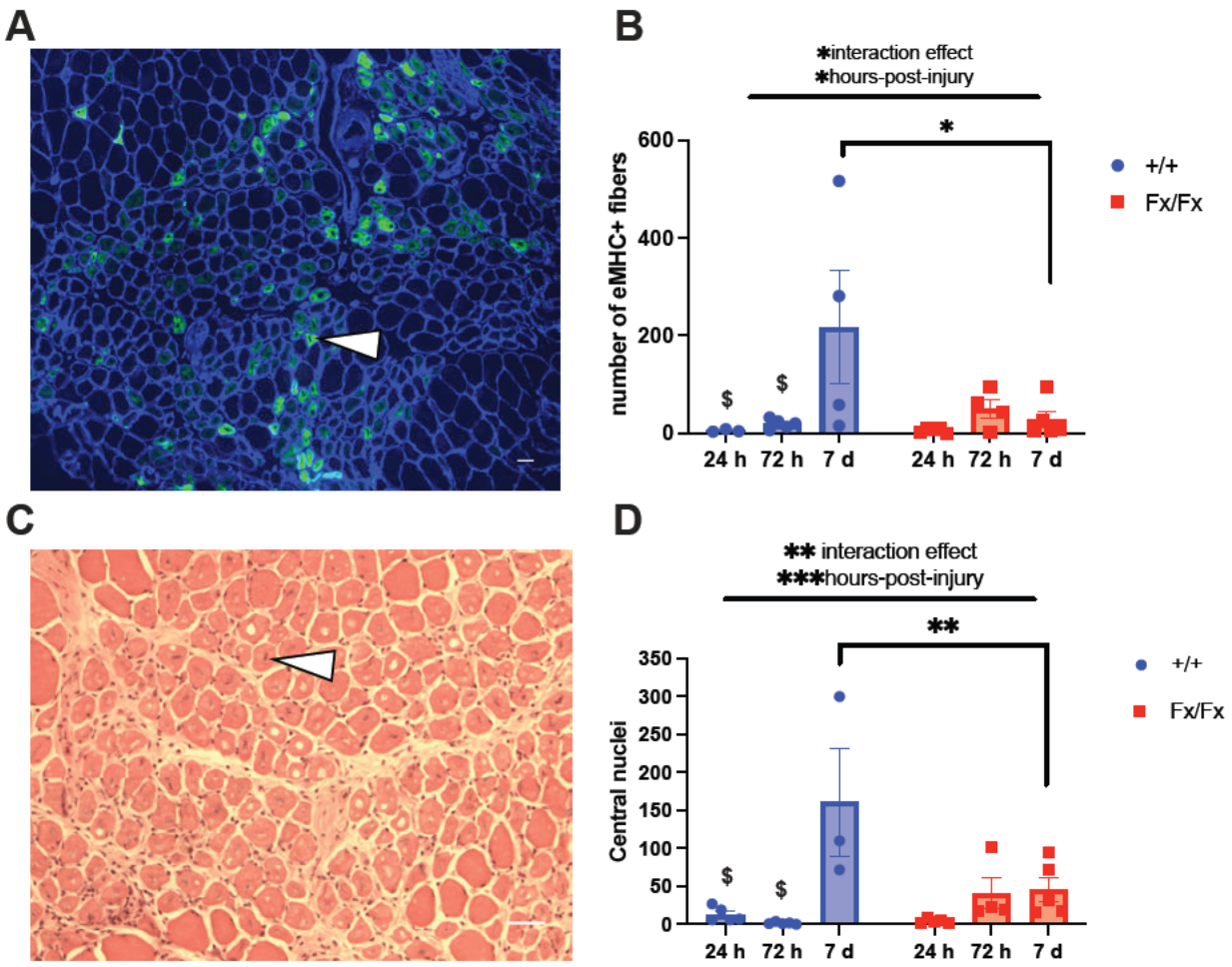

Figure 8.4: SC-Bmal1^{iKO} animals exhibit lesser degrees of muscle repair on day seven post-injury

5A, 5D) Representative images showing an uninjured and a 7 day post-injury cross-section stained for laminin (blue)/eMHC+ (green) and a H&E cross-section reflective of centralized nuclei fibers, respectively (arrows indicate eMHC+ fiber and a fiber with a centralized nuclei, respectively). 5B) Total number of fibers expressing eMHC+ across timepoints and groups (n=3-5). 6D) Total number of fibers containing centralized nuclei across timepoints and groups (n=4-5). Scale bar for all images set to 100 μm. All data shown as mean ± s.e.m. Groups were compared using two-way ANOVA for main effects of hours-post-injury and treatment-group with post-hoc Sidak's multiple comparison tests (, refer to results for Cntrl versus iKO comparisons*

and, ***$,*** *refer to results for intra-group significance) ($p < 0.05$*) ($p < 0.005$**) ($p < 0.001$***) ($p < 0.0001$****).*

8.4.5 Reduced neutrophil response following contractile muscle injury in SC-*Bmal1*^{iKO} animals

Figure 8.5A is a representative image showing a cross-section stained for dystrophin, Ly6G/C^{+} content (referred to as Ly6+), DAPI and a merged image. Overall, using a two-way ANOVA, main effects of treatment-group and time (h) post-injury were observed as well as an interaction effect. Control SC-*Bmal1*^{Cntrl} mice demonstrated greater Ly6+ content at 24 versus 72 h and 7 d (Fig 8.5B, Sidak's multiple comparisons). However, no such differences were detected within SC-*Bmal1*^{iKO} groups. Neutrophil content (Ly6+ content) was ~83% reduced at 24 h in SC-*Bmal1*^{iKO} versus control animals (neutrophil content at 24 h: SC-*Bmal1*^{Cntrl} 2.4 ± 0.4; SC-*Bmal1*^{iKO} 0.4 ± 0.2, % area fraction, Sidak's multiple comparisons, Fig 8.5B). Furthermore, across all timepoints in both SC-*Bmal1*^{Cntrl} and SC-*Bmal1*^{iKO} groups, the number of dystrophin^{negative} and necrosing fibers were positively associated with neutrophil content (dystrophin^{negative} fibers $r^2 = 0.85$ and 0.41; necrosing fibers $r^2 = 0.42$ and 49, respectively).

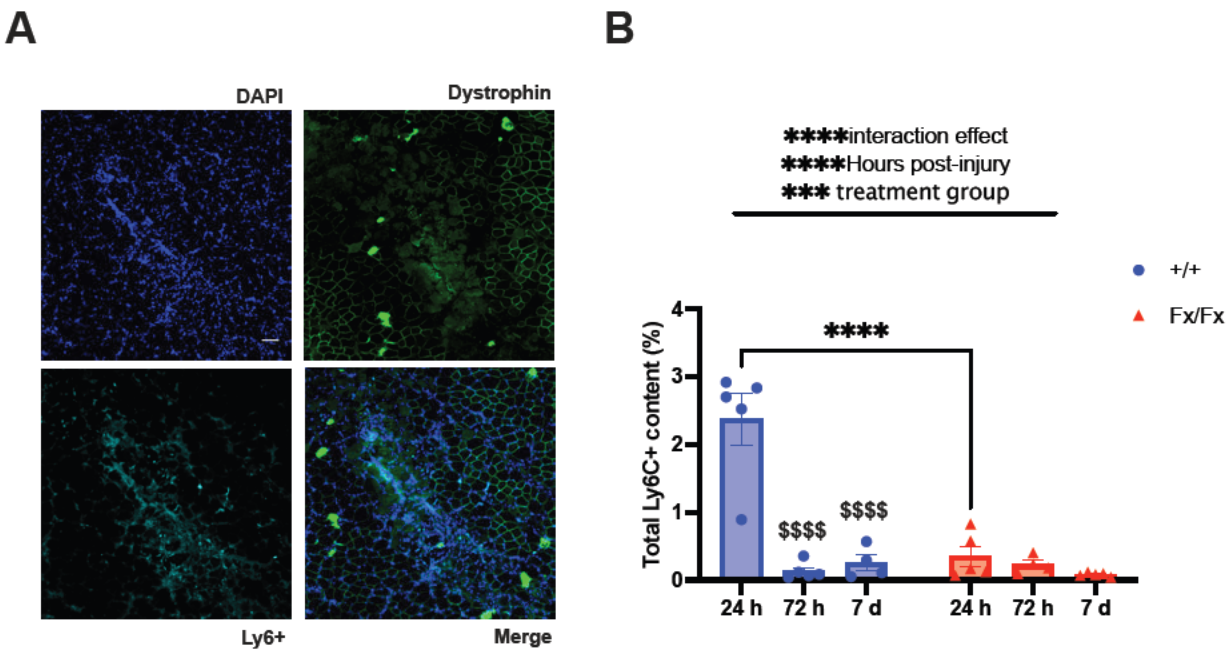

Figure 8.5: SC-Bmal1^{iKO} animals experience less neutrophil infiltration

5A) Representative image showing a cross-section stained for DAPI, dystrophin, Ly6^{+} content, and a merge image. 5B) Total Ly6^{+} content in either group across all timepoints (n=4-5). Scale bar for all images set to 100 µm. All data shown as mean ± s.e.m. Groups were compared using two-way ANOVA for main effects of hours-post-injury and treatment-group with post-hoc Sidak's multiple comparison tests (, refer to results for Cntrl versus iKO comparisons and,* ***$,*** *refer to results for intra-group significance) (p < 0.05*) (p < 0.005**) (p < 0.001***) (p < 0.0001****).*

8.4.6 Altered satellite cell activation and proliferation following contractile muscle injury in SC-*Bmal1*^{iKO} animals

There were no group differences in baseline tdTomato^{+} SCs in the uninjured limb in a subset of animals (SC-*Bmal1*^{Cntrl}: 24.9 ± 2.2; SC-*Bmal1*^{iKO}: 25 ± 2.4 SC/100fibers, Supplemental Figure 8.S.1A). Figure 8.6A and 8.6C are representative images showing a cross-section with DAPI,

tdTomato^{+} (Pax7), MyoD or Ki67 (respectively) and a merged image. In both SC-activation and proliferation, using a two-way ANOVA, main effects of treatment-group and time as well as an interaction effect were observed (Fig 8.6B, 8.6D). SC-*Bmal1*^{Cntrl} mice demonstrated greater SC-activation and proliferation at 72 h compared to 24 h and 7 days (Fig 8.6B, 8.6D, Sidak's multiple comparisons). In SC-*Bmal1*^{iKO}, SC-activation and proliferation was greatest at 24 h versus 72 h, 7 days (Fig 8.6B, 8.6D). Additionally, in SC-*Bmal1*^{iKO}, SC-activation was increased at 7 days compared to 72 h (Fig 8.6B). There was greater SC-activation in SC-*Bmal1*^{iKO} versus SC-*Bmal1*^{Cntrl} animals at 24 h and 7 days but, lower levels of activation at 72 h (SC-activation 24 h, 72 h, 7day: SC-*Bmal1*^{Cntrl} 2.9 ± 0.4, 8.5 ± 0.9, 0.2 ± 0.1; SC-*Bmal1*^{iKO} 13.6 ± 1.3, 0.1 ± 0.04, 5.6 ± 1.6, all units in tdTomato+/MyoD+ cells/100 fibers, Sidak post-hoc analysis) (Fig 8.6B).

Similarly, compared to SC-*Bmal1*^{Cntrl} animals, SC-*Bmal1*^{iKO} animals exhibited significantly greater SC-proliferation at 24 h and lower proliferation at 72 h post-injury (SC-proliferation 24 h, 72 h, 7day: SC-*Bmal1*^{Cntrl} 0.4 ± 0.1, 1.3 ± 0.3, 0.3 ± 0.1; SC-*Bmal1*^{iKO} 2.4 ± 0.5, 0.3 ± 0.1, 0.4 ± 0.1, all units in tdTomato+/Ki67+ cells/100 fibers) (Fig 8.6D). There were positive associations between SC-proliferation and neutrophil content at 24 h post-injury, when neutrophil content was greatest (SC-*Bmal1*^{Cntrl} $r^2 = 0.75$, $p = 0.058$; SC- *Bmal1*^{iKO} $r^2 = 0.86$, $p < 0.05$). A positive association was also observed in both SC-*Bmal1*^{Cntrl} and SC-*Bmal1*^{iKO} for SC-activation and SC-proliferation ($r^2 = 0.45$, $r^2 = 0.68$, respectively).

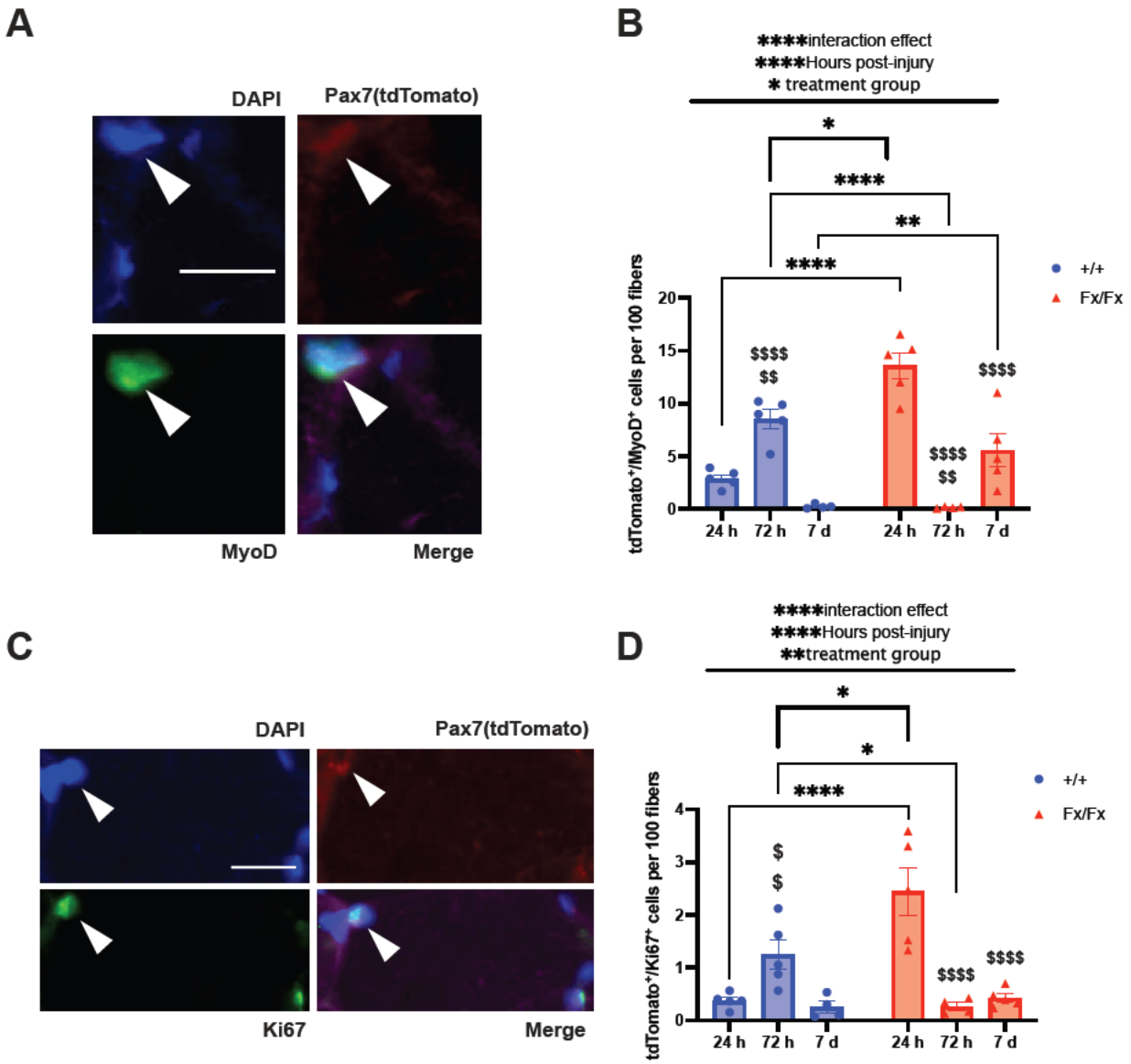

Figure 8.6: Altered SC-activation and proliferation kinetics in SC- Bmal1^{iKO} animals vs control animals

6A, 6C) Representative images showing a cross-section stained for DAPI, tdTomato (Pax7), MyoD or Ki67 (respectively), and a merge image. 6B) Comparison of Pax7^{+}/MyoD^{+} activated SCs across timepoints and between groups (n=4-5). 6D) Comparison of Pax7^{+}/Ki67^{+} proliferating SCs across timepoints and between groups (n=4-5). Scale bar for all images set to

100 µm. All data shown as mean ± s.e.m. Groups were compared using two-way ANOVA for main effects of hours-post-injury and treatment-group with post-hoc Sidak's multiple comparison tests (, refer to results for Cntrl versus iKO comparisons and, **$**, refer to results for intra-group significance) ($p < 0.05$*) ($p < 0.005$**) ($p < 0.001$***) ($p < 0.0001$****).*

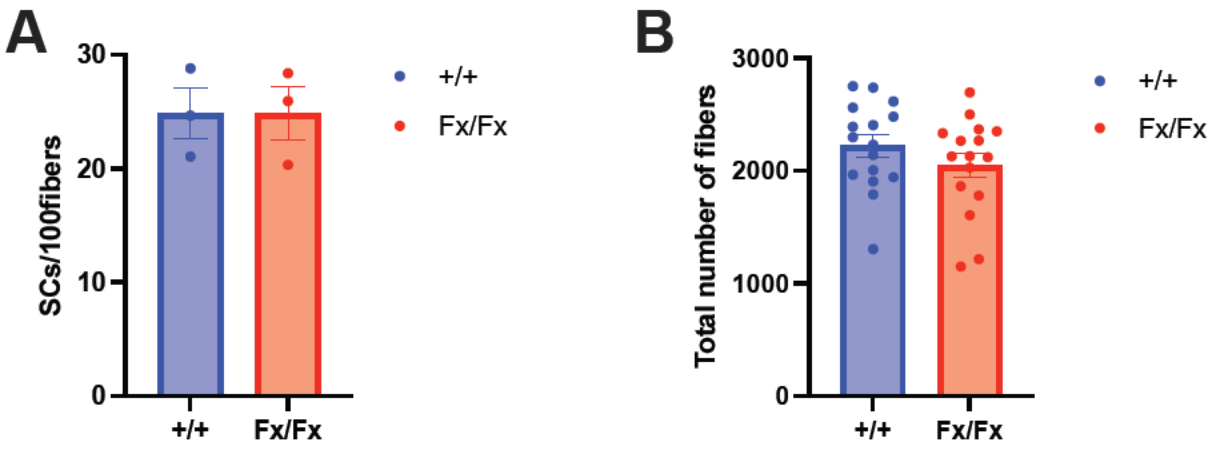

Figure 8.S.1: No difference in baseline satellite cell abundance between SC-Bmal1^{Cntrl} and SC-Bmal1^{iKO} animals

S1A) Baseline satellite cell abundance between groups (n=3). S1B: Total number of fibers analyzed. All data shown as mean ± s.e.m. Groups were compared using unpaired t-tests ($p<0.05$).

8.5 Discussion

Using an inducible depletion model of SC-specific clock gene, *Bmal1* (SC-*Bmal1*^{iKO}), I measured contractile function, contractile-induced injury muscle damage, repair, and myogenic progression. The major findings were 1) ablation of SC-*Bmal1* reduced force production (*in vivo*

and *ex vivo*) versus control animals, 2) SC-*Bmal1*^{iKO} animals experienced less muscle damage (determined by muscle fiber necrosis, dystrophin^{negative} fibers, and neutrophil content) and subsequently displayed fewer regenerating fibers, and 3) the SC myogenic trajectory (activation and proliferation) was altered in SC-*Bmal1*^{iKO} animals with SC-activation/proliferation occurring earlier and activated to a greater extent compared to control animals. These data suggest SC specific *Bmal1* plays a regulatory role on force-production and, following contractile injury, may influence the magnitude of damage/repair and SC-myogenic progression.

Following *in vivo* eccentric injury, both SC-*Bmal1*^{iKO} and control animals exhibited reductions in maximal torque, with the ~50% decrease being in close agreement with previous contractile injury models (207, 209, 215). Yet despite similar percentage reductions in maximal torque, SC-*Bmal1*^{iKO} animals displayed reduced damage/necrosis and neutrophil infiltration following contractile-injury. A likely explanation for these reductions in markers of muscle damage could be the lower forces produced by SC-*Bmal1*^{iKO} animals, although the precise mechanisms underpinning such force reductions are not easily explained and were not linked to differences in muscle fiber-type, myofiber area, or contractile kinetics. As such, I reason that SC-molecular clocks may exert regulation on contractility via modulation of sarcoplasmic reticulum (SR) Ca^{++} availability for contractile units. This is supported by previous findings that showed SCs have time-of-day specific control over contractile function via Ca^{++} availability (91) with evidence elsewhere showing muscle molecular clocks harbor regulation over Ca^{++} contractile proteins and signaling pathways (26, 56, 139). Elsewhere, whole body and muscle-specific *Bmal1* KO animals exhibit lower force-production with the underlying mechanism in these studies being a result of long-term dysregulations on titin, leading to sarcomere-length modifications (13, 52, 54, 55). However, these animal models were either bred from birth

lacking *Bmal1* or assessed 22 and 58 weeks following *muscle-Bmal1* ablation (52) and therefore it is likely the mechanisms underpinning such force-alterations are different than the current study in which animals were assessed 10 days following SC-*Bmal1* ablation.

Following muscle fiber damage, a first wave of immune cells and neutrophils infiltrate damaged-regions to initiate a necrotic microenvironment that subsequently necessitates a reparative response from SCs upon further immune-myogenic crosstalk signaling (70, 73, 216). In this regard, I show that the amount of damaged/necrosing fibers is associated with the neutrophil response across all timepoints in both SC-*Bmal1*^{Cntrl} and SC-*Bmal1*^{iKO} animals, confirming that neutrophils are a function of damage-induced necrosis independent of the extent of damage that occurred in the absence of SC-*Bmal1*. SC-*Bmal1*^{iKO} animals experienced significantly less damaged/necrosing fibers compared to their SC-*Bmal1*^{Cntrl} counterparts at 24 h and consequently less neutrophil infiltration. One explanation for this observation is that the lower forces generated by SC-*Bmal1*^{iKO} animals did not induce widespread damage adequate to trigger a more extensive immune response. Others have reported that when contractile-injury is induced via low versus high forces, the extent of injury scales as force increases (67). In line with this, SC-*Bmal1*^{iKO} animals exhibited less eMHC+ fibers and centralized nuclei seven days post-injury suggesting that these animals indeed experienced lesser degrees of muscle repair as well. I note however, in cases of extreme injury (i.e. cardiotoxin) when the extent of damage exceeds what contractile forces are capable of inducing, the relationship between SC-molecular clocks and the damage-induced neutrophil response may manifest differently (89). This is likely because models of extreme injury can expose the maximum capacities of cellular events in the muscle regenerative cascade compared to contractile injuries (217). In this regard, the regulatory mechanisms observed in *Zhu et al* 2024 between SC-molecular clocks and neutrophils following

cardiotoxin injury might also be at play in this work here as well but, may be masked by the higher/lower forces that induced the contractile injury. Potential evidence for this may, in part, be the dysregulated temporal relationship of necrosis, dystrophin^{negative} fibers, and neutrophil infiltration observed across timepoints post-injury in SC-*Bmal1*^{iKO} animals.

Following contractile-induced muscle injury, the necrotic and neutrophil response necessitates SC myogenic progression to facilitate muscle repair (15, 70, 73, 218, 219). Consistent with this notion, I show that across all animals and timepoints, SC activation/proliferation proceeded following contractile injury induced damage. However, the timeline of SC progression differed between groups as SC activation/proliferation in SC-*Bmal1*^{iKO} peaked at 24 h compared to a later response (72 h) in SC-*Bmal1*^{Cntrl} animals. One explanation for this earlier timeline of SC progression could be that these animals experienced less damage/neutrophil infiltration permitting SCs to become activated sooner. Indirect support for this premise can be seen in human models of eccentric damage in which SC activation following voluntary versus electrically-stimulated (ES) eccentric contraction occurs at an earlier timepoint, likely due to there being no "delay" in activation as there is less fiber-necrosis that occurs after voluntary versus ES eccentric contractions (15, 36, 90).

Despite having experienced less damage/repair, SC-*Bmal1*^{iKO} animals displayed higher relative peaks in SC-activation/proliferation at 24 h and an unexplained increase in activation at 7 days post-injury versus control animals. Since SC-*Bmal1*^{iKO} animals underwent less damage/necrosis, neutrophil infiltration, and muscle repair, the greater extents of SC activation/proliferation are somewhat surprising. These findings may be related to the critical role *Bmal1* plays in MyoD's rhythmicity (26, 88) where, upon inducible depletion of *Bmal1* in SCs, MyoD's trajectory/amplitude during myogenesis may have been perturbed. *Bmal1* binds to

the core-enhancer (CE) region of MyoD during homeostasis which in-turn induces MyoD's rhythmic expression throughout the day. However, the ablation of the CE region blunts such rhythmicity and dysregulates MyoD's timing/amplitude of expression during myogenesis (86, 88). This may partially explain the observations of an increased amplitude at 24 h and altered timing at 7 days post-injury of SC-MyoD content in SC-*Bmal1*^{iKO} animals. Collectively, these data suggest SC-*Bmal1* may be required for the appropriate timing of MyoD's response throughout regenerative-myogenesis, which is in line with previous work demonstrating that animals lacking Bmal1's binding site on MyoD had dysregulated MyoD expression during embryonic myogenesis ultimately blunting muscle growth (86-88). Additional evidence shows that SCs and SC-derived myogenic progenitors of Bmal1 KO animals (whole-body and SC-specific) harbor alterations in activation and proliferation following injury, offering further support that *Bmal1* regulates MyoD and thus SC activation/proliferation (11, 76, 85, 161).

In contrast to the work here, a previous study from the group demonstrated that SC expansion following cardiotoxin injury is reduced following SC-*Bmal1* ablation leading to inhibited muscle repair. However, as extreme non-physiological injuries cause far more damage vs contractile injuries, the mode of injury utilized across the two studies may underlie the differences observed in SC activation. Speculatively, the augmented SC activation noted in this study may be a compensatory mechanism to still successfully carry out adequate muscle repair in the absence of *Bmal1* whereas the limitations of SCs to carry out repair when damage is much greater is exposed during repair following non-physiological injury.

8.6. Conclusion

In conclusion, ablation of SC-*Bmal1* resulted in ~20-25% lower force-production *in vivo* and *ex vivo* compared to control animals. Following *in vivo* contractile injury, SC-*Bmal1*^{iKO} animals experienced less necrosis and muscle repair, suggesting their reduced forces led to a lesser extent of injury. In line with this notion, SC-*Bmal1*^{iKO} animals exhibited less neutrophil infiltration post-injury as well. Additionally, SC activation and proliferation occurred earlier (24 h versus 72 h) in SC-*Bmal1*^{iKO} animals indicating the reduced neutrophil response allowed for an earlier timeline of SC myogenic progression. Finally, although SC-*Bmal1*^{iKO} may have experienced less damage, potentially explaining the earlier peaks in SC progression, these mice exhibited a greater extent of SC activation as well as an unexplained increase in activation 7 days post-injury. These findings indicate SC-*Bmal1* may be required for the appropriate response and timing of MyoD during regenerative myogenesis. Collectively, ablation of SC-*Bmal1* lowered force-production and altered the magnitude of muscle-damage/repair and SC-myogenic progression following eccentric contractile injury.

Acknowledgements

I acknowledge discussions with Orly Lacham-Kaplan and Leonidas Karagounis. I thank Rick Lieber for the use of his *ex vivo* contractility setup. This work was supported, in part, by a Novo Nordisk Foundation Challenge Grant (NNF14OC0011493) to J.A.H, National Institutes of Health grant HD094602 to S.D.

Data Availability Statement

All data used within the results and to create figures are included in the material of this manuscript. Additional analysis and files can be provided upon request.

Competing Interests

The authors declare no competing interests.

Author Contributions

RK, SD, JAH contributed to conceptualization and preparation of this manuscript. RK performed all experimentation. RK drafted manuscript. CP and PZ provided the animals used in these experiments and were involved in data interpretation and determining experimental direction. IR provided the *in vivo* contractile apparatus setup used on all animals. RK, JAH, SD, CP, PZ, IR contributed to manuscript editing and revising.

Chapter 9: General Discussion and Concluding Remarks

9.1 Summary

The overall aim of the experiments undertaken for this thesis was to investigate the effects of the SC-molecular clock on muscle mitochondrial function, contractile function and contractile-induced injury and repair processes. To address these aims, two mouse models capable of either whole (Pax7DTA) or partial (SC-Bmal1^{iKO}) KO of the SC-molecular clock were utilized. Experiments also involved time-of-day study-designs (morning, afternoon, evening) and *ex vivo*, *in situ*, or *in vivo* measurements of muscle mitochondria, contractility, and muscle damage/repair across three studies (chapters 3, 5, 8). In the first experimental study (chapter 3), mitochondrial function was assessed in glycolytic and oxidative muscles in the morning, afternoon, and evening in the presence and absence of SCs (Pax7DTA mice) to identify any SC time-of-day regulation. At timepoints exhibiting time-of-day differences in study-1 (chapter 3), study-2 (chapter 5) utilized the same timepoints and animal-model to investigate if force-production displayed diurnal variance due to SC time-of-day influences. In study-3 (chapter 8), utilizing a SC-specific Bmal1 KO model, the SC-molecular clock was evaluated for its role in muscle repair following contractile-induced injury. Collectively, the findings from this series of independent but related investigations have provided novel insights regarding SC-molecular clock regulations on muscle mitochondria, contractility, and muscle repair.

The results from study-1 (described in chapter 3) revealed that SCs are not a factor that influence mitochondrial respiration according to time-of-day. At a peak and trough in *Bmal1* and *CLOCK* molecular clock gene expression, I found that mitochondrial-dependent submaximal fatigue in glycolytic muscle (EDL) was ~35% more fatigue resistant in the morning versus afternoon. Given the evidence provided in study-1 (chapter-3), SCs do not influence diurnal

mitochondrial function and therefore time-of-day differences noted in submaximal fatigue are unlikely due to time-of-day regulations (SC, muscle, or otherwise) on mitochondrial respiration. As a main finding from study-1 demonstrated time-of-day differences in submaximal contractile fatigue independent of SC influence on mitochondria, the subsequent experimental chapter therefore focused solely on SC time-of-day influence of contractility.

The major findings from study-2 (chapter 5) revealed that SCs differentially regulate force-production by time-of-day and such variation in force production altered the magnitude of *ex vivo* eccentric contractile injury. Specifically, eccentric force was reduced in the morning in the presence of SCs with these animals experiencing lesser degrees of contractile injury versus their SC^{-} counterparts. The mechanism underpinning these force reductions in the morning are suggested to be lower volumes of Ca^{++} available to contractile units (assessed via caffeine-contracture force). No differences in force production or magnitude of injury were observed between afternoon groups suggesting that SCs regulate force-production early, but not later in the day. This work is the first to demonstrate that SCs have an influence on contractile function according to time-of-day with this effect, in part, likely to be mediated by the SC-molecular clock. As differences were noted in extents of injury due to SC time-of-day alterations in force, the next experiment focused on how/if SC-molecular clocks regulate repair following *contractile* induced injury.

The major findings for the final study in this thesis were that SC-molecular clocks have a regulatory role in contractile function, the extent of muscle damage, repair, and SC myogenic progression following contractile injury. Of note, ablation of SC-Bmal1 led to reduced force production with these animals experiencing concordantly lesser degrees of muscle damage and repair. This phenomenon of higher/lower degrees of force-production leading to concordant

magnitudes of muscle damages in in agreement with past works (67, 68) (reduced force equates reduced injury) with evidence from this study suggesting SC-molecular clocks also harbor influence over this mechanism. Additionally, as a result of less damages sustained, these animals experienced earlier peaks (24 h versus control animals 72 h) in SC activation and proliferation, with the relative increase in SC activation and proliferation being approximately two-fold higher versus control animals, despite less damages and repair 7 days post-injury. This evidence of dysregulated SC myogenic progression aligns with past work showing that ablation of the bindings site of Bmal1 on MyoD altered both MyoD's circadian rhythmicity and the temporal expression pattern of MyoD/Pax7 cells during myogenesis (86, 88). Collectively, the findings from this study demonstrate that SC-molecular clocks regulate force-production and thus the extent of muscle damage/repair while also having independent regulation on SC myogenic progression during repair.

9.2 Study limitations

In the experimental studies described, several limitations exist. In the experiments described in chapters 3, and 5, animals were assessed across times of day in the presence/absence of SCs and it was assumed that any effects observed were due to SC-molecular clocks. However, as the entire SC was ablated (not just molecular clocks), the results may be impacted by factors related to SC ablation. Additionally, muscles and/or the muscle microenvironment may adapt when experiments are conducted long-term following SCs ablation (64). Also of note, a previous study has reported the drug-metabolizing enzymes involved in tamoxifen pharmacokinetics exhibit marginal circadian behavior (220). Therefore, to mitigate any such aforementioned effects, experiments were conducted after a washout period of at least 10-14 days following tamoxifen-

treatment in line with past works (95, 118). Secondly, in study-1, as the number of experimental mice were limited, submaximal fatigue experiments were only performed on SC^+ mice aligned to selected time-points reflective of time-of-day differences in clock gene expression and not performed in SC^- mice. Lastly, in studies 1 and 2, *Gapdh* was used as a housekeeping gene however, I recognize the importance of using multiple housekeeping genes for assessing gene expression. In chapter 8, a novel mouse model that allowed for SC-specific ablation of molecular clock gene, *Bmal1*, was utilized. A limitation to the findings described in chapter 8 is that experiments were performed at a single time-of-day and it is unknown if the effects from SC-Bmal1 ablation are different across various times of day. Therefore, the findings from this project in chapter 8 are limited in their interpretations for time-of-day related contexts. Additionally, while experimental mice were limited, a higher sample size for experiments would have been desired to add more validation to the findings throughout this thesis.

9.3 Future directions

A major finding from the experimental studies undertaken for this thesis is that the SC-molecular clock harbors regulations on force-production. Throughout the thesis, such regulations on force-production have shown to impact muscle fatigue (chapter 3), extents of contractile-injury (chapter 5), and the magnitudes of muscle repair (chapter 8). The consistency of the SC-molecular clock regulation on contractility was unexpected and although the experimental studies from this thesis were able to show the physiological consequences of such regulations (fatigue, damage, repair), a basic question remains: *how* do SC-molecular clocks exert a regulatory role on force-production.

Although little evidence exists showing the relationship between SC-molecular clocks and contractility, a few studies have highlighted the connection between SCs and contractile mechanics. A recent report demonstrated that SCs of fiber bundles subject to passive mechanical strain (60% fiber strain) deform to the same extent as the bundles they reside on (60% strain of SC cell length) (221). This work highlighted that SCs are mechanically in-tuned with the forces/stresses their host myofibers experience and similar work has since reported this phenomenon exists in human muscle fiber bundles as well (222). While such evidence shows SCs may experience the same stresses/forces as their host myofibers, it remains unknown if and how SCs actively regulate forces produced by muscle. In this regard, the evidence from this thesis demonstrates that SCs actively reduce force in the morning and potentially do so via lowering the volume of Ca^{++} available to contractile units (chapter 5). Evidence from two reports using the same mouse model (Pax7DTA) have shown that animals having undergone SC ablation also display altered force-production (63, 64). However, differences in these reports appear due to blunted growth in post-natal development and excess ECM accumulation following long-term SC ablation (63, 64). Chapter 5 of this thesis is perhaps the first experiment to report that SCs have an active role in regulating force-production via modulation of Ca^{++} and that this phenomenon is time-of-day dependent. Additionally, work from chapter 8 provided confirmation that SC-molecular clocks alter force-production, although it was not possible to determine whether alterations stemmed from Ca^{++} kinetics were responsible for this observation. However, it was recently reported that SCs express E-C coupling and Ca^{++} related genes on a circadian basis and are likely regulated by SC molecular clocks (17).

Future work can help build on the lines of evidence reported in this thesis. One of the first experiments that could help shed light on if Ca^{++} is the mechanistic "culprit" would be to assess

Ca^{++} volume in myofiber bundles (223) at times of day aligned to peak/trough SC-specific molecular clock gene expression. This first set of experiments could help identify if Ca^{++} *volume* within the SR changes throughout the day and if such rhythmicity is a function of the SC-molecular clock. An additional set of experiments should assess Ca^{++} transients during *ex vivo* twitch contractions (rate of releases, rate of sequestering) (224, 225) to assess if Ca^{++} *handling* is the mechanistic culprit versus Ca^{++} volume. Such experiments might elucidate if SC-molecular clocks truly modulate force-production via Ca^{++} related mechanisms. Moving forward, the evidence and insights provided in this thesis will hopefully guide future works into unraveling the complicated, but most intriguing mechanisms behind SC-molecular clock regulation of force-production.

9.4 Concluding Remarks

In this thesis, the effects of the SC-molecular clock on muscle mitochondria, contractile function, and muscle repair were evaluated across three related, but independent experimental studies. Three major novel findings are reported: 1) Mitochondrial function is not dependent on time-of-day influence by SCs however, submaximal mitochondrial-dependent fatigue does differ by time-of-day; 2) SCs differentially regulate maximal force-production according to time-of-day and such alterations in force lead to diverging magnitudes of contractile-injury, and 3) SC-molecular clocks alter force-production with such alterations underpinning the subsequent magnitudes of muscle damage and repair.

Prior to the work presented in this thesis, there had been little investigation into how SC-molecular clocks regulate critical processes in muscle physiology including metabolism, contractility, and repair. In this regard, the findings from this thesis have provided preliminary evidence that SC-molecular clocks harbor regulations over such key processes in muscle. Although

speculative, the combined evidence from the work presented in this thesis suggests SC-molecular clock regulation of force-production may protect muscle from injury at times of day muscle may be more vulnerable to high-eccentric forces that can lead to injury. The results described in Chapter 3 demonstrate that muscle was more fatigue-resistant in the morning and the findings described in chapter 5 revealed that muscle was also more vulnerable to injury in the morning, with the presence of SCs at this time lowering force-production and thus the severity of injury. In this regard, prior work has shown that fatigue "protects" muscle from high-eccentric forces resultant in injury (226) and thus, enhanced fatigue resistance (chapter 3) and lowered maximum forces in the morning (chapter 5) may be a dual protective mechanism SC-molecular clocks enact to protect against injury early in the day. Additionally, this protective effect may hinge on molecular clock gene, *Bmal1*, as the absence of SC-specific Bmal1 led to lower maximal forces and thus lesser extents of contractile induced damages and repair (chapter 8).

In broader contexts, the "take-home" message from the results of this thesis is that SC-molecular clocks play a previously underappreciated role in muscle contractile function. The physiological consequences of these regulations on contractility are demonstrated herein to be time-dependent rates of fatigue (chapter 3), altered maximal force-production (chapter 5), and altered magnitudes of muscle damage and repair (chapter 8). The precise mechanisms underlying SC-molecular clock regulation of contractility remains unknown but, is an exciting untapped area of research worthy of further investigation. Collectively, the work from this thesis has provided novel initial insights into the roles SC-molecular clocks play in muscle physiology which will hopefully serve as useful tools in guiding future works to come.

References

1. **Bass J**. Circadian topology of metabolism. *Nature* 491: 348-356, 2012.
2. **Mohawk JA, Green CB, and Takahashi JS**. Central and peripheral circadian clocks in mammals. *Annu Rev Neurosci* 35: 445-462, 2012.
3. **Dvornyk V, Vinogradova O, and Nevo E**. Origin and evolution of circadian clock genes in prokaryotes. *Proceedings of the National Academy of Sciences of the United States of America* 100: 2495-2500, 2003.
4. **Esser K**. Circadian Rhythms, Skeletal Muscle Molecular Clocks, and Exercise. 2013.
5. **Zhang R, Lahens NF, Ballance HI, Hughes ME, and Hogenesch JB**. A circadian gene expression atlas in mammals: implications for biology and medicine. *Proc Natl Acad Sci U S A* 111: 16219-16224, 2014.
6. **Gemmink A, Daemen S, Wefers J, Hansen J, van Moorsel D, Astuti P, Jorgensen JA, Kornips E, Schaart G, Hoeks J, Schrauwen P, and Hesselink MKC**. Twenty-four hour rhythmicity in mitochondrial network connectivity and mitochondrial respiration; a study in human skeletal muscle biopsies of young lean and older individuals with obesity. *Molecular Metabolism* 101727, 2023.
7. **Gabriel BM, and Zierath JR**. Zeitgebers of skeletal muscle and implications for metabolic health. *J Physiol* 2021.
8. **Douglas CM, Hesketh SJ, and Esser KA**. Time of Day and Muscle Strength: A Circadian Output? *Physiology (Bethesda)* 36: 44-51, 2021.
9. **Gutierrez-Monreal MA, Harmsen JF, Schrauwen P, and Esser KA**. Ticking for Metabolic Health: The Skeletal-Muscle Clocks. *Obesity (Silver Spring)* 28 Suppl 1: S46-S54, 2020.
10. **van Moorsel D, Hansen J, Havekes B, Scheer F, Jorgensen JA, Hoeks J, Schrauwen-Hinderling VB, Duez H, Lefebvre P, Schaper NC, Hesselink MKC, Staels B, and Schrauwen P**. Demonstration of a day-night rhythm in human skeletal muscle oxidative capacity. *Mol Metab* 5: 635-645, 2016.
11. **Chatterjee S, Yin H, Nam D, Li Y, and Ma K**. Brain and muscle Arnt-like 1 promotes skeletal muscle regeneration through satellite cell expansion. *Exp Cell Res* 331: 200-210, 2015.
12. **Chatterjee S, Nam D, Guo B, Kim JM, Winnier GE, Lee J, Berdeaux R, Yechoor VK, and Ma K**. Brain and muscle Arnt-like 1 is a key regulator of myogenesis. *J Cell Sci* 126: 2213-2224, 2013.
13. **Andrews JL, Zhang X, McCarthy JJ, McDearmon EL, Hornberger TA, Russell B, Campbell KS, Arbogast S, Reid MB, Walker JR, Hogenesch JB, Takahashi JS, and Esser KA**. CLOCK and BMAL1 regulate MyoD and are necessary for maintenance of skeletal muscle phenotype and function. *Proc Natl Acad Sci U S A* 107: 19090-19095, 2010.
14. **Kiho B, Kisoo L, Younguk S, Haesang L, Dongyong K, and Inho C**. Differential Effects of Two Period Genes on the Physiology and Proteomic Profiles of Mouse Anterior Tibialis Muscles. *Mol Cells* 22: 275-284, 2006.
15. **Mackey AL, and Kjaer M**. The breaking and making of healthy adult human skeletal muscle in vivo. *Skelet Muscle* 7: 24, 2017.
16. **Yin H, Price F, and Rudnicki MA**. Satellite cells and the muscle stem cell niche. *Physiol Rev* 93: 23-67, 2013.
17. **Solanas G, Peixoto FO, Perdiguero E, Jardi M, Ruiz-Bonilla V, Datta D, Symeonidi A, Castellanos A, Welz PS, Caballero JM, Sassone-Corsi P, Munoz-Canoves P, and Benitah**

SA. Aged Stem Cells Reprogram Their Daily Rhythmic Functions to Adapt to Stress. *Cell* 170: 678-692 e620, 2017.
18. **Gerhart-Hines Z, and Lazar MA**. Circadian Metabolism in the Light of Evolution. *Endocrine Reviews* 36: 289-304, 2015.
19. **Robinson I, and Reddy AB**. Molecular mechanisms of the circadian clockwork in mammals. *FEBS Letters* 588: 2477-2483, 2014.
20. **Panda S**. Circadian physiology of metabolism. *Science* 354: 1008-1015, 2016.
21. **Ding G, Gong Y, Eckel-Mahan KL, and Sun Z**. Central Circadian Clock Regulates Energy Metabolism. *Advances in experimental medicine and biology* 1090: 79-103, 2018.
22. **Koronowski KB, Kinouchi K, Welz P-S, Smith JG, Zinna VM, Shi J, Samad M, Chen S, Magnan CN, Kinchen JM, Li W, Baldi P, Benitah SA, and Sassone-Corsi P**. Defining the Independence of the Liver Circadian Clock. *Cell* 177: 1448-1462.e1414, 2019.
23. **Gabriel BM, and Zierath JR**. Circadian rhythms and exercise - re-setting the clock in metabolic disease. *Nat Rev Endocrinol* 15: 197-206, 2019.
24. **Harfmann BD, Schroder EA, and Esser KA**. Circadian rhythms, the molecular clock, and skeletal muscle. *J Biol Rhythms* 30: 84-94, 2015.
25. **Ezagouri S, Zwighaft Z, Sobel J, Baillieul S, Doutreleau S, Ladeuix B, Golik M, Verges S, and Asher G**. Physiological and Molecular Dissection of Daily Variance in Exercise Capacity. *Cell Metab* 30: 78-91 e74, 2019.
26. **McCarthy JJ, Andrews JL, McDearmon EL, Campbell KS, Barber BK, Miller BH, Walker JR, Hogenesch JB, Takahashi JS, and Esser KA**. Identification of the circadian transcriptome in adult mouse skeletal muscle. *Physiol Genomics* 31: 86-95, 2007.
27. **Mayeuf-Louchart A**. Skeletal Muscle Functins around the Clock. 2017.
28. **Hargreaves M, and Spriet LL**. Skeletal muscle energy metabolism during exercise. *Nat Metab* 2: 817-828, 2020.
29. **Smith JAB, Murach KA, Dyar KA, and Zierath JR**. Exercise metabolism and adaptation in skeletal muscle. *Nat Rev Mol Cell Biol* 2023.
30. **Zierath JR, and Hawley JA**. Skeletal muscle fiber type: influence on contractile and metabolic properties. *PLoS Biol* 2: e348, 2004.
31. **Hamner SR, and Delp SL**. Muscle contributions to fore-aft and vertical body mass center accelerations over a range of running speeds. *J Biomech* 46: 780-787, 2013.
32. **Place N, Yamada T, Bruton JD, and Westerblad H**. Muscle fatigue: from observations in humans to underlying mechanisms studied in intact single muscle fibres. *Eur J Appl Physiol* 110: 1-15, 2010.
33. **Allen DG, Lamb GD, and Westerblad H**. Skeletal muscle fatigue: cellular mechanisms. *Physiol Rev* 88: 287-332, 2008.
34. **Lieber RL**. Biomechanical response of skeletal muscle to eccentric contractions. *J Sport Health Sci* 7: 294-309, 2018.
35. **Warren GL, Ingalls CP, Lowe DA, and Armstrong RB**. Excitation-Contraction Uncoupling: Major Role in Contraction-Induced Muscle Injury. *Exercise and Sport Sciences Reviews* 29: 82-87, 2001.
36. **Mackey AL, and Kjaer M**. Connective tissue regeneration in skeletal muscle after eccentric contraction-induced injury. *J Appl Physiol (1985)* 122: 533-540, 2017.
37. **Snijders T, Nederveen JP, McKay BR, Joanisse S, Verdijk LB, van Loon LJC, and Parise G**. Satellite cells in human skeletal muscle plasticity. *Frontiers in Physiology* 6: 2015.

38. **Maier G, Delezie J, Westermark PO, Santos G, Ritz D, and Handschin C**. Transcriptomic, proteomic and phosphoproteomic underpinnings of daily exercise performance and zeitgeber activity of training in mouse muscle. *J Physiol* 2021.
39. **Adamovich Y, Dandavate V, Ezagouri S, Manella G, Zwighaft Z, Sobel J, Kuperman Y, Golik M, Auerbach A, Itkin M, Malitsky S, and Asher G**. Clock proteins and training modify exercise capacity in a daytime-dependent manner. *Proc Natl Acad Sci U S A* 118: 2021.
40. **Jordan SD, Kriebs A, Vaughan M, Duglan D, Fan W, Henriksson E, Huber AL, Papp SJ, Nguyen M, Afetian M, Downes M, Yu RT, Kralli A, Evans RM, and Lamia KA**. CRY1/2 Selectively Repress PPARdelta and Limit Exercise Capacity. *Cell Metab* 26: 243-255 e246, 2017.
41. **Kent-Braun JA, Fitts RH, and Christie A**. Skeletal muscle fatigue. *Compr Physiol* 2: 997-1044, 2012.
42. **de Goede P, Wust RCI, Schomakers BV, Denis S, Vaz FM, Pras-Raves ML, van Weeghel M, Yi CX, Kalsbeek A, and Houtkooper RH**. Time-restricted feeding during the inactive phase abolishes the daily rhythm in mitochondrial respiration in rat skeletal muscle. *FASEB J* 36: e22133, 2022.
43. **Gabriel BM, Altıntaş A, Smith JAB, Sardon-Puig L, Zhang X, Basse AL, Laker RC, Gao H, Liu Z, Dollet L, Treebak JT, Zorzano A, Huo Z, Rydén M, Lanner JT, Esser KA, Barrès R, Pillon NJ, Krook A, and Zierath JR**. Disrupted circadian oscillations in type 2 diabetes are linked to altered rhythmic mitochondrial metabolism in skeletal muscle. *Science Advances* 7: eabi9654, 2021.
44. **Peek CB, Levine DC, Cedernaes J, Taguchi A, Kobayashi Y, Tsai SJ, Bonar NA, McNulty MR, Ramsey KM, and Bass J**. Circadian Clock Interaction with HIF1alpha Mediates Oxygenic Metabolism and Anaerobic Glycolysis in Skeletal Muscle. *Cell Metab* 25: 86-92, 2017.
45. **Peek CB, Affinati AH, Ramsey KM, Kuo HY, Yu W, Sena LA, Ilkayeva O, Marcheva B, Kobayashi Y, Omura C, Levine DC, Bacsik DJ, Gius D, Newgard CB, Goetzman E, Chandel NS, Denu JM, Mrksich M, and Bass J**. Circadian clock NAD+ cycle drives mitochondrial oxidative metabolism in mice. *Science* 342: 1243417, 2013.
46. **Levine DC, Kuo HY, Hong HK, Cedernaes J, Hepler C, Wright AG, Sommars MA, Kobayashi Y, Marcheva B, Gao P, Ilkayeva OR, Omura C, Ramsey KM, Newgard CB, Barish GD, Peek CB, Chandel NS, Mrksich M, and Bass J**. NADH inhibition of SIRT1 links energy state to transcription during time-restricted feeding. *Nat Metab* 2021.
47. **Levine DC, Hong H, Weidemann BJ, Ramsey KM, Affinati AH, Schmidt MS, Cedernaes J, Omura C, Braun R, Lee C, Brenner C, Peek CB, and Bass J**. NAD(+) Controls Circadian Reprogramming through PER2 Nuclear Translocation to Counter Aging. *Mol Cell* 78: 835-849 e837, 2020.
48. **Leckey JJ, Hoffman NJ, Parr EB, Devlin BL, Trewin AJ, Stepto NK, Morton JP, Burke LM, and Hawley JA**. High dietary fat intake increases fat oxidation and reduces skeletal muscle mitochondrial respiration in trained humans. *FASEB J* 32: 2979-2991, 2018.
49. **Jackson JR, Kirby TJ, Fry CS, Cooper RL, McCarthy JJ, Peterson CA, and Dupont-Versteegden EE**. Reduced voluntary running performance is associated with impaired coordination as a result of muscle satellite cell depletion in adult mice. *Skelet Muscle* 5: 41, 2015.

50. **Englund DA, Murach KA, Dungan CM, Figueiredo VC, Vechetti IJ, Jr., Dupont-Versteegden EE, McCarthy JJ, and Peterson CA**. Depletion of resident muscle stem cells negatively impacts running volume, physical function, and muscle fiber hypertrophy in response to lifelong physical activity. *Am J Physiol Cell Physiol* 318: C1178-c1188, 2020.
51. **Tavi P, Korhonen T, Hänninen SL, Bruton JD, Lööf S, Simon A, and Westerblad H**. Myogenic skeletal muscle satellite cells communicate by tunnelling nanotubes. *J Cell Physiol* 223: 376-383, 2010.
52. **Schroder EA, Harfmann BD, Zhang X, Srikuea R, England JH, Hodge BA, Wen Y, Riley LA, Yu Q, Christie A, Smith JD, Seward T, Wolf Horrell EM, Mula J, Peterson CA, Butterfield TA, and Esser KA**. Intrinsic muscle clock is necessary for musculoskeletal health. *J Physiol* 593: 5387-5404, 2015.
53. **Dyar KA, Ciciliot S, Wright LE, Biensø RS, Tagliazucchi GM, Patel VR, Forcato M, Paz MI, Gudiksen A, Solagna F, Albiero M, Moretti I, Eckel-Mahan KL, Baldi P, Sassone-Corsi P, Rizzuto R, Bicciato S, Pilegaard H, Blaauw B, and Schiaffino S**. Muscle insulin sensitivity and glucose metabolism are controlled by the intrinsic muscle clock. *Mol Metab* 3: 29-41, 2014.
54. **Riley LA, Zhang X, Douglas CM, Mijares JM, Hammers DW, Wolff CA, Wood NB, Olafson HR, Du P, Labeit S, Previs MJ, Wang ET, and Esser KA**. The skeletal muscle circadian clock regulates titin splicing through RBM20. *eLife* 11: e76478, 2022.
55. **Hodge BA, Zhang X, Gutierrez-Monreal MA, Cao Y, Hammers DW, Yao Z, Wolff CA, Du P, Kemler D, Judge AR, and Esser KA**. MYOD1 functions as a clock amplifier as well as a critical co-factor for downstream circadian gene expression in muscle. *Elife* 8: 2019.
56. **Small L, Altintas A, Laker RC, Ehrlich A, Pattamaprapanont P, Villarroel J, Pillon NJ, Zierath JR, and Barres R**. Contraction influences Per2 gene expression in skeletal muscle through a calcium-dependent pathway. *J Physiol* 598: 5739-5752, 2020.
57. **Baumann CW, Ingalls CP, and Lowe DA**. Mechanisms of weakness in Mdx muscle following in vivo eccentric contractions. *J Muscle Res Cell Motil* 43: 63-72, 2022.
58. **Länngergren J, and Westerblad H**. Force decline due to fatigue and intracellular acidification in isolated fibres from mouse skeletal muscle. *J Physiol* 434: 307-322, 1991.
59. **Isaacson A, Hinkes MJ, and Taylor SR**. Contracture and twitch potentiation of fast and slow muscles of the rat at 20 and 37 C. *Am J Physiol* 218: 33-41, 1970.
60. **Cavieres-Lepe J, and Ewer J**. Reciprocal Relationship Between Calcium Signaling and Circadian Clocks: Implications for Calcium Homeostasis, Clock Function, and Therapeutics. *Front Mol Neurosci* 14: 666673, 2021.
61. **Enoki R, Ono D, Kuroda S, Honma S, and Honma K-i**. Dual origins of the intracellular circadian calcium rhythm in the suprachiasmatic nucleus. *Scientific Reports* 7: 41733, 2017.
62. **Colwell CS**. Circadian modulation of calcium levels in cells in the suprachiasmatic nucleus. *Eur J Neurosci* 12: 571-576, 2000.
63. **Bachman JF, Klose A, Liu W, Paris ND, Blanc RS, Schmalz M, Knapp E, and Chakkalakal JV**. Prepubertal skeletal muscle growth requires Pax7-expressing satellite cell-derived myonuclear contribution. *Development* 145: 2018.
64. **Fry CS, Lee JD, Jackson JR, Kirby TJ, Stasko SA, Liu H, Dupont-Versteegden EE, McCarthy JJ, and Peterson CA**. Regulation of the muscle fiber microenvironment by activated satellite cells during hypertrophy. *FASEB J* 28: 1654-1665, 2014.

65. **Gattazzo F, Laurent B, Relaix F, Rouard H, and Didier N**. Distinct Phases of Postnatal Skeletal Muscle Growth Govern the Progressive Establishment of Muscle Stem Cell Quiescence. *Stem Cell Reports* 15: 597-611, 2020.
66. **Dhawan J, and Rando TA**. Stem cells in postnatal myogenesis: molecular mechanisms of satellite cell quiescence, activation and replenishment. *Trends Cell Biol* 15: 666-673, 2005.
67. **Hentzen ER, Lahey M, Peters D, Mathew L, Barash IA, Fridén J, and Lieber RL**. Stress-dependent and -independent expression of the myogenic regulatory factors and the MARP genes after eccentric contractions in rats. *J Physiol* 570: 157-167, 2006.
68. **Warren GL, Hayes DA, Lowe DA, and Armstrong RB**. Mechanical factors in the initiation of eccentric contraction-induced injury in rat soleus muscle. *The Journal of Physiology* 464: 457-475, 1993.
69. **De Micheli AJ, Laurilliard EJ, Heinke CL, Ravichandran H, Fraczek P, Soueid-Baumgarten S, De Vlaminck I, Elemento O, and Cosgrove BD**. Single-Cell Analysis of the Muscle Stem Cell Hierarchy Identifies Heterotypic Communication Signals Involved in Skeletal Muscle Regeneration. *Cell Rep* 30: 3583-3595 e3585, 2020.
70. **He Y, Heng Y, Qin Z, Wei X, Wu Z, and Qu J**. Intravital microscopy of satellite cell dynamics and their interaction with myeloid cells during skeletal muscle regeneration. *Science Advances* 9: eadi1891, 2023.
71. **Hindi SM, and Millay DP**. All for One and One for All: Regenerating Skeletal Muscle. *Cold Spring Harb Perspect Biol* 2021.
72. **Webster MT, Manor U, Lippincott-Schwartz J, and Fan CM**. Intravital Imaging Reveals Ghost Fibers as Architectural Units Guiding Myogenic Progenitors during Regeneration. *Cell Stem Cell* 18: 243-252, 2016.
73. **Gurevich DB, Nguyen PD, Siegel AL, Ehrlich OV, Sonntag C, Phan JMN, Berger S, Ratnayake D, Hersey L, Berger J, Verkade H, Hall TE, and Currie PD**. Asymmetric division of clonal muscle stem cells coordinates muscle regeneration in vivo. *Science* 353: aad9969, 2016.
74. **Nederveen JP, Fortino SA, Baker JM, Snijders T, Joanisse S, McGlory C, McKay BR, Kumbhare D, and Parise G**. Consistent expression pattern of myogenic regulatory factors in whole muscle and isolated human muscle satellite cells after eccentric contractions in humans. *J Appl Physiol (1985)* 127: 1419-1426, 2019.
75. **Hernandez-Hernandez JM, Garcia-Gonzalez EG, Brun CE, and Rudnicki MA**. The myogenic regulatory factors, determinants of muscle development, cell identity and regeneration. *Semin Cell Dev Biol* 72: 10-18, 2017.
76. **Singh K, and Dilworth FJ**. Differential modulation of cell cycle progression distinguishes members of the myogenic regulatory factor family of transcription factors. *FEBS J* 280: 3991-4003, 2013.
77. **Paatela E, Munson D, and Kikyo N**. Circadian Regulation in Tissue Regeneration. *Int J Mol Sci* 20: 2019.
78. **Kowalska E, Ripperger JA, Hoegger DC, Bruegger P, Buch T, Birchler T, Mueller A, Albrecht U, Contaldo C, and Brown SA**. NONO couples the circadian clock to the cell cycle. *Proc Natl Acad Sci U S A* 110: 1592-1599, 2013.
79. **Maier CE, and Singer M**. The effect of prolactin on the rate of forelimb regeneration in newts exposed to photoperiod extremes. *Journal of Experimental Zoology* 216: 395-397, 1981.
80. **Maier CE, and Singer M**. The effect of light on forelimb regeneration in the newt. *Journal of Experimental Zoology* 202: 241-244, 1977.

81. **Schauble MK, and Tyler DB**. The effect of prolactin on the seasonal cyclicity of newt forelimb regeneration. *Journal of Experimental Zoology* 182: 41-46, 1972.
82. **Schauble MK**. Seasonal variation of newt forelimb regeneration under controlled environmental conditions. *Journal of Experimental Zoology* 181: 281-286, 1972.
83. **Katoku-Kikyo N, Paatela E, Houtz DL, Lee B, Munson D, Wang X, Hussein M, Bhatia J, Lim S, Yuan C, Asakura Y, Asakura A, and Kikyo N**. Per1/Per2-Igf2 axis-mediated circadian regulation of myogenic differentiation. *J Cell Biol* 220: 2021.
84. **Lowe M, Lage J, Paatela E, Munson D, Hostager R, Yuan C, Katoku-Kikyo N, Ruiz-Estevez M, Asakura Y, Staats J, Qahar M, Lohman M, Asakura A, and Kikyo N**. Cry2 Is Critical for Circadian Regulation of Myogenic Differentiation by Bclaf1-Mediated mRNA Stabilization of Cyclin D1 and Tmem176b. *Cell Rep* 22: 2118-2132, 2018.
85. **Zhu P, Hamlish NX, Thakkar AV, Steffeck AWT, Rendleman EJ, Khan NH, Waldeck NJ, DeVilbiss AW, Martin-Sandoval MS, Mathews TP, Chandel NS, and Peek CB**. BMAL1 drives muscle repair through control of hypoxic NAD(+) regeneration in satellite cells. *Genes Dev* 2022.
86. **Chen JC, and Goldhamer DJ**. The core enhancer is essential for proper timing of MyoD activation in limb buds and branchial arches. *Dev Biol* 265: 502-512, 2004.
87. **Chen JCJ, Love CM, and Goldhamer DJ**. Two upstream enhancers collaborate to regulate the spatial patterning and timing of MyoD transcription during mouse development. *Developmental Dynamics* 221: 274-288, 2001.
88. **Zhang X, Patel SP, McCarthy JJ, Rabchevsky AG, Goldhamer DJ, and Esser KA**. A non-canonical E-box within the MyoD core enhancer is necessary for circadian expression in skeletal muscle. *Nucleic Acids Res* 40: 3419-3430, 2012.
89. **Zhu P, Pfrender E, Steffeck A, Reczek C, Zhou Y, Thakkar A, Gupta N, Willbanks A, Lieber R, Roy I, Chandel NS, and Peek CB**. Immunomodulatory Role of the Stem Cell Circadian Clock in Muscle Repair. *bioRxiv* 2024.
90. **Nederveen JP, Joanisse S, Snijders T, Thomas ACQ, Kumbhare D, and Parise G**. The influence of capillarization on satellite cell pool expansion and activation following exercise-induced muscle damage in healthy young men. *J Physiol* 596: 1063-1078, 2018.
91. **Kahn RE, Lieber RL, Meza G, Dinnunhan F, Lacham-Kaplan O, Dayanidhi S, and Hawley JA**. Time-of-day effects on ex vivo muscle contractility following short-term satellite cell ablation. *Am J Physiol Cell Physiol* 2024.
92. **Kemler D, Wolff CA, and Esser KA**. Time-of-day dependent effects of contractile activity on the phase of the skeletal muscle clock. *J Physiol* 598: 3631-3644, 2020.
93. **Deschenes MR, Sharma JV, Brittingham KT, Casa DJ, Armstrong LE, and Maresh CM**. Chronobiological effects on exercise performance and selected physiological responses. *Eur J Appl Physiol Occup Physiol* 77: 249-256, 1998.
94. **Murach KA, Peck BD, Policastro RA, Vechetti IJ, Van Pelt DW, Dungan CM, Denes LT, Fu X, Brightwell CR, Zentner GE, Dupont-Versteegden EE, Richards CI, Smith JJ, Fry CS, McCarthy JJ, and Peterson CA**. Early satellite cell communication creates a permissive environment for long-term muscle growth. *iScience* 24: 102372, 2021.
95. **Englund DA, Figueiredo VC, Dungan CM, Murach KA, Peck BD, Petrosino JM, Brightwell CR, Dupont AM, Neal AC, Fry CS, Accornero F, McCarthy JJ, and Peterson CA**. Satellite Cell Depletion Disrupts Transcriptional Coordination and Muscle Adaptation to Exercise. *Function (Oxf)* 2: zqaa033, 2021.

96. **Relaix F, and Zammit PS**. Satellite cells are essential for skeletal muscle regeneration: the cell on the edge returns centre stage. *Development* 139: 2845-2856, 2012.
97. **Fry CS, Lee JD, Mula J, Kirby TJ, Jackson JR, Liu F, Yang L, Mendias CL, Dupont-Versteegden EE, McCarthy JJ, and Peterson CA**. Inducible depletion of satellite cells in adult, sedentary mice impairs muscle regenerative capacity without affecting sarcopenia. *Nat Med* 21: 76-80, 2015.
98. **McCarthy JJ, Mula J, Miyazaki M, Erfani R, Garrison K, Farooqui AB, Srikuea R, Lawson BA, Grimes B, Keller C, Van Zant G, Campbell KS, Esser KA, Dupont-Versteegden EE, and Peterson CA**. Effective fiber hypertrophy in satellite cell-depleted skeletal muscle. *Development* 138: 3657-3666, 2011.
99. **Guo M, McDermott MM, Dayanidhi S, Leeuwenburgh C, Wohlgemuth S, Ferrucci L, Peterson CA, Kosmac K, Tian L, Zhao L, Sufit R, Ho K, Criqui M, Xu S, Zhang D, and Greenland P**. Cigarette smoking and mitochondrial dysfunction in peripheral artery disease. *Vasc Med* 28: 28-35, 2022.
100. **Thompson SD, Barrett KL, Rugel CL, Redmond R, Rudofski A, Kurian J, Curtin JL, Dayanidhi S, and Lavasani M**. Sex-specific preservation of neuromuscular function and metabolism following systemic transplantation of multipotent adult stem cells in a murine model of progeria. *GeroScience* 2023.
101. **Dayanidhi S, Buckner EH, Redmond RS, Chambers HG, Schenk S, and Lieber RL**. Skeletal muscle maximal mitochondrial activity in ambulatory children with cerebral palsy. *Dev Med Child Neurol* 63: 1194-1203, 2021.
102. **LaBarge SA, Migdal CW, Buckner EH, Okuno H, Gertsman I, Stocks B, Barshop BA, Nalbandian SR, Philp A, McCurdy CE, and Schenk S**. p300 is not required for metabolic adaptation to endurance exercise training. *FASEB J* 30: 1623-1633, 2016.
103. **Pfaffl MW**. A new mathematical model for relative quantification in real-time RT-PCR. *Nucleic Acids Res* 29: e45, 2001.
104. **Palmisano MG, Bremner SN, Hornberger TA, Meyer GA, Domenighetti AA, Shah SB, Kiss B, Kellermayer M, Ryan AF, and Lieber RL**. Skeletal muscle intermediate filaments form a stress-transmitting and stress-signaling network. *J Cell Sci* 128: 219-224, 2015.
105. **Chapman MA, Zhang J, Banerjee I, Guo LT, Zhang Z, Shelton GD, Ouyang K, Lieber RL, and Chen J**. Disruption of both nesprin 1 and desmin results in nuclear anchorage defects and fibrosis in skeletal muscle. *Hum Mol Genet* 23: 5879-5892, 2014.
106. **Sam M, Shah S, Fridén J, Milner DJ, Capetanaki Y, and Lieber RL**. Desmin knockout muscles generate lower stress and are less vulnerable to injury compared with wild-type muscles. *Am J Physiol Cell Physiol* 279: C1116-1122, 2000.
107. **Nogueira L, Gilmore NK, and Hogan MC**. Role of parvalbumin in fatigue-induced changes in force and cytosolic calcium transients in intact single mouse myofibers. *J Appl Physiol (1985)* 132: 1041-1053, 2022.
108. **Gandra PG, Nogueira L, and Hogan MC**. Mitochondrial activation at the onset of contractions in isolated myofibres during successive contractile periods. *The Journal of Physiology* 590: 3597-3609, 2012.
109. **Nogueira L, Ramirez-Sanchez I, Perkins GA, Murphy A, Taub PR, Ceballos G, Villarreal FJ, Hogan MC, and Malek MH**. (–)-Epicatechin enhances fatigue resistance and oxidative capacity in mouse muscle. *The Journal of Physiology* 589: 4615-4631, 2011.
110. **Delfinis LJ, Bellissimo CA, Gandhi S, DiBenedetto SN, Garibotti MC, Thuhan AK, Tsitkanou S, Rosa-Caldwell ME, Rahman FA, Cheng AJ, Wiggs MP, Schlattner U,**

Quadrilatero J, Greene NP, and Perry CGR. Muscle weakness precedes atrophy during cancer cachexia and is linked to muscle-specific mitochondrial stress. *JCI Insight* 2022.
111. **Meyer GA, Thomopoulos S, Abu-Amer Y, and Shen KC**. Tenotomy-induced muscle atrophy is sex-specific and independent of NFκB. *eLife* 11: e82016, 2022.
112. **Wen Y, Murach KA, Vechetti IJ, Jr., Fry CS, Vickery C, Peterson CA, McCarthy JJ, and Campbell KS**. MyoVision: software for automated high-content analysis of skeletal muscle immunohistochemistry. *J Appl Physiol (1985)* 124: 40-51, 2018.
113. **Dungan CM, Murach KA, Frick KK, Jones SR, Crow SE, Englund DA, Vechetti IJ, Jr., Figueiredo VC, Levitan BM, Satin J, McCarthy JJ, and Peterson CA**. Elevated myonuclear density during skeletal muscle hypertrophy in response to training is reversed during detraining. *Am J Physiol Cell Physiol* 316: C649-C654, 2019.
114. **Mayeuf-Louchart A, Hardy D, Thorel Q, Roux P, Gueniot L, Briand D, Mazeraud A, Bouglé A, Shorte SL, Staels B, Chrétien F, Duez H, and Danckaert A**. MuscleJ: a high-content analysis method to study skeletal muscle with a new Fiji tool. *Skelet Muscle* 8: 25, 2018.
115. **Fitzgerald LS, Bremner SN, Ward SR, Cho Y, and Schenk S**. Intrinsic Skeletal Muscle Function and Contraction-stimulated Glucose Uptake Do Not Vary by Time-of-day in Mice. *Function* zqae035, 2024.
116. **Zhang SJ, Bruton JD, Katz A, and Westerblad H**. Limited oxygen diffusion accelerates fatigue development in mouse skeletal muscle. *J Physiol* 572: 551-559, 2006.
117. **Dayanidhi S, Kinney MC, Dykstra PB, and Lieber RL**. Does a Reduced Number of Muscle Stem Cells Impair the Addition of Sarcomeres and Recovery from a Skeletal Muscle Contracture? A Transgenic Mouse Model. *Clin Orthop Relat Res* 478: 886-899, 2020.
118. **Murach KA, White SH, Wen Y, Ho A, Dupont-Versteegden EE, McCarthy JJ, and Peterson CA**. Differential requirement for satellite cells during overload-induced muscle hypertrophy in growing versus mature mice. *Skelet Muscle* 7: 14, 2017.
119. **Kinney MC, Dayanidhi S, Dykstra PB, McCarthy JJ, Peterson CA, and Lieber RL**. Reduced skeletal muscle satellite cell number alters muscle morphology after chronic stretch but allows limited serial sarcomere addition. *Muscle Nerve* 55: 384-392, 2017.
120. **Brooks SV, and Faulkner JA**. Contractile properties of skeletal muscles from young, adult and aged mice. *J Physiol* 404: 71-82, 1988.
121. **Egan B, and Zierath JR**. Exercise metabolism and the molecular regulation of skeletal muscle adaptation. *Cell Metab* 17: 162-184, 2013.
122. **Kinney MC, Dayanidhi S, Dykstra PB, McCarthy JJ, Peterson CA, and Lieber RL**. Reduced skeletal muscle satellite cell number alters muscle morphology after chronic stretch but allows limited serial sarcomere addition. *Muscle Nerve* 55: 384-392, 2017.
123. **Murach KA, White SH, Wen Y, Ho A, Dupont-Versteegden EE, McCarthy JJ, and Peterson CA**. Differential requirement for satellite cells during overload-induced muscle hypertrophy in growing versus mature mice. *Skeletal Muscle* 7: 14, 2017.
124. **Lieber R**. Desmin knockout muscles generate lower stress and are less vulnerable to injury compared with wild-type muscles. 2000.
125. **Warren GL, Lowe DA, Hayes DA, Karwoski CJ, Prior BM, and Armstrong RB**. Excitation failure in eccentric contraction-induced injury of mouse soleus muscle. *J Physiol* 468: 487-499, 1993.
126. **Hunter KD, and Faulkner JA**. Pliometric contraction-induced injury of mouse skeletal muscle: effect of initial length. *Journal of Applied Physiology* 82: 278-283, 1997.

127. **Faulkner JA, Jones DA, and Round JM**. Injury to skeletal muscles of mice by forced lengthening during contractions. *Q J Exp Physiol* 74: 661-670, 1989.
128. **Lindsay A, Baumann CW, Rebbeck RT, Yuen SL, Southern WM, Hodges JS, Cornea RL, Thomas DD, Ervasti JM, and Lowe DA**. Mechanical factors tune the sensitivity of mdx muscle to eccentric strength loss and its protection by antioxidant and calcium modulators. *Skelet Muscle* 10: 3, 2020.
129. **Camera DM, West DW, Burd NA, Phillips SM, Garnham AP, Hawley JA, and Coffey VG**. Low muscle glycogen concentration does not suppress the anabolic response to resistance exercise. *J Appl Physiol (1985)* 113: 206-214, 2012.
130. **Sato S, Parr EB, Devlin BL, Hawley JA, and Sassone-Corsi P**. Human metabolomics reveal daily variations under nutritional challenges specific to serum and skeletal muscle. *Mol Metab* 16: 1-11, 2018.
131. **Zhang BT, Whitehead NP, Gervasio OL, Reardon TF, Vale M, Fatkin D, Dietrich A, Yeung EW, and Allen DG**. Pathways of Ca^{2+} entry and cytoskeletal damage following eccentric contractions in mouse skeletal muscle. *J Appl Physiol (1985)* 112: 2077-2086, 2012.
132. **Zhang BT, Yeung SS, Allen DG, Qin L, and Yeung EW**. Role of the calcium-calpain pathway in cytoskeletal damage after eccentric contractions. *J Appl Physiol (1985)* 105: 352-357, 2008.
133. **Crameri RM, Aagaard P, Qvortrup K, Langberg H, Olesen J, and Kjaer M**. Myofibre damage in human skeletal muscle: effects of electrical stimulation versus voluntary contraction. *J Physiol* 583: 365-380, 2007.
134. **Rinard J, Clarkson PM, Smith LL, and Grossman M**. Response of males and females to high-force eccentric exercise. *J Sports Sci* 18: 229-236, 2000.
135. **Lieber RL, Schmitz MC, Mishra DK, and Friden J**. Contractile and cellular remodeling in rabbit skeletal muscle after cyclic eccentric contractions. *J Appl Physiol (1985)* 77: 1926-1934, 1994.
136. **Mackey AL, Rasmussen LK, Kadi F, Schjerling P, Helmark IC, Ponsot E, Aagaard P, Durigan JL, and Kjaer M**. Activation of satellite cells and the regeneration of human skeletal muscle are expedited by ingestion of nonsteroidal anti-inflammatory medication. *FASEB J* 30: 2266-2281, 2016.
137. **Barash IA, Peters D, Fridén J, Lutz GJ, and Lieber RL**. Desmin cytoskeletal modifications after a bout of eccentric exercise in the rat. *Am J Physiol Regul Integr Comp Physiol* 283: R958-963, 2002.
138. **Lieber RL, Thornell LE, and Friden J**. Muscle cytoskeletal disruption occurs within the first 15 min of cyclic eccentric contraction. *Journal of Applied Physiology* 80: 278-284, 1996.
139. **Miller BH, McDearmon EL, Panda S, Hayes KR, Zhang J, Andrews JL, Antoch MP, Walker JR, Esser KA, Hogenesch JB, and Takahashi JS**. Circadian and CLOCK-controlled regulation of the mouse transcriptome and cell proliferation. *Proc Natl Acad Sci U S A* 104: 3342-3347, 2007.
140. **Krauss RS, and Kann AP**. Muscle stem cells get a new look: Dynamic cellular projections as sensors of the stem cell niche. *Bioessays* e2200249, 2023.
141. **Palla AR, Hilgendorf KI, Yang AV, Kerr JP, Hinken AC, Demeter J, Kraft P, Mooney NA, Yucel N, Burns DM, Wang YX, Jackson PK, and Blau HM**. Primary cilia on muscle stem cells are critical to maintain regenerative capacity and are lost during aging. *Nat Commun* 13: 1439, 2022.

142. **Kann AP, Hung M, Wang W, Nguyen J, Gilbert PM, Wu Z, and Krauss RS**. An injury-responsive Rac-to-Rho GTPase switch drives activation of muscle stem cells through rapid cytoskeletal remodeling. *Cell Stem Cell* 2022.
143. **Ma N, Chen D, Lee JH, Kuri P, Hernandez EB, Kocan J, Mahmood H, Tichy ED, Rompolas P, and Mourkioti F**. Piezo1 regulates the regenerative capacity of skeletal muscles via orchestration of stem cell morphological states. *Sci Adv* 8: eabn0485, 2022.
144. **Burkholder TJ, Fingado B, Baron S, and Lieber RL**. Relationship between muscle fiber types and sizes and muscle architectural properties in the mouse hindlimb. *J Morphol* 221: 177-190, 1994.
145. **Powell PL, Roy RR, Kanim P, Bello MA, and Edgerton VR**. Predictability of skeletal muscle tension from architectural determinations in guinea pig hindlimbs. *J Appl Physiol Respir Environ Exerc Physiol* 57: 1715-1721, 1984.
146. **Méndez J, and Keys AB**. Density and composition of mammalian muscle. *Metabolism-clinical and Experimental* 9: 184-188, 1960.
147. **Crane BR, and Young MW**. Interactive features of proteins composing eukaryotic circadian clocks. *Annu Rev Biochem* 83: 191-219, 2014.
148. **Asher G, and Sassone-Corsi P**. Time for food: the intimate interplay between nutrition, metabolism, and the circadian clock. *Cell* 161: 84-92, 2015.
149. **Adamovich Y, Aviram R, and Asher G**. The emerging roles of lipids in circadian control. *Biochim Biophys Acta* 1851: 1017-1025, 2015.
150. **Asher G, and Schibler U**. Crosstalk between components of circadian and metabolic cycles in mammals. *Cell Metab* 13: 125-137, 2011.
151. **Manella G, Sabath E, Aviram R, Dandavate V, Ezagouri S, Golik M, Adamovich Y, and Asher G**. The liver-clock coordinates rhythmicity of peripheral tissues in response to feeding. *Nature Metabolism* 3: 829-842, 2021.
152. **Dyar KA, Hubert MJ, Mir AA, Ciciliot S, Lutter D, Greulich F, Quagliarini F, Kleinert M, Fischer K, Eichmann TO, Wright LE, Peña Paz MI, Casarin A, Pertegato V, Romanello V, Albiero M, Mazzucco S, Rizzuto R, Salviati L, Biolo G, Blaauw B, Schiaffino S, and Uhlenhaut NH**. Transcriptional programming of lipid and amino acid metabolism by the skeletal muscle circadian clock. *PLOS Biology* 16: e2005886, 2018.
153. **Dyar KA, Ciciliot S, Wright LE, Biensø RS, Tagliazucchi GM, Patel VR, Forcato M, Paz MIP, Gudiksen A, Solagna F, Albiero M, Moretti I, Eckel-Mahan KL, Baldi P, Sassone-Corsi P, Rizzuto R, Bicciato S, Pilegaard H, Blaauw B, and Schiaffino S**. Muscle insulin sensitivity and glucose metabolism are controlled by the intrinsic muscle clock. *Molecular Metabolism* 3: 29-41, 2014.
154. **Sato S, Dyar KA, Treebak JT, Jepsen SL, Ehrlich AM, Ashcroft SP, Trost K, Kunzke T, Prade VM, Small L, Basse AL, Schönke M, Chen S, Samad M, Baldi P, Barrès R, Walch A, Moritz T, Holst JJ, Lutter D, Zierath JR, and Sassone-Corsi P**. Atlas of exercise metabolism reveals time-dependent signatures of metabolic homeostasis. *Cell Metabolism* 2022.
155. **Brack AS, and Rando TA**. Tissue-specific stem cells: lessons from the skeletal muscle satellite cell. *Cell Stem Cell* 10: 504-514, 2012.
156. **Pawlikowski B, Pulliam C, Betta ND, Kardon G, and Olwin BB**. Pervasive satellite cell contribution to uninjured adult muscle fibers. *Skelet Muscle* 5: 42, 2015.
157. **van Velthoven CTJ, and Rando TA**. Stem Cell Quiescence: Dynamism, Restraint, and Cellular Idling. *Cell Stem Cell* 24: 213-225, 2019.

158. **van Velthoven CTJ, de Morree A, Egner IM, Brett JO, and Rando TA**. Transcriptional Profiling of Quiescent Muscle Stem Cells In Vivo. *Cell Rep* 21: 1994-2004, 2017.
159. **Lepper C, Partridge TA, and Fan CM**. An absolute requirement for Pax7-positive satellite cells in acute injury-induced skeletal muscle regeneration. *Development* 138: 3639-3646, 2011.
160. **Zammit PS, Relaix F, Nagata Y, Ruiz AP, Collins CA, Partridge TA, and Beauchamp JR**. Pax7 and myogenic progression in skeletal muscle satellite cells. *J Cell Sci* 119: 1824-1832, 2006.
161. **Vicente-García C, Hernández-Camacho JD, and Carvajal JJ**. Regulation of myogenic gene expression. *Experimental Cell Research* 419: 113299, 2022.
162. **Massenet J, Gardner E, Chazaud B, and Dilworth FJ**. Epigenetic regulation of satellite cell fate during skeletal muscle regeneration. *Skelet Muscle* 11: 4, 2021.
163. **Madamtzoglou D, and Relaix F**. From cyclins to CDKIs: Cell cycle regulation of skeletal muscle stem cell quiescence and activation. *Exp Cell Res* 113275, 2022.
164. **Ganassi M, Badodi S, Wanders K, Zammit PS, and Hughes SM**. Myogenin is an essential regulator of adult myofibre growth and muscle stem cell homeostasis. *Elife* 9: 2020.
165. **Yamamoto M, Legendre NP, Biswas AA, Lawton A, Yamamoto S, Tajbakhsh S, Kardon G, and Goldhamer DJ**. Loss of MyoD and Myf5 in Skeletal Muscle Stem Cells Results in Altered Myogenic Programming and Failed Regeneration. *Stem Cell Reports* 10: 956-969, 2018.
166. **Wood WM, Etemad S, Yamamoto M, and Goldhamer DJ**. MyoD-expressing progenitors are essential for skeletal myogenesis and satellite cell development. *Dev Biol* 384: 114-127, 2013.
167. **Biressi S, Bjornson CR, Carlig PM, Nishijo K, Keller C, and Rando TA**. Myf5 expression during fetal myogenesis defines the developmental progenitors of adult satellite cells. *Dev Biol* 379: 195-207, 2013.
168. **Kanisicak O, Mendez JJ, Yamamoto S, Yamamoto M, and Goldhamer DJ**. Progenitors of skeletal muscle satellite cells express the muscle determination gene, MyoD. *Dev Biol* 332: 131-141, 2009.
169. **Megeney LA, Kablar B, Garrett K, Anderson JE, and Rudnicki MA**. MyoD is required for myogenic stem cell function in adult skeletal muscle. *Genes Dev* 10: 1173-1183, 1996.
170. **Sambasivan R, Comai G, Le Roux I, Gomès D, Konge J, Dumas G, Cimper C, and Tajbakhsh S**. Embryonic founders of adult muscle stem cells are primed by the determination gene Mrf4. *Dev Biol* 381: 241-255, 2013.
171. **Masri S, Cervantes M, and Sassone-Corsi P**. The circadian clock and cell cycle: interconnected biological circuits. *Curr Opin Cell Biol* 25: 730-734, 2013.
172. **Tamai TK, Young LC, Cox CA, and Whitmore D**. Light acts on the zebrafish circadian clock to suppress rhythmic mitosis and cell proliferation. *J Biol Rhythms* 27: 226-236, 2012.
173. **Dong G, Yang Q, Wang Q, Kim YI, Wood TL, Osteryoung KW, van Oudenaarden A, and Golden SS**. Elevated ATPase activity of KaiC applies a circadian checkpoint on cell division in Synechococcus elongatus. *Cell* 140: 529-539, 2010.
174. **Salter MG, Franklin KA, and Whitelam GC**. Gating of the rapid shade-avoidance response by the circadian clock in plants. *Nature* 426: 680-683, 2003.

175. **Dekens MP, Santoriello C, Vallone D, Grassi G, Whitmore D, and Foulkes NS**. Light regulates the cell cycle in zebrafish. *Curr Biol* 13: 2051-2057, 2003.
176. **Mori T, Binder B, and Johnson CH**. Circadian gating of cell division in cyanobacteria growing with average doubling times of less than 24 hours. *Proc Natl Acad Sci U S A* 93: 10183-10188, 1996.
177. **Matsuo T, Yamaguchi S, Mitsui S, Emi A, Shimoda F, and Okamura H**. Control mechanism of the circadian clock for timing of cell division in vivo. *Science* 302: 255-259, 2003.
178. **Chatterjee S, and Ma K**. Circadian clock regulation of skeletal muscle growth and repair. *F1000Res* 5: 1549, 2016.
179. **Eliazer S, Muncie JM, Christensen J, Sun X, D'Urso RS, Weaver VM, and Brack AS**. Wnt4 from the Niche Controls the Mechano-Properties and Quiescent State of Muscle Stem Cells. *Cell Stem Cell* 25: 654-665 e654, 2019.
180. **von Maltzahn J**. Regulation of muscle stem cell function. *Vitam Horm* 116: 295-311, 2021.
181. **Chatterjee S, Yin H, Li W, Lee J, Yechoor VK, and Ma K**. The Nuclear Receptor and Clock Repressor Rev-erbalpha Suppresses Myogenesis. *Sci Rep* 9: 4585, 2019.
182. **Relaix F, Bencze M, Borok MJ, Der Vartanian A, Gattazzo F, Mademtzoglou D, Perez-Diaz S, Prola A, Reyes-Fernandez PC, Rotini A, and Taglietti t**. Perspectives on skeletal muscle stem cells. *Nat Commun* 12: 692, 2021.
183. **Nguyen JH, Chung JD, Lynch GS, and Ryall JG**. The Microenvironment Is a Critical Regulator of Muscle Stem Cell Activation and Proliferation. *Front Cell Dev Biol* 7: 254, 2019.
184. **Ryall JG**. Metabolic reprogramming as a novel regulator of skeletal muscle development and regeneration. *FEBS J* 280: 4004-4013, 2013.
185. **Siddle K**. Signalling by insulin and IGF receptors: supporting acts and new players. *Journal of Molecular Endocrinology* 47: R1-R10, 2011.
186. **Taniguchi CM, Emanuelli B, and Kahn CR**. Critical nodes in signalling pathways: insights into insulin action. *Nature Reviews Molecular Cell Biology* 7: 85-96, 2006.
187. **Rodgers JT, Schroeder MD, Ma C, and Rando TA**. HGFA Is an Injury-Regulated Systemic Factor that Induces the Transition of Stem Cells into GAlert. *Cell Rep* 19: 479-486, 2017.
188. **Rodgers JT, King KY, Brett JO, Cromie MJ, Charville GW, Maguire KK, Brunson C, Mastey N, Liu L, Tsai CR, Goodell MA, and Rando TA**. mTORC1 controls the adaptive transition of quiescent stem cells from G0 to G(Alert). *Nature* 510: 393-396, 2014.
189. **Esser K**. Phosphorylation of p70S6k correlates with increased skeletal muscle mass following resistance exercise. 1999.
190. **Marcotte GR, West DW, and Baar K**. The molecular basis for load-induced skeletal muscle hypertrophy. *Calcif Tissue Int* 96: 196-210, 2015.
191. **Wang W, Duan X, Huang Z, Pan Q, Chen C, and Guo L**. The GH-IGF-1 Axis in Circadian Rhythm. *Front Mol Neurosci* 14: 742294, 2021.
192. **McKay BR, Nederveen JP, Fortino SA, Snijders T, Joanisse S, Kumbhare DA, and Parise G**. Brain-derived neurotrophic factor is associated with human muscle satellite cell differentiation in response to muscle-damaging exercise. *Appl Physiol Nutr Metab* 45: 581-590, 2020.
193. **Hyldahl RD, Nelson B, Xin L, Welling T, Groscost L, Hubal MJ, Chipkin S, Clarkson PM, and Parcell AC**. Extracellular matrix remodeling and its contribution to

protective adaptation following lengthening contractions in human muscle. *Faseb j* 29: 2894-2904, 2015.
194. **Hyldahl RD, Olson T, Welling T, Groscost L, and Parcell AC**. Satellite cell activity is differentially affected by contraction mode in human muscle following a work-matched bout of exercise. *Front Physiol* 5: 485, 2014.
195. **McKay BR, Toth KG, Tarnopolsky MA, and Parise G**. Satellite cell number and cell cycle kinetics in response to acute myotrauma in humans: immunohistochemistry versus flow cytometry. *J Physiol* 588: 3307-3320, 2010.
196. **McKay BR, De Lisio M, Johnston AP, O'Reilly CE, Phillips SM, Tarnopolsky MA, and Parise G**. Association of interleukin-6 signalling with the muscle stem cell response following muscle-lengthening contractions in humans. *PLoS One* 4: e6027, 2009.
197. **O'Reilly C, McKay B, Phillips S, Tarnopolsky M, and Parise G**. Hepatocyte growth factor (HGF) and the satellite cell response following muscle lengthening contractions in humans. *Muscle Nerve* 38: 1434-1442, 2008.
198. **Dreyer HC, Blanco CE, Sattler FR, Schroeder ET, and Wiswell RA**. Satellite cell numbers in young and older men 24 hours after eccentric exercise. *Muscle Nerve* 33: 242-253, 2006.
199. **Karlsen A, Soendenbroe C, Malmgaard-Clausen NM, Wagener F, Moeller CE, Senhaji Z, Damberg K, Andersen JL, Schjerling P, Kjaer M, and Mackey AL**. Preserved capacity for satellite cell proliferation, regeneration, and hypertrophy in the skeletal muscle of healthy elderly men. *Faseb j* 34: 6418-6436, 2020.
200. **Farup J, Rahbek SK, Knudsen IS, de Paoli F, Mackey AL, and Vissing K**. Whey protein supplementation accelerates satellite cell proliferation during recovery from eccentric exercise. *Amino Acids* 46: 2503-2516, 2014.
201. **Shamim B, Hawley JA, and Camera DM**. Protein Availability and Satellite Cell Dynamics in Skeletal Muscle. *Sports Med* 48: 1329-1343, 2018.
202. **Yamazaki S, and Takahashi JS**. Real-Time Luminescence Reporting of Circadian Gene Expression in Mammals. In: *Methods in Enzymology*, edited by Young MWAcademic Press, 2005, p. 288-301.
203. **Kahn RE, Dayanidhi S, Lacham-Kaplan O, and Hawley JA**. Molecular clocks, satellite cells, and skeletal muscle regeneration. *American Journal of Physiology-Cell Physiology* 2023.
204. **Xue Y, Liu P, Wang H, Xiao C, Lin C, Liu J, Dong D, Fu T, Yang Y, Wang Z, Pan H, Chen J, Li Y, Cai D, and Li Z**. Modulation of Circadian Rhythms Affects Corneal Epithelium Renewal and Repair in Mice. *Investigative Ophthalmology & Visual Science* 58: 1865-1874, 2017.
205. **Kumar A, Vaca-Dempere M, Mortimer T, Deryagin O, Smith JG, Petrus P, Koronowski KB, Greco CM, Segalés J, Andrés E, Lukesova V, Zinna VM, Welz P-S, Serrano AL, Perdiguero E, Sassone-Corsi P, Benitah SA, and Muñoz-Cánoves P**. Brain-muscle communication prevents muscle aging by maintaining daily physiology. *Science* 384: 563-572, 2024.
206. **Barash IA, Mathew L, Ryan AF, Chen J, and Lieber RL**. Rapid muscle-specific gene expression changes after a single bout of eccentric contractions in the mouse. *Am J Physiol Cell Physiol* 286: C355-364, 2004.

207. **Ingalls CP, Wenke JC, Nofal T, and Armstrong RB**. Adaptation to lengthening contraction-induced injury in mouse muscle. *Journal of Applied Physiology* 97: 1067-1076, 2004.
208. **Sidky SR, Ingalls CP, Lowe DA, and Baumann CW**. Membrane Proteins Increase with the Repeated Bout Effect. *Med Sci Sports Exerc* 54: 57-66, 2022.
209. **Devor ST, and Faulkner JA**. Regeneration of new fibers in muscles of old rats reduces contraction-induced injury. *Journal of Applied Physiology* 87: 750-756, 1999.
210. **Warren GL, Hayes DA, Lowe DA, and Armstrong RB**. Mechanical factors in the initiation of eccentric contraction-induced injury in rat soleus muscle. *J Physiol* 464: 457-475, 1993.
211. **Brooks SV, and Faulkner JA**. Contraction-induced injury: recovery of skeletal muscles in young and old mice. *Am J Physiol* 258: C436-442, 1990.
212. **McCully KK, and Faulkner JA**. Injury to skeletal muscle fibers of mice following lengthening contractions. *J Appl Physiol (1985)* 59: 119-126, 1985.
213. **Newham DJ, McPhail G, Mills KR, and Edwards RH**. Ultrastructural changes after concentric and eccentric contractions of human muscle. *J Neurol Sci* 61: 109-122, 1983.
214. **Kahn RE, Krater T, Larson JE, Encarnacion M, Karakostas T, Patel NM, Swaroop VT, and Dayanidhi S**. Resident muscle stem myogenic characteristics in postnatal muscle growth impairments in children with cerebral palsy. *American Journal of Physiology-Cell Physiology* 2023.
215. **Ingalls CP, Warren GL, Williams JH, Ward CW, and Armstrong RB**. E-C coupling failure in mouse EDL muscle after in vivo eccentric contractions. *J Appl Physiol (1985)* 85: 58-67, 1998.
216. **Bentzinger CF, Wang YX, Dumont NA, and Rudnicki MA**. Cellular dynamics in the muscle satellite cell niche. *EMBO Rep* 14: 1062-1072, 2013.
217. **Warren GL, Summan M, Gao X, Chapman R, Hulderman T, and Simeonova PP**. Mechanisms of skeletal muscle injury and repair revealed by gene expression studies in mouse models. *J Physiol* 582: 825-841, 2007.
218. **Bernard C, Jomard C, Chazaud B, and Gondin J**. Kinetics of skeletal muscle regeneration after mild and severe muscle damage induced by electrically-evoked lengthening contractions. *The FASEB Journal* 37: e23107, 2023.
219. **Ratnayake D, Nguyen PD, Rossello FJ, Wimmer VC, Tan JL, Galvis LA, Julier Z, Wood AJ, Boudier T, Isiaku AI, Berger S, Oorschot V, Sonntag C, Rogers KL, Marcelle C, Lieschke GJ, Martino MM, Bakkers J, and Currie PD**. Macrophages provide a transient muscle stem cell niche via NAMPT secretion. *Nature* 591: 281-287, 2021.
220. **Binkhorst L, Kloth JSL, de Wit AS, de Bruijn P, Lam MH, Chaves I, Burger H, van Alphen RJ, Hamberg P, van Schaik RHN, Jager A, Koch BCP, Wiemer EAC, van Gelder T, van der Horst GTJ, and Mathijssen RHJ**. Circadian variation in tamoxifen pharmacokinetics in mice and breast cancer patients. *Breast Cancer Res Treat* 152: 119-128, 2015.
221. **Haroon M, Klein-Nulend J, Bakker AD, Jin J, Seddiqi H, Offringa C, de Wit GMJ, Le Grand F, Giordani L, Liu KJ, Knight RD, and Jaspers RT**. Myofiber stretch induces tensile and shear deformation of muscle stem cells in their native niche. *Biophys J* 120: 2665-2678, 2021.

222. **Dykstra PB, Dayanidhi S, Chambers HG, and Lieber RL**. Stretch-induced satellite cell deformation incontracturedmuscles in children with cerebral palsy. *J Biomech* 126: 110635, 2021.
223. **Xu H, Ahn B, and Van Remmen H**. Impact of aging and oxidative stress on specific components of excitation contraction coupling in regulating force generation. *Science Advances* 8: eadd7377, 2022.
224. **Rome LC**. Design and function of superfast muscles: new insights into the physiology of skeletal muscle. *Annu Rev Physiol* 68: 193-221, 2006.
225. **Rome LC, Syme DA, Hollingworth S, Lindstedt SL, and Baylor SM**. The whistle and the rattle: the design of sound producing muscles. *Proc Natl Acad Sci U S A* 93: 8095-8100, 1996.
226. **McCully KK, and Faulkner JA**. Characteristics of lengthening contractions associated with injury to skeletal muscle fibers. *J Appl Physiol (1985)* 61: 293-299, 1986.

Research Portfolio Index

List of Publications

Kahn RE, Dinnunhan F, Meza G, Lieber RL, Lacham-Kaplan O, Hawley JA, & Dayanidhi S. (2024). Time-of-day mitochondrial respiration in glycolytic and oxidative skeletal muscle in the presence and following ablation of satellite cells. *Revised and resubmitting to MSSE.*

Kahn, R. E., Lieber, R. L., Dinnuhan, F., Lacham-Kaplan, O., Dayanidhi, S., & Hawley, J. A. (2024). Satellite cells differentially regulate *ex vivo* force production according to time-of-day. *American Journal of Physiology-Cell Physiology.* https://doi.org/10.1152/ajpcell.00157.2024

The above original article is available at the link below

https://journals.physiology.org/doi/abs/10.1152/ajpcell.00157.2024

Kahn, R. E., Dayanidhi, S., Lacham-Kaplan, O., & Hawley, J. A. (2023). Molecular clocks, satellite cells, and skeletal muscle regeneration. *American Journal of Physiology-Cell Physiology*. https://doi.org/10.1152/ajpcell.00073.2023

The above review article is available at the link below

https://journals.physiology.org/doi/abs/10.1152/ajpcell.00073.2023

Kahn RE, Zhu P, Roy I, Peek C, Hawley JA, & Dayanidhi S. (2024). Ablation of satellite cell-specific clock gene, *Bmal1*, alters force production, muscle damage, and repair following contractile injury. *Submitted to FASEB.*

Statement of Contribution of Others

As a requirement from the Australian Catholic University Higher Degree Research policies with regard to the degree of Doctor of Philosophy with Publication, this statement is provided to summarize and clearly identify the nature and extent of the intellectual input by the candidate and any co-authors.

Kahn RE, Dinnunhan F, Meza G, Lieber RL, Lacham-Kaplan O, Hawley JA, & Dayanidhi S. (2024). Time-of-day mitochondrial respiration in glycolytic and oxidative skeletal muscle in the presence and following ablation of satellite cells. *Revised and resubmitting to MSSE.*

Statement of Contribution: RK, SD, OLK, JAH contributed to conceptualization and preparation of this manuscript. RK performed all physiology and IHC experimentation. RK drafted manuscript. GM performed activity assay experiments. OLK and FD performed gene expression experiments. RLL contributed in helping develop the novel submaximal contractile fatigue protocol used in this study. RK, SD, OLK, JAH, RLL edited and revised the manuscript. All authors approved of its content.

“I acknowledge that my contribution was 70%

Date: 21/05/2024

Ryan Kahn

“I acknowledge that my contribution was 5%

-non-responsive Date: 21/05/2024

-Fawzan Dinnunhan

“I acknowledge that my contribution was 5%

Date: 21/05/2024

-Guadalupe Meza

“I acknowledge that my contribution was 5%

Date: 21/05/2024

-Rick L. Lieber

“I acknowledge that my contribution was 5%

Date: 21/05/2024

-Orly Lacham-Kaplan

“I acknowledge that my contribution was 5%

Date: 21/05/2024

-John A. Hawley

“I acknowledge that my contribution was 5%

Date: 21/05/2024

-Sudarshan Dayanidhi

Kahn, R. E., Lieber, R. L., Meza, G., Dinnunhan, F., Lacham-Kaplan, O., Dayanidhi, S., & Hawley, J. A. (2024). Time-of-day effects on *ex vivo* muscle contractility following short-term satellite cell ablation. *American Journal of Physiology-Cell Physiology.* https://doi.org/10.1152/ajpcell.00157.2024

Statement of Contribution: RK, SD, OLK, JAH contributed to conceptualization and preparation of this manuscript. RK performed all physiology and most IHC experimentation. RK drafted manuscript. GM performed some IHC experimentation. OLK and FD performed gene expression experiments. RLL contributed to RK's *ex vivo* contractile training, overseeing of RK's contractile experimentation, and data interpretation. RK, SD, OLK, JAH, RLL edited and revised the manuscript. All authors approved of its content.

"I acknowledge that my contribution was 70%

Date: 21/05/2024

-Ryan E. Kahn

“I acknowledge that my contribution was 5%

Date: 21/05/2024

-Richard L. Lieber

“I acknowledge that my contribution was 5%

Date: 21/05/2024

-Guadalupe Meza

“I acknowledge that my contribution was 5%

-non-responsive Date: 21/05/2024

-Fawzan Dinnunhan

“I acknowledge that my contribution was 5%

Date: 21/05/2024

-Orly Lacham-Kaplan

“I acknowledge that my contribution was 5%

Date: 21/05/2024

-Sudarshan Dayanidhi

“I acknowledge that my contribution was 5%

Date: 21/05/2024

-John A. Hawley

Kahn, R. E., Dayanidhi, S., Lacham-Kaplan, O., & Hawley, J. A. (2023). Molecular clocks, satellite cells, and skeletal muscle regeneration. *American Journal of Physiology-Cell Physiology*. https://doi.org/10.1152/ajpcell.00073.2023

Statement of contribution: RK, OLK, SD, JAH conceptualized and outlined the structure of the review paper. RK drafted manuscript. RK, OLK, SD, JAH edited and revised manuscript. All authors approved final content.

"I acknowledge that my contribution was 70%

Date: 21/05/2024

-Ryan E. Kahn

"I acknowledge that my contribution was 10%

Date: 21/05/2024

-Sudarshan Dayanidhi

“I acknowledge that my contribution was 10%

Date: 21/05/2024

-Orly Lacham-Kaplan

“I acknowledge that my contribution was 10%

Date: 21/05/2024

-John A. Hawley

Kahn RE, Zhu P, Roy I, Peek C, Hawley JA, & Dayanidhi S. (2024). Ablation of satellite cell-specific clock gene, *Bmal1*, alters force production, muscle damage, and repair following contractile injury. *Submitted to FASEB.*

Statement of Contribution: RK, SD, JAH contributed to conceptualization and preparation of this manuscript. RK performed all experimentation. RK drafted manuscript. CP and PZ provided the animals used in these experiments and were involved in data interpretation and determining experimental direction. IR provided the *in vivo* contractile apparatus setup used on all animals. RK, JAH, SD contributed to manuscript editing and revising thus far.

“I acknowledge that my contribution was 70%

Date: 21/05/2024

-Ryan E. Kahn

“I acknowledge that my contribution was 5%

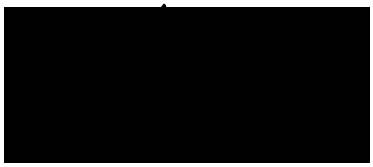

Date: 21/05/2024

-Pei Zhu

“I acknowledge that my contribution was 5%

Date: 21/05/2024

-Ishan Roy

“I acknowledge that my contribution was 5%

Date: 21/05/2024

-Clara Peek

“I acknowledge that my contribution was 5%

Date: 21/05/2024

-John A. Hawley

“I acknowledge that my contribution was 10%

Date: 21/05/2024

-Sudarshan Dayanidhi